NOTE TO USERS

This reproduction is the best copy available.

UMI®

Selective caffeine removal by microbial consortia

By

Jean-Philippe Gaulin

Department of Chemical Engineering
McGill University, Montreal

November 2003

A thesis submitted to the Faculty of Graduate Studies and Research in partial fulfillment of the requirements of the degree of Master of Science

©Jean-Philippe Gaulin 2003

Library and Archives Canada

Published Heritage Branch

395 Wellington Street
Ottawa ON K1A 0N4
Canada

Bibliothèque et Archives Canada

Direction du Patrimoine de l'édition

395, rue Wellington
Ottawa ON K1A 0N4
Canada

Your file Votre référence
ISBN: 0-612-98641-1
Our file Notre référence
ISBN: 0-612-98641-1

NOTICE:
The author has granted a non-exclusive license allowing Library and Archives Canada to reproduce, publish, archive, preserve, conserve, communicate to the public by telecommunication or on the Internet, loan, distribute and sell theses worldwide, for commercial or non-commercial purposes, in microform, paper, electronic and/or any other formats.

The author retains copyright ownership and moral rights in this thesis. Neither the thesis nor substantial extracts from it may be printed or otherwise reproduced without the author's permission.

AVIS:
L'auteur a accordé une licence non exclusive permettant à la Bibliothèque et Archives Canada de reproduire, publier, archiver, sauvegarder, conserver, transmettre au public par télécommunication ou par l'Internet, prêter, distribuer et vendre des thèses partout dans le monde, à des fins commerciales ou autres, sur support microforme, papier, électronique et/ou autres formats.

L'auteur conserve la propriété du droit d'auteur et des droits moraux qui protège cette thèse. Ni la thèse ni des extraits substantiels de celle-ci ne doivent être imprimés ou autrement reproduits sans son autorisation.

In compliance with the Canadian Privacy Act some supporting forms may have been removed from this thesis.

While these forms may be included in the document page count, their removal does not represent any loss of content from the thesis.

Conformément à la loi canadienne sur la protection de la vie privée, quelques formulaires secondaires ont été enlevés de cette thèse.

Bien que ces formulaires aient inclus dans la pagination, il n'y aura aucun contenu manquant.

Canada

Abstract

Coffee processing presents a considerable waste disposal problem, mainly because of the large volumes generated and the chemical composition of the by-products, particularly the caffeine levels. The use of *Pseudomonas putida* IF-3, a caffeine-degrading microorganism, in a microbial consortium for bioremediation of caffeine found in coffee wastes was investigated. Caffeine degradation was observed in fed-batch reactor experiments with caffeine as sole source of carbon and nitrogen. Metabolic regulation and caffeine removal potential by *Pseudomonas putida* IF-3 were investigated by supplementing with other nutrient sources. Diauxic growth was not observed. Nitrogen release from caffeine breakdown was found to be rate-limiting.

Effects of caffeine on microbial consortia were studied using denaturing gradient gel electrophoresis (DGGE), providing a community-scale view of changes in microbial consortia upon caffeine addition. Surprisingly, caffeine removal was achieved indigenously by the microbial consortium. Principal component analysis was used to analyze differences in DGGE banding patterns between control and caffeine-exposed mixed cultures.

Résumé

Le processus de tranformation du café engendre un important problème de disposition des déchets, principalement à cause de l'importance des volumes générés et de la composition chimique des sous-produits, particulièrement les taux de caféine. L'utilisation de *Pseudomonas putida* IF-3, un microorganisme dégradant la caféine, dans un consortium microbien pour la bioremédiation de la caféine contenue dans les déchets de l'industrie du café a été étudiée. La dégradation de la caféine a été observée lors d'expériences en bioéracteur d'apport de substrat avec la caféine comme seule source de carbone et d'azote. La régulation métabolique et le potentiel de dégradation de la caféine par *Pseudomonas putida* IF-3 ont été étudiés par addition d'autres sources de nutriments. Une croissance diauxique n'a pas été observée. L'étape limitante lors de la dégradation de la caféine serait le relâchement d'azote associé au clivage de la caféine.

L'impact de la caféine sur un consortium microbien a aussi été étudié en utilisant l'électrophorèse en gel de gradient dénaturant (DGGE), qui fournit une vision à l'échelle de la communauté des changements dans le consortium microbien suite à l'addition de caféine. L'analyse de composantes principales de séquences de bandes obtenues par DGGE a été utilisé afin de déceler des changements entre les séquences de bandes obtenues avec une culture mixte contrôle et celles obtenues avec une culture mixte exposée à la caféine.

Acknowledgements

I would like to give sincere thanks to my supervisor, Dr. Brown, for his precious advice, support, and financial aid throughout the whole duration of my Master's degree. He helped me "reinvent" myself by allowing me to pursue Graduate studies in Chemical Engineering, coming from a Biochemistry background. This new engineering perspective I acquired will be of great help in future projects. I would also like to thank Dr. Cooper for his much needed advice.

I also need to acknowledge the daily help and contributions from all coworkers. Special thanks to Michael Bratty for showing me the basics of bioreactor work. To all others, Dominic, Soren, Sandro, Adam, Owen, Esther, Robbie, Carl and Annie, thank you for answering the dumb questions a biochemist can ask...Sorry if I forgot anyone. I must also recognize the work of the Chemical Engineering department secretaries, which do their best to ease the burden of McGill bureaucratic tasks on us.

Marie-Ève, thanks for listening and understanding me in my hectic periods, and sleeping on the couch on the 7^{th} floor at 2 AM while I was sampling. Many thanks to my parents for believing in me and supporting me from start to finish. To all my friends, you're a great crew.

TABLE OF CONTENTS

LIST OF FIGURES

LIST OF TABLES

1. LITERATURE REVIEW

1.1. COFFEE PRODUCTION AND PROCESSING

The production of coffee beans is a major industry in many countries in the Southern hemisphere. The world's biggest coffee producers are Brazil, Colombia and Vietnam, but coffee production also has significant economic importance in countries including Venezuela, Guatemala, Costa Rica, Mexico, El Salvador and India (Elias 1979). The US. Department of agriculture estimated the world coffee production for 1993 to be 5.43 x 10^6 tonnes, with 1.26 x 10^6 tonnes coming form Brazil alone (Lundsberg 1998). As for importers, the U.S.A. and Germany lead all consuming countries with 22 and 17% of the world coffee imports, respectively (Lundsberg 1998).

Coffee plants belong to the botanical family *Rubiaceae*, which is comprised of 500 genera and over 6000 different species (Clark 1985). The coffee berry consists of four anatomical fractions: the beans or endosperm; the hull or endocarp; the mucilage or mesocarp; and the pulp or esocarp. There are two beans per fruit, and their flat surfaces face each other. The hulls cover the beans, and are surrounded by a 0.5-2 mm thick layer of mucilage. The mucilage is in turn covered by a thick layer of spongy cells called the coffee pulp (Bressani 1979).

Two commercial methods are used to harvest the bean from the fruit. They are referred to as the "wet" and "dry" methods. In the early stages of the wet processing operation, the fruits, or cherries, of the plants are harvested. Following harvesting, the berries are dumped into a water tank to remove foreign material and unripe fruits, which rise to the surface. The berries are then passed to the wet processing step. In this step, the berries are dumped into a large tank of water resembling an inverted pyramid. The fruits are siphoned from the bottom, and mechanical friction separates the pulp from the rest of the fruit. The berries, with the pulp removed, are then transported to fermentation tanks where the mucilage is removed by an anaerobic process. The hydrolysis products of the mucilage remain in the water. The coffee beans are then washed and dehydrated, first by

sun-drying then with hot air. Finally, a dry processing step separates the hulls from the beans (Bressani 1979). The wet method is mostly used for *Arabica* coffees (Clarke and Macrae 1987). Table 1-1 shows the associated material balance of the coffee cherry. All coffee by-products, besides the bean, are discarded to the environment.

Component	% (Dry weight)
Coffee beans	55.4
Coffee pulp	28.7
Mucilage	4.9
Coffee hulls	11.9
Coffee berry (Total)	100

Table 1-1: Material balance of the coffee fruit (Elias 1979).

A dry processing method can also be used, which involves the drying of the fruit as a whole. First, the harvested fruits are manually separated from unripe and damaged fruits. The coffee cherries are spread out in the sun on large, flat surfaces. As the cherries dry, they are raked or turned to ensure even drying. The cherries are dried to a moisture content of about 12.5%, and the drying process can take up to four weeks. The dried cherries are stored in bulk in special silos before being sent to the mill, where all unwanted layers of the coffee cherry are removed by the hulling machine (Clarke and Macrae 1987).

1.2. ENVIRONMENTAL SIGNIFICANCE

1.2.1. Waste disposal

Coffee processing, being a major economic activity in many countries, releases large volumes of solid wastes, as 45% of the whole fruit is discarded (Table 1-1). It is estimated that for every two tonnes coffee cherries processed, a whole ton of coffee pulp is generated (Roussos, de los Angeles Aquiahuatl et al. 1995). The process also releases

significant volumes of wastewaters, since the wet process used relies on water to serve as a transport medium and to remove spoiled fruits and foreign material (Bressani 1979). As an example of the large volumes generated by coffee wastes, in Columbia for the year 1988, processing of coffee cherries produced the same amount of organic waste as was produced by 80% of its total population of 30 million (Zuluaga 1989).

Coffee processing effluents have limited economic uses, due to the presence of undesirable organic components such as caffeine, caffeic acid and chlorogenic acid. Hence, they are discarded as waste products in the surrounding effluent streams. They are considered to be the major polluting agents in water streams located near coffee-processing sites (Roussos, de los Angeles Aquiahuatl et al. 1995). Table 1-2 presents the organic components of the major by-product generated, coffee pulp.

Component	% (Dry weight)
Moisture	7.9
Dry matter	92.1
Ether extract	2.6
Crude fibre	20.8
Crude protein	10.7
Ash	8.8
Nitrogen-free extract	49.2
Tannins	1.80-8.56
Total pectic substances	6.5
Reducing sugars	12.4
Nonreducing sugars	2.0
Caffeine	1.3
Chlorogenic acid	2.6
Total caffeic acid	1.6

Table 1-2: Organic components of coffee pulp (Elias 1979).

1.2.2. Caffeine

Caffeine (1,3,7-trimethylxanthine) is a purine alkaloid, present in numerous plant species (Figure 1-1). Caffeine and other methylxanthines, such as theobromine and theophylline

have been detected in over a hundred plant species, most notably from the genera: *Camellia*, *Coffea*, *Cola*, *Ilex*, *Paullinia*, and *Theobromia*. In most coffee plants, caffeine is present at concentrations ranging from 0.4 to 2.4% (w/w) on a dry weight basis (Ashihara and Crozier 1999).

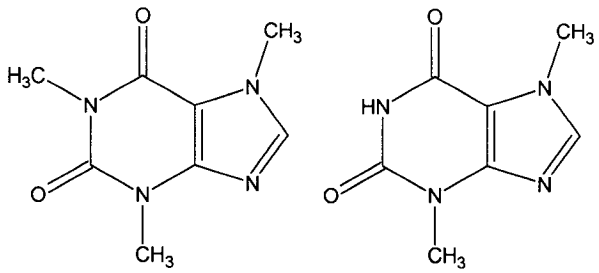

Caffeine Theobromine

Figure 1-1: Chemical structure of caffeine and theobromine.

Caffeine and other methylxanthines are present in vast variety of non-alcoholic beverages and foods such as coffee, tea, chocolate, mate and numerous soft drinks. Caffeine is ubiquitous in the human diet, and is probably the most widely consumed drug in the world (Barone and Roberts 1984). A 5-ounce cup of coffee contains approximately 75-155 mg caffeine, and the U.S. daily caffeine consumption in 1979 was estimated to be on the order 200 mg per person, based solely on consumption of coffee and tea (Barone and Roberts 1984).

The purine alkaloid accumulates in leaves and fruits of coffee plants, and is thought to be produced for two main reasons. First, high concentrations of caffeine in young leaves, buds and fruits of *Coffea arabica* and *Camellia sinensis* (tea) plants, could act as a chemical defense against predators, such as small animals and insects (Ashihara and Crozier 1999). Second, caffeine would be produced as an allelopathic and slightly autotoxic compound, inhibiting weed growth under the coffee plants, as well as being toxic to the roots of coffee plants (Friedman and Waller 1985; Waller, Kumari et al. 1986). This mechanism would prevent overwhelming growth in its surroundings.

Caffeine has notable effects upon ingestion, as it stimulates the central nervous system, increases cardiac muscle activity, widens the heart, kidney and skin vessels, and also exhibits broncholytical and diurectical activity (Glück and Lingens 1987). The molecule probably exerts its effects through antagonism of adenosine receptors (Curatolo and Robertson 1984). Moreover, it may lead to abnormal behavorial effects including depression and hyperactivity, and might also be linked to myocardial infarction and arrhythmia (Dews 1984; Spiller 1984). It is thought to be associated with cancers of the urinary tract, kidney and pancreas. However, conflicting results do not allow confirmation on the implication of caffeine in cancer development (Curatolo and Robertson 1983). When tested to evaluate its teratogenic effects, caffeine, when consumed in moderate amounts, poses little hazard to the developing mammalian embryo. However, the molecule does induce teratogenic synergism with other known teratogens, although at doses higher than the average human intake (Wilson and Scott Jr. 1984).

Studies of caffeine effects on animal health showed that mixing caffeine-containing coffee pulp with regular feedstocks resulted in slower weight gain in both chicken and rats, and a high level of mortality for both species (Molina, de la Fuente et al. 1974; Braham 1979; Penaloza, Molina et al. 1985). It also has similar stimulating and diuretic effects on ruminants and swine as those noted for humans (Bressani 1979). Rats submitted to high doses of caffeine suffered an endocrine stress syndrome characterized by elevated hormonal levels (Spindel and Wurtman 1984). Caffeine also acts on bacteria and yeasts, impairing cell growth and inducing inhibition of both RNA and protein synthesis in *E. coli* and *S. cerevisiae* strains (Putrament, Rabanowska et al. 1972).

1.2.3. Environmental effects of organic components in coffee by-products

Polyphenols such as caffeic acid and chlorogenic acid, and the polymeric phenol-containing tannins are other components of coffee by-products suspected of having physiological effects on humans and animals. Tannins are polymeric substances of

phenolic nature. There are two groups of tannins: the hydrolysable tannins and the condensed tannins. Tannins act by binding to proteins and rendering them unavailable to organisms. They can therefore act as enzyme inhibitors. Tannins can alter animal performance regarding feed intake by decreasing protein availability, and inhibiting enzyme activity (Bressani 1979). Free polyphenols may interfere with protein utilization by binding to proteins, such as digestive enzymes (McLeod 1974). Caffeic acid and chlorogenic acid have been reported to act as antithiamine substances (Somogyi and Näegli 1976). There is also biochemical evidence that low blood-glucose levels are associated with animals fed with coffee pulp rations (Bressani 1979). Finally, the high levels of fermentable sugars released as waste in the coffee by-product can lead to quick assimilation by the surrounding aquatic vegetation, therefore promoting eutrophication of the waste streams located in the vicinity of the coffee processing sites.

Although coffee by-products do contain harmful compounds, they are potentially a good and inexpensive source of protein, fibers, carbohydrates and minerals, especially potassium (Roussos, de los Angeles Aquiahuatl et al. 1995). The dry coffee pulp contains 8 to 11% protein with an amino acid profile similar to those found in soy, cotton, and fish flours (Molina, de la Fuente et al. 1974). The crude fiber content, around 21%, is also high, and the elevated concentrations of fermentable sugars make it a very rich product (Table 1-2). However, because of the toxic and physiological effects of the components mentioned above, no large-scale commercial use of the coffee wastes has been developed.

1.3. APPLICATIONS AND LIMITATIONS OF COFFEE BY-PRODUCTS

The high levels of protein, fibers, and fermentable sugars present in coffee wastes, combined with the environmental problems associated with its disposal, have motivated research for finding alternate uses for these products. Converting coffee wastes into single-cell proteins by using solid coffee by-products as substrates for fungi has been investigated (Orue and Bahar 1985; Roussos, Aquiahuatl et al. 1994; Hakil, Denis et al.

1998). The mycelia formed could then be used as feed for ruminants. Coffee pulp has shown to be a good substrate for *Aspergillus oryzae*, *Bacillus megatherium*, and *Saccharomyces cerevisiae*. However, slow growth and only partial caffeine removal kept these processes from being commercialized (Bressani 1979). Using coffee pulp as an organic fertilizer in coffee plantations has been a good way to fertilize caffeine-containing soils, mainly because of the high potassium content of the coffee pulp. However, handling of the pulp was problematic because of the high moisture content, containing 80 to 88% water (Bressani 1979). Coffee hulls could be used as fillers in animal feeds, having a high concentration of crude fibre, which is characteristic of other fillers used for ruminant feeding.

An interesting option is the potential use of coffee by-products directly as part of an animal feedstock. This would address the issue of supplying a nutrient-rich, low-cost resource for feedstock for swine, poultry and cattle, a problem encountered by many farmers and cattle producers. Mixing dehydrated coffee pulp with conventional feedstocks was attempted for ruminants, swine and poultry rations (Braham 1979; Cabezas, Flores et al. 1979; Jarquin 1979). However, as mentioned in sections 1.2.2 and 1.2.3, the significant levels of caffeine, caffeic acid, chlorogenic acid and polyphenolic compounds greatly limit the proportion in which the coffee wastes can be mixed in with the standard animal feed preparation. The high levels of potassium can also inhibit feed intake. The maximum proportion of coffee by-products that could be introduced without impairing animal growth or causing mortality was found to be 20-30% on a dry-weight basis (Sideso, Marvier et al. 2001). Above this concentration, effects on nitrogen absorption, voluntary feed intake and weight gain are significant in cattle crops (Cabezas, Flores et al. 1979). Coffee pulp can be used in swine rations at a ratio up to 16% without any detrimental effects on animal weight gain and nitrogen absorption (Jarquin 1979). Feeding chicks with rations containing coffee by-products proved to have even greater effects, leading to mortality in some cases at a proportion of 30% coffee by-product in the feed (Braham 1979).

Based on these studies, reducing the caffeine concentration in the coffee wastes could allow an increase in the ratio of these substances in animal feed preparation. Such work has already been attempted, and the best success was achieved by physically or chemically treating the wastes to remove the undesired compounds. Conclusions drawn from these experiments were that the treatments were either inefficient in eliminating the toxicity or too expensive for large-scale use (Roussos, Aquiahuatl et al. 1994).

1.4. DECAFFEINATION METHODS

Decaffeination of the coffee beans is achieved on an industrial scale by several methods. Chemical solvent decaffeination is widely used, where the beans are treated with the solvent under pressure and at a temperature close to the boiling point of the solvent. Methylene chloride and ethyl acetate are the two most commonly used solvents for this decaffeination method (Clarke and Macrae 1987). Percolation at 94°C with water as solvent, or solvent extraction at room temperature using either ethyl alcohol or water are other efficient ways to extract the caffeine from the bean into the solvent (Molina, de la Fuente et al. 1974; Braham and Bressani 1979). The latest technological advance for decaffeination involves the use of supercritical fluid extraction with carbon dioxide. While effective, this method has proven to be less viable economically (Ashihara and Crozier 1999). Another popular technique is the swiss hot process, in which the caffeine is first removed from the beans by soaking in hot water. The water is then stripped of its caffeine by percolation through activated charcoal. The beans are then returned to the water, where they reabsorb the remaining caffeine-free constituents from the water (Davis 1996). Recently, genetically engineered plants in which the caffeine content was reduced to up to 70% have been developed (Ogita, Uefuji et al. 2003). However, legal considerations and public apprehension have greatly limited the commercial applications for such plants. A more recent approach is the removal of the caffeine content by biological means. This would allow complete and specific removal of caffeine, without altering the composition and taste of the end product. Furthermore, the worry about solvent residues would be eliminated (Bressani 1979). Caffeine degradation has been

achieved using different strains of the genus *Pseudomonads*, and different strains of fungi (Kurtzmann and Schwimmer 1971; Woolfolk 1975; Roussos, Aquiahuatl et al. 1994; Hakil, Denis et al. 1998)).

Although much effort has been put on decaffeination of the coffee bean in order to produce a caffeine-free beverage, little research has been aimed at the efficient removal of caffeine from the coffee by-products. Different white-rot fungi were investigated to treat coffee pulp and succeeded in decreasing the holocellulosic and lignitic content, but the treatment did not manage to reduce the caffeine content (Rolz, de Leon et al. 1988). Microbiological methods could be used to reduce the caffeine content in the coffee processing wastes. Selective bioremediation of coffee wastes by microorganisms could address part of the waste disposal problem, reducing the concern for environmental pollution exacerbated by the presence of caffeine. Use of coffee pulp as a substrate for solid-state fermentation by fungi has been investigated, with mixed success in removing the contaminants (Orue and Bahar 1985; Penaloza, Molina et al. 1985; Roussos, de los Angeles Aquiahuatl et al. 1995). However, selective biological caffeine removal, with an effort to minimize consumption of other nutrient sources, has not yet been achieved. This process, combined with the naturally high nutritional value of the coffee wastes, could allow an increase in the proportion of coffee by-products that could be used as feedstock by swine, poultry and cattle crops, therefore converting a widely produced waste product into an inexpensive, highly nutritious resource.

1.4.1. Biological decaffeination by *Pseudomonas putida* IF-3

The bacterial strain *Pseudomonas putida* IF-3 is capable of growing on caffeine as sole source of carbon and nitrogen, and possesses a series of demethylases that lead to complete mineralization of the caffeine molecule (Koide 1996). *P. putida* IF-3 is a Gram-negative rod of 0.8 x 2.3 μm dimension. It grows under aerobic conditions, at an optimal temperature at 30°C (Koide 1996). Similar to other members of the *Pseudomonads* genus, IF-3 produces a yellow fluorescent pigment that can be visualized under UV light.

Caffeine degradation occurs through three subsequent demethylation steps (Blecher and Lingens 1977; Asano, Komeda et al. 1993). Following demethylation, xanthine is converted to uric acid, which gets broken down as glyoxylic acid and urea, before complete mineralization into carbon dioxide and water (Figure 1-2). NADH and oxygen are needed as cofactors in the demethylation steps. Formaldehyde is released as demethylation occurs.

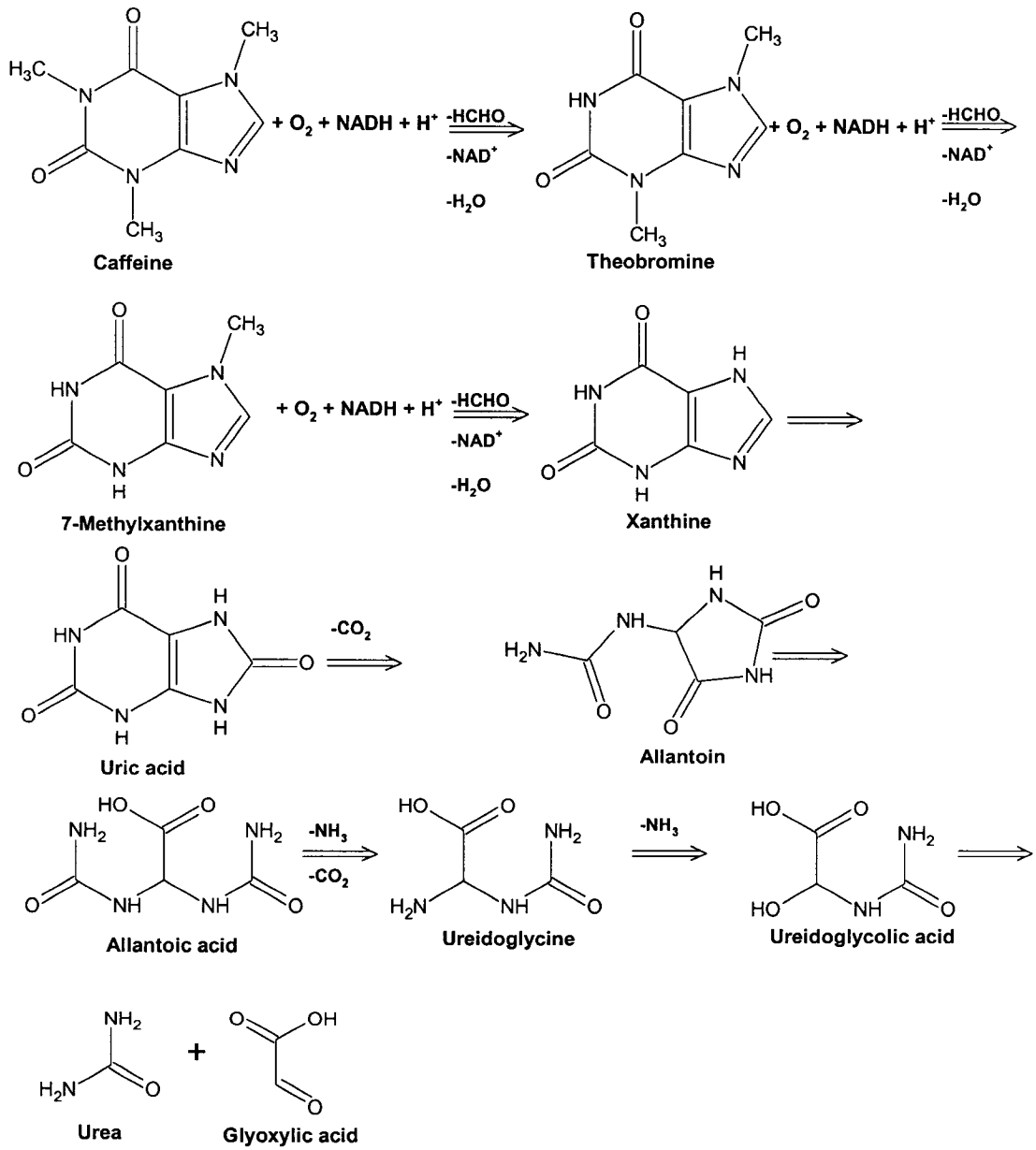

Figure 1-2: Caffeine degradation pathway by *Pseudomonas putida* IF-3.

1.5. MICROBIAL ECOLOGY

In order to achieve efficient caffeine removal using microbiological methods, it is important to have a good understanding of the effects of caffeine on bacterial species, in terms of the microbial communities rather than individual species. Near the coffee processing sites, where the coffee by-products are discarded, a variety of microorganisms respond to the environmental stresses imposed upon them. Caffeine can have harmful effects on certain populations of microorganisms within the consortium. Therefore, finding a way to monitor the response of the microbial populations to caffeine exposure is of interest. Focusing on the effects of caffeine, or any other contaminant, on a single bacterial or fungal strain will yield information of limited value with respect to the natural ecosystem. In most cases, it is assumed that microbial communities within contaminated ecosystems tend to be dominated by the organisms that are capable of metabolizing the contaminant or surviving its exposure (Macnaugton, Stephen et al. 1999). The presence of such organisms can have a protective effect on the more susceptible populations.

Therefore, studying population changes and their dynamics in response to an environmental stress will help elucidate the changes in tightly regulated microbial consortia, and may provide insight on which bacterial species can cope with the added environmental pressure exerted by caffeine exposure. However, studying changes in environmental populations using conventional culture techniques in microbiology is not adequate. This is mainly because of the inherent limitations in laboratory culture conditions, since selective enrichment cultures fail to mimic the conditions required by microorganisms to proliferate in their natural habitat (Muyzer, De Waal et al. 1993). There is only limited information available on the nutritional needs of bacteria, and it is practically impossible to develop a culture medium that would be representative of what is available in selective environments where organisms are isolated. It is estimated that only a small fraction (1-5%) of all microorganisms in nature can be isolated in pure cultures using the conventional microbiology techniques, such as isolation by growth on defined culture media and identification based on biochemical responses (Amann,

Ludwig et al. 1995). Therefore, other tools must be used in order to gain a valuable understanding of the microbial diversity.

1.5.1. Molecular markers and genetic fingerprinting

Recent technological advances in molecular biology have led to the development of culture independent tools, therefore eliminating the restrictions imposed by traditional microbiology techniques. It is now possible to study microbial diversity and population changes at the genetic level, by using molecular markers. This area of work is called genetic fingerprinting, and the techniques available provide a pattern, or profile, of the genetic diversity in a microbial community (Muyzer and Smalla 1998). Bacterial species can be grouped according to similarities in sequences on specific genes. The gene selected for this purpose must be common to all species of interest, and must have both conserved and variable regions. Species with similarities in the variable region of the DNA are assumed to have a similar ancestry (Woese 1987). Phylogenetic classification of bacteria is often achieved upon sequence analysis of genes encoding small-subunit ribosomal RNA (16S rRNA), a molecule present in all bacterial species. This gene contains regions of high homology between species, separated by other DNA stretches of high variability. Therefore, comparative sequence analysis of the variable regions can dictate the evolutionary discrepancy between bacterial strains. Evolutionary classification of bacterial genus or species is usually represented in the form of a phylogenetic tree, on which the physical distance between two species represents the similarity in their evolution (Figure 1-3). For example, in figure 1-3, the *Saccharomyces* genus would be more closely related in evolution terms, to the *Paramecium* genus than to the *Bacillus* genus. Through the application of 16S rRNA genes fragments as molecular markers, a community-scale view of the changes in a microbial community upon exposure to a contaminant, such as caffeine, can be assembled.

1.5.2. DNA amplification

After total DNA extraction of bacterial species from a microbial community, an exponential amplification of the 16S rDNA fragments can be achieved by using the polymerase chain reaction (PCR), an enzymatic method for double-stranded DNA synthesis. The principle of PCR relies on the use of primers, which are usually 15-30 bp oligonucleotides with complementary sequences to the 3' region of the fragment to be amplified. One primer is required for each of the two strands of a fragment. The primers anneal directly to the complementary regions on the template DNA, and total genomic DNA is used directly as a template for the PCR reaction. Only small quantities (<1 μg) of DNA are required. Both primers, all four deoxynucleotides (dATP, dCTP, dGTP, dTTP), a thermostable *Taq* DNA polymerase and an appropriate buffer are added to the reaction mixture.

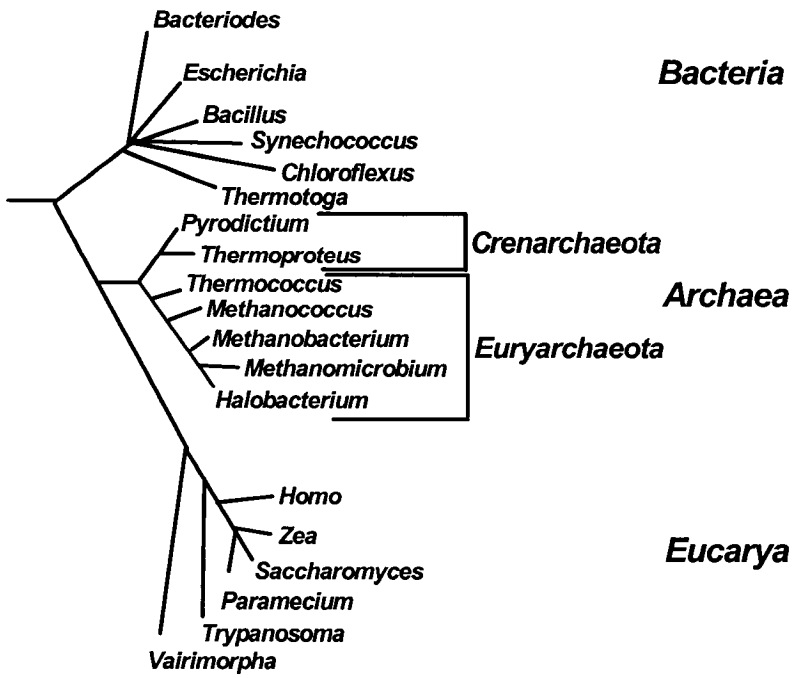

Figure 1-3: Example of a phylogenetic tree, relating the major subdivisions of all three life groups: Bacteria, Archaeabacteria and Eucarya. The physical distance on the image represents the actual evolutionary distance between two genuses.

In the first step of the process, the reaction mixture is heated to 95 °C to denature the double-stranded DNA. At high temperature, double-stranded DNA unwinds to give two single strands that will serve as template strands for the DNA polymerase. The second step is the annealing of the primers to their complementary sequences on the 3' ends of each strand. The choice of the annealing temperature is determined by the length and nucleotidic sequence of the primers, mainly their guanine and cytosine (G+C) content. During the elongation step, the thermostable DNA polymerase synthesizes the complementary strand. This is achieved at 72 °C, which is the optimal temperature for the *Taq* DNA polymerase family, but can vary with different polymerases. The three steps are then repeated for 25-30 cycles, to allow subsequent amplification of the newly formed strands (Figure 1-4). A standard PCR reaction can give an amplification factor on the order of 10^6, with high efficiency (Lodish, Baltimore et al. 1995).

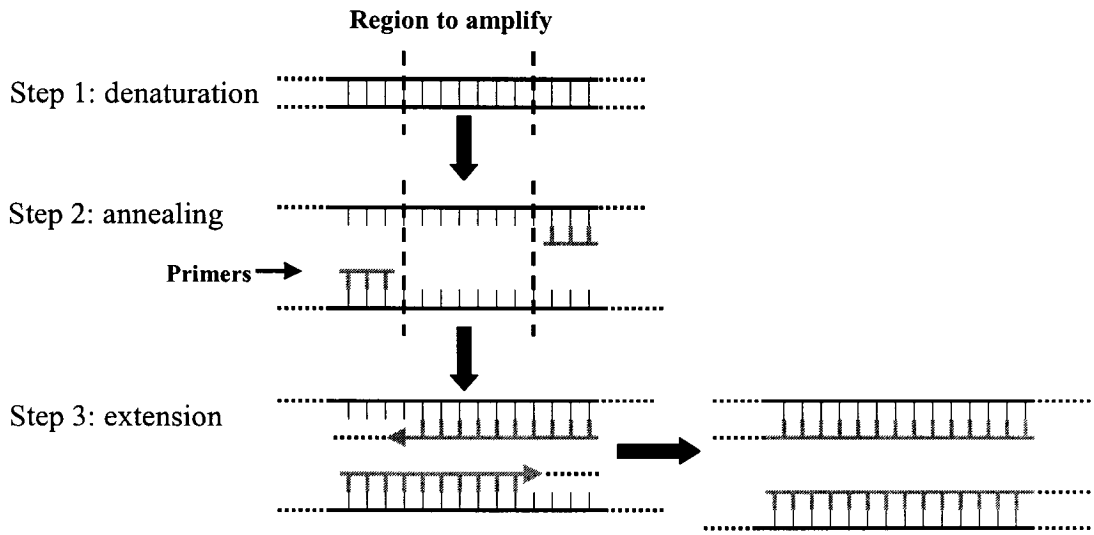

Figure 1-4: The polymerase chain reaction.

The genes coding for 16S rRNA contain segments of highly conserved DNA sequences interspersed among highly variable regions. These highly conserved regions are good target sites for the design of primers for PCR. Thus, using the conserved regions as primer binding sites allows for the amplification of the adjacent variable region. Universal primers have been developed to anneal to the specific conserved regions of the 16S rRNA gene that are common to all species present in the bacterial domain (Juck,

Charles et al. 2000). Therefore, it is theoretically possible to amplify gene fragments from all the bacterial species present in a sample.

1.5.3. Denaturing gradient gel electrophoresis (DGGE) and other community analysis techniques

PCR amplification of 16S rRNA gene fragments from the different bacterial strains present in an environmental sample yields a large number of fragments of the same length, differing only in their nucleotidic sequence. These fragments cannot be resolved using conventional gel electrophoresis, which separates DNA fragments according to their size only.

In order to resolve the different DNA fragments obtained by PCR amplification and retrieve the desired information on the status of the bacterial community, a technique called denaturing gradient gel electrophoresis is used. This technique was first developed to identify single base-pair differences in DNA fragments, including point mutations (Muyzer 1999). It is now widely used as a genetic fingerprinting tool in microbial ecology, allowing the health and status of microbial consortia to be monitored during a bioremediation treatment, or upon exposure to a environmental stress (Macnaugton, Stephen et al. 1999).

DGGE differs from conventional electrophoresis in that it allows a separation of DNA fragments of identical length based upon their DNA sequence. In a polyacrylamide gel, the double-stranded DNA fragments are submitted to a linear, increasing denaturing gradient composed of urea and formamide. When an electric potential is applied to the gel, the fragments begin to migrate. Since all fragments have the same length, they all migrate initially at the same rate. When exposed to the denaturing agents, the DNA fragments will "melt", or partially unwind due to the breakage of the hydrogen bonding between base pairs, in segments called "melting domains". These melting domains are short base pair stretches having identical melting behaviours, which are dependent upon

the nucleotidic G + C content of the fragment. Therefore, the concentration at which a fragment denatures is sequence-specific. At the concentration of denaturing agent in the gel corresponding to the lowest melting domain, the DNA will partially denature from the helical to a partially open structure (Muyzer and Smalla 1998). A 40 base-pair GC clamp is added to one of the primers, preventing complete unwinding of the double-stranded amplified fragment in the denaturing gel. This melting decreases the electrophoretic mobility of the DNA fragment, separating it from the other fragments in the gel matrix. The critical concentration of the denaturing agents at which a fragment first melts is dictated by the sequence variations within the discrete melting domains. In this way, molecules of the same length but different sequences will migrate to different extents in the same electric field.

DGGE can be used to analyze community diversity without further characterization of the individual species (Muyzer 1999). It yields a banding pattern that is specific to a microbial consortium, where each band is thought to represent a dominant organism in the consortium (Muyzer and Smalla 1998). It is also assumed that relative band intensities will give a rough estimate of the relative species abundance in the sample (Eichner, Erb et al. 1999; Iwamoto, Tani et al. 2000). Therefore, it is possible to monitor changes in a microbial community over time upon exposure to caffeine, and to follow the presence of metabolically active members of the community in response to high caffeine loadings.

Other genetic fingerprinting techniques can also be used to study microbial populations dynamics. A variation to DGGE is thermal gradient gel electrophoresis (TGGE), where DNA fragments are separated by a temperature gradient in the gel. TGGE can be used for similar purposes as DGGE, such as studying microbial population changes in bioremediation treatments (Eichner, Erb et al. 1999). When the sequence of the gene coding for a specific enzyme is known, genes probes can be used to detect the presence of the gene of interest. Oligonucleotides with sequences complementary to short regions of the gene are used as primers for PCR amplification (Mesarch, Nakatsu et al. 2000). Genes coding for dehalogenases have been detected in kraft pulp mill effluents using this

technique (Fortin, Fulthorpe et al. 1998). Terminal restriction fragment length polymorphism (T-RFLP) is another technique used to characterize microbial diversity. The technique relies on the use of PCR in which one primer was fluorescently labeled at the 5' end and was used to amplify a selected region of bacterial genes encoding 16S rRNA (Liu, Marsh et al. 1997). PCR products were digested with restriction enzymes, and the fluorescently labeled terminal restriction fragments sequenced. Computer analysis of T-RFLP can allow a classification of bacterial strains present in a microbial consortium. Population changes during bioremediation of an oil spill were monitored by the measurement of lipid biomarkers such as phospholipid fatty acid analysis (PLFA), combined with DGGE (Macnaugton, Stephen et al. 1999). Another technique allowing the study of the distribution of bacterial species within a defined environment is fluorescent *in situ* hybridization (FISH), where tagged DNA oligomers are used as probes targeting intact microbial communities (Schneegurt and Kulpa 1998).

1.5.4. Applications of community analyses

Genetic fingerprinting using DGGE has been applied to a number of studies. The most common approach is to amplify the 16S rDNA from the entire community, separate the mixture using DGGE, and finally to sequence the bands of interest on the resulting banding profile. This leads to direct identification of the predominant bacterial species present in the bacterial communities studied (Muyzer, De Waal et al. 1993; Vallaeys, Topp et al. 1997; Juck, Charles et al. 2000). Iwamoto *et al.* (2000) used DGGE to monitor the impact of an *in situ* biostimulation treatment on a groundwater bacterial community by injecting methane as a stimulus for trichloroethylene (TCE) degrading-bacteria. Groundwater samples were run on DGGE and the banding patterns analyzed using the Shannon index of bacterial diversity, which provides an indication of bacterial diversity within a community (Eichner, Erb et al. 1999). Other researchers have used DGGE to monitor changes in a microbial population during bioremediation of an oil spill. Data obtained from sequencing DGGE bands was used to perform a dendogram analysis, where relationships of sequences retrieved from the gel were attributed to known

microorganisms (Macnaugton, Stephen et al. 1999). The effects of herbicides on microbial communities were also studied using this approach (El Fantroussi, Verschuere et al. 1999). Here again, dominant bands were excised from the gel and sequenced for species identification. A different approach was used by (Santegoeds, Ferdelman et al. 1998) to study population dynamics of sulfate-reducing populations in biofilms. They used hybridization analysis for DGGE, with probes targeted for specific sulfate-reducing species.

Determining similarities between banding patterns is a difficult task. A number of approaches have been used, with the most successful being related to the application of multivariate analyses (MVA). In one study, banding patterns were also analyzed for similarity by using two similarity coefficients, the coefficient of Jaccard, used to determine a proportionality index between bands of the same lane, and the area-sensitive coefficient, used to detect matching bands in between lanes (El Fantroussi, Verschuere et al. 1999). In another work, banding patterns were analyzed by multidimensional scaling analysis (MDS), a mathematical method which generates a spatial configuration map where proximity between data points reflect the relationship between the underlying variables (Iwamoto, Tani et al. 2000). A number of studies have used principal component analysis (PCA) to detect relationships amongst banding patterns on DGGE. For instance, changes in a microbial consortium during a biostimulation treatment of an oil spill were assessed using this technique (Ogino, Koshikawa et al. 2001).

2. OBJECTIVES

The objective of this study was to selectively remove caffeine from a complex mixture, using *Pseudomonas putida* IF-3. Specific goals were:

- To achieve total caffeine removal;
- To determine the caffeine degradation potential with pure cultures in presence of other nutrient sources;
- To maximize selective caffeine removal while minimizing depletion of other nutrient sources;
- To study the effects of caffeine loading on mixed cultures;
- To monitor the health of microbial consortia by genetic fingerprinting.

3. MATERIALS AND METHODS

3.1. CULTURES

Organisms used in this study were obtained from the sources described in Table 3-1. *Escherichia coli* BL21(DE3), *Rhodococcus rhodochrous* ATCC 21766 and *Pseudomonas putida* IF-3 cultures were initially grown in shake flasks at 30°C on Luria-Bertani (LB) medium (Table 3-2). A volume of 150 mL of medium was used in all cases, and flasks were shaken at 200 RPM. The pH of the medium was adjusted to 7.0 by addition of concentrated HCl prior to autoclaving. Cultures were then plated on Luria-Bertani agar plates, consisting of LB medium to which was added 2% (w/v) agar prior to autoclaving. Single colonies were selected from the agar plates, streaked again and stored at 4°C for up to two months.

Organism	Gram stain	Source
Pseudomonas putida IF-3	-	(Koide 1996)
Escherichia coli BL21(DE3)	-	(Derman, Prinz et al. 1993)
Rhodococcus rhodochrous ATCC 21766	+	ATCC

Table 3-1: Organisms used in this study.

Component	g/L
Bactotryptone	10
Yeast extract	5
NaCl	10

Table 3-2: Luria-Bertani (LB) medium.

Mixed cultures used in this study were obtained from samples of activated sludge obtained from a municipal wastewater treatment plant (St-Canut, Québec). They were used for reactor work within 24 hours of sampling and were therefore not cultured in the laboratory for long-term storage.

3.2. CULTURE CONDITIONS

Pseudomonas putida IF-3 was grown on caffeine growth medium in which caffeine was the sole source of carbon and nitrogen (Table 3-3). Glucose was added as the supplemental carbon source and ammonium sulfate was used as the supplemental nitrogen source, where indicated in the text.

Component	g/L
Calcium chloride	0.08
Potassium chloride	0.37
Magnesium sulphate (heptahydrate)	0.1
Potassium phosphate (monobasic)	0.67
Sodium phosphate (dibasic)	0.71
Ferric chloride	0.005
Caffeine	5
	µg/L
Boric acid	10
Cobaltous nitrate (hexahydrate)	10
Copper sulphate	10
Manganous sulphate (monohydrate)	10
Sodium molybdate (dihydrate)	10
Zinc sulphate	10

Table 3-3: Caffeine growth medium.

Microbial populations from activated sludge were cultured at 30°C on an undefined sludge medium as described in table 3-4 (Nitschke, Wagner et al. 1996).

Component	mg/L
Peptone	73
Beef extract	51
Urea	14
Sodium chloride	3.2
Potassium phosphate (dibasic)	12.9
Sodium bicarbonate	90
Tap water up to 1L	

Table 3-4: Activated sludge growth medium.

3.3. BIOREACTOR

The bioreactor used in this study was a 4L stainless steel vessel with a 2L working volume (Figure 3-1). The reactor offgas carbon dioxide was measured using an Oxymax 451 Series analyzer. Dissolved oxygen (DO) was monitored with an Ingold probe. A four-blade impeller with a 7.5 cm diameter driven by a variable speed mixer (Caframo model RZR1) set to 850 RPM was used for mixing. Air was regulated to the reactor using a gas flow controller coupled to the CO_2 analyzer. Air was dispersed through a rotometer, a glass wool air filter, and bubbled through the bottom of the reactor, below the impeller at a flow rate of 1.0 L/min. Offgas was passed through a condenser and then a glass wool air filter, and finally sampled by the CO_2 analyzer through an air dryer. Temperature was kept constant at 30°C ±0.1°C in the bioreactor using a thermocouple and a temperature controller (Omega Instrument Co., model 9000) with deadband control.

Medium was introduced in the vessel by gravity, through a stainless steel solenoid valve located on the top of the bioreactor. Draining was achieved by the same process, through another valve located at the bottom of the reactor, and the waste was collected in a 10L bottle. The valves were controlled *via* computer using a data acquisition board and associated control system. Software was written in Visual Basic (Softwire Technology, Palo Alto, USA).

"Cycling" of the reactor consisted of draining half of the liquid volume (1L) from the reactor, after turning off aeration and mixing, and replacing the removed volume with fresh medium. Mixing and aeration were then reactivated. A "cycle" consists of the time period bracketed by "cycling" events. The end of the cycle is usually determined based on the extent of the completion of the biological processes within the reactor, as inferred by carbon dioxide evolution rate.

Samples were taken through a sample port, equipped with a 50 mL glass vial. The first 10 mL volume of each sample was discarded, to account for the dead volume in the sample

line. Samples of 10-30 mL were drawn into the glass vial, and either stored at –20°C or analyzed immediately, as described in the text.

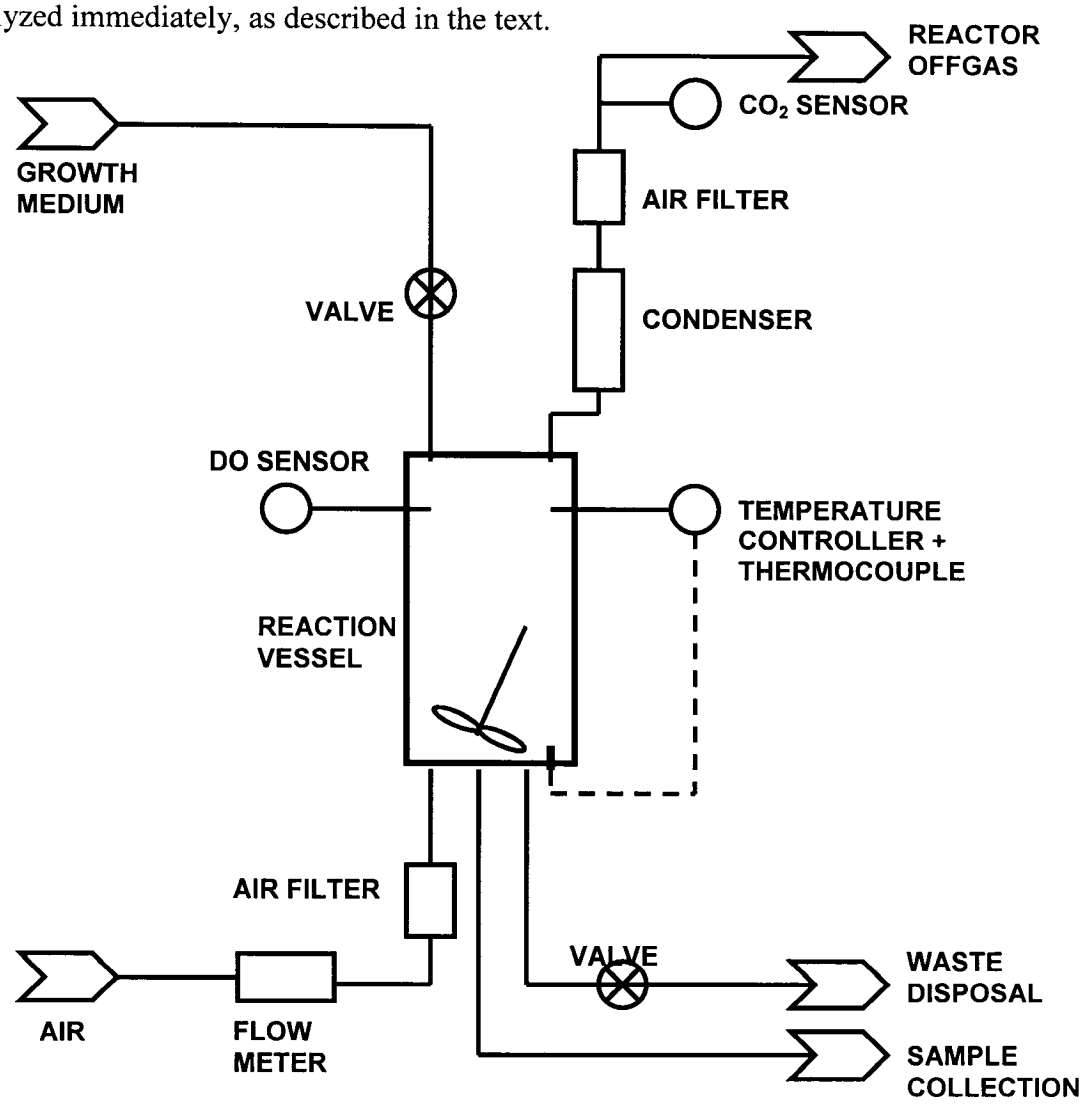

Figure 3-1: Fed-batch bioreactor instrument diagram.

3.4. ANALYTICAL PROCEDURES

3.4.1. Biomass

Biomass from the reactor samples was measured either by dry weight or by absorbance. For the dry weight experiments, a 25 mL volume from the reactor was centrifuged at 10,000 x g for 10 minutes at 4°C (Model B-22M, International Equipment Co., Needham

Heights, USA,). The supernatant was discarded and the cells were washed once by addition of 25 ml of Tris-Cl buffer pH 8.0, and centrifuged again for 10 minutes. The supernatant was discarded and the pellet resuspended to 10 mL in distilled H_2O. The sample was then loaded into a desiccated, tared weighing dish. The dishes were dried at 105°C for 6 hours. The weighing dish was weighed again using an analytical balance with a weighing accuracy of +/- 0.0001 g (Denver Instrument Co., model TR-204). The net difference in weight was divided by the sample volume, to yield a dry weight in g/L.

For mixed cultures, due to the low cell density maintained in the reactor, the dry weight assay could not be used. Therefore, optical density readings at 560 nm were used to measure biomass, using a Bio 100 UV spectrophotometer (Varian Inc., Palo Alto, USA). A 2 mL sample from the reactor was centrifuged at 10,000 x g for 5 minutes at 4°C (Micromax RF microcentrifuge, International Equipment Co.). The supernatant was discarded and the pellet resuspended in 2 mL of a 1M TRIS-Cl buffer (pH 8.0). Buffer was used as the reference solution, and samples were diluted if necessary to obtain an absorbance reading below 1.5 AU.

This technique was also used for pure culture samples in parallel with the dry weight assay to build a calibration curve relating absorbance and dry weight. A calibration curve of absorbance versus measured dry weight for *Pseudomonas putida* IF-3 is provided in figure 3-2.

3.4.2. Dissolved oxygen

As an indicator of bacterial metabolism, dissolved oxygen was measured using an Ingold autoclavable DO probe (Cole-Parmer, Model E05644-02) in conjunction with a Cole-Parmer transmitter (Model 01971-00). The probe was calibrated prior to autoclaving using a two-point calibration method performed at 30°C. The zero point was taken as the signal given when the probe was disconnected from the transmitter. The saturation point was defined as the response of the probe in distilled water saturated with air. Saturation

was achieved by bubbling air in distilled water until the probe response remained at its highest value. The probe was then autoclaved once fixed in the reactor body.

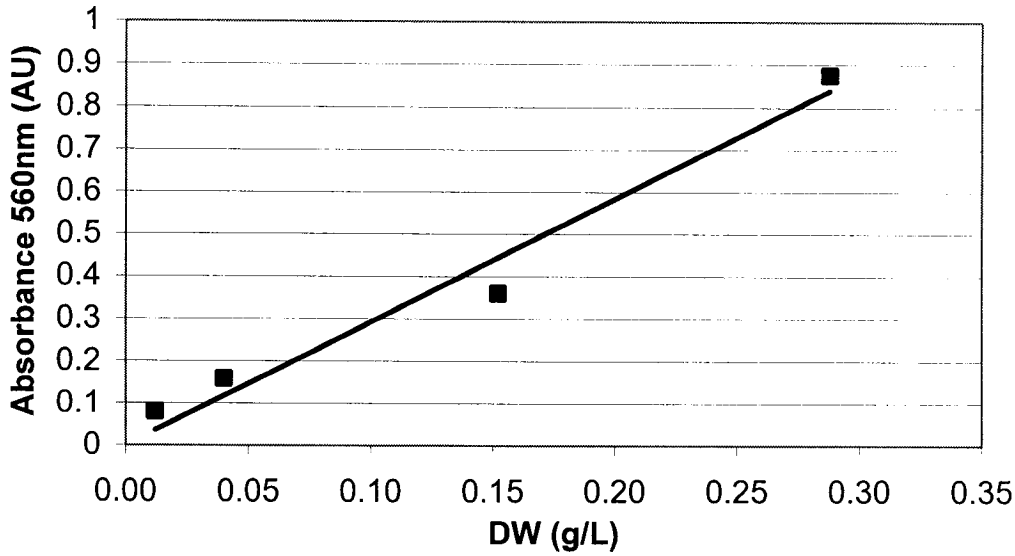

Figure 3-2: Calibration curve relating dry weight to Absorbance measurements for *Pseudomonas putida* IF-3. The trendline was used to determine the correlation factor between absorbance at 560 nm and cell dry weight.

3.4.3. Carbon dioxide evolution

Carbon dioxide in the reactor offgas was measured with an Oxymax 451 series analyzer. The unit was coupled to a gas flow control valve (Columbia Instrument Co.) and an Oxymax MS-DOS based data acquisition and control system. The system was not calibrated, and therefore yielded only qualitative data about the carbon dioxide evolution and metabolism of the microorganisms in the bioreactor.

3.4.4. Caffeine

Caffeine was measured by gas chromatography using a Varian CP 3800 GC equipped with a flame ionization detector (FID). A 1 mL volume of the supernatant broth from a reactor sample was contacted with 1 mL of a mixture of chloroform containing pentadecane at 750 ppm as the internal standard. The sample was then mixed using a Vortex Genie Model 2 (Fisher Scientific, Hampton, USA) for about 30 seconds. The phases were allowed to separate for 2 minutes. A 0.5 µL sample of the organic phase was then injected in the gas chromatograph. Separation was achieved with a SPB-5 column (Supelco Inc., St-Louis, USA) with an immobilized phase consisting of poly(5% diphenyl/ 95% dimethylsiloxane). The injector temperature was maintained at 250°C. A split ratio of 10:1 was used, with a column flow of 4 ml/min. The oven was at 30°C initially, and the temperature ramped up at a rate of 20°C/min to a final temperature of 320°C, for a total run time of 14.5 minutes. The detector temperature was kept at 320°C. Figure 3-3 shows the calibration curve generated using standard caffeine solutions. Caffeine concentration are shown in parts per million, on a weight per volume basis. To test for repeatability, the method was run five times with the same sample, at a fixed concentration of 0.25 g/L. The standard deviation obtained was 8.14×10^{-3}, with 11% variability, which indicated good repeatability. A two-point calibration was done with standard solutions every time measurements were done.

3.4.5. Glucose

The glucose hexokinase assay (Thermo DMA Inc., St-Louis, USA) was used to quantify the glucose concentrations in the bioreactor broth. A 10 µL sample of the cell free broth was added to 1 mL of the glucose reagent, and vortexed for 5 seconds before incubating at 37°C for 3 minutes. Absorbance was then read at 340 nm. The reference cell contained 1 mL of the glucose reagent and the blank consisted of 1 mL of the glucose reagent to which was added 10 µL of distilled H_2O. A calibration curve relating absorbance at 340 nm to glucose concentration of standard solutions is shown in figure 3-4. Repeatability

and error were tested by running a standard solution at 0.25 g/L glucose each time the assay was used. The average of 12 measurements was 0.256 g/L with a standard deviation of 7.78 x 10^{-3} and 7% variability.

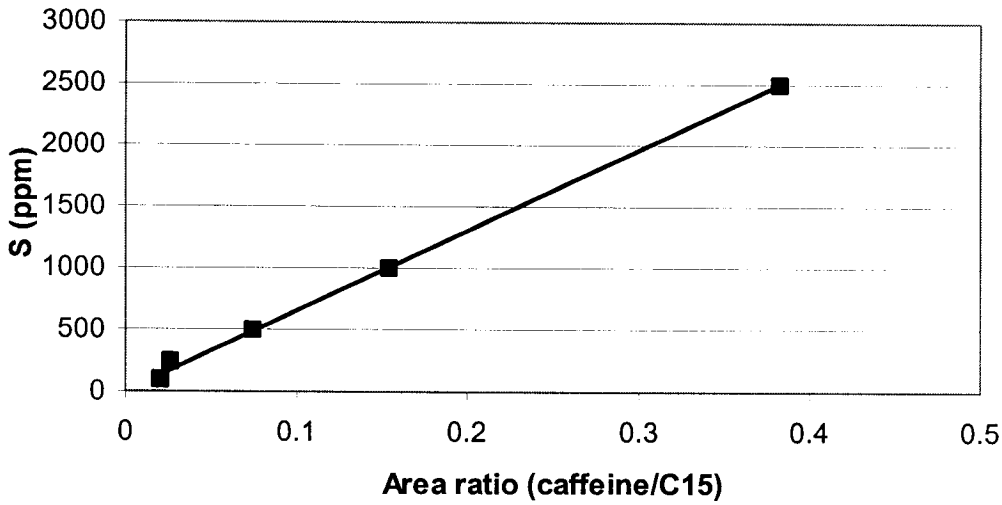

Figure 3-3: Calibration curve for caffeine in the Gas Chromatograph, with C15 as internal standard. The trendline was used to determine the correlation between caffeine concentration and area ratio on the chromatogram.

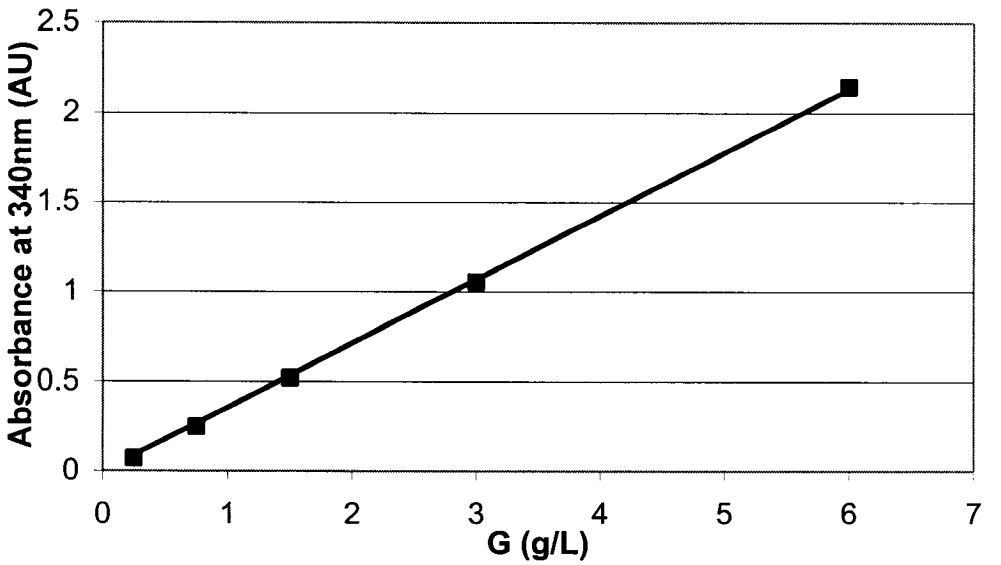

Figure 3-4: Calibration curve for the glucose hexokinase enzymatic assay. The trendline was used to determine the correlation between absorbance at 340 nm and glucose concentration.

3.4.6. Ammonium ion

Nitrogen released as ammonium in the culture broth was quantified by Conway diffusion (Conway 1957). A 0.5 mL of cell free culture broth was added to the outside annular well of the diffusion apparatus. A 0.5 mL volume of a saturated sodium bicarbonate solution was also added to the outside well, without mixing the two solutions. A 0.5 mL volume of the pink indicator solution (1% boric acid, 0.033% bromocresol green, 0.066% methyl red) was added in the inner well of the apparatus. The lid, sealed with silicone grease, was then pressed on and the two solutions in the outer well were mixed. After incubation overnight, the indicator solution was titrated back to pink with 0.02N HCl using a 2 mL (+/- 0.001 mL) microsyringe (Gilmont Instruments, Barrington, USA). A calibration curve relating ammonium concentrations of standard ammonium sulfate solutions with the volume of HCl needed for the titration was created (figure 3-5) and used to determine ammonium ion concentrations in the bioreactor samples.

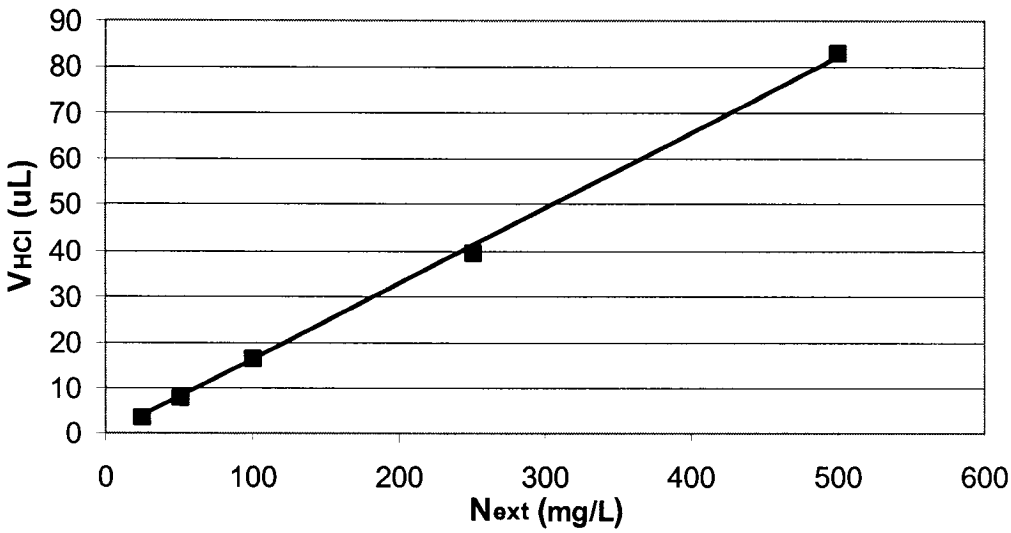

Figure 3-5: Calibration curve for Conway diffusion assay for ammonium ion quantification. The trendline was used to determine the correlation between the volume of HCl 0.02N added and the concentration of ammonium sulfate. N_{ext} represents the ammonium sulfate concentration.

Repeatability and error were tested, with a standard solution of 250 mg/L ammonium sulfate. The method proved to be reliable, with less than 2% error on the average of 10 samples. The percent error was calculated by subtracting the measured concentration from the standard concentration, and by dividing the result by the standard concentration.

3.5. MOLECULAR BIOLOGY

3.5.1. Cell lysis

Lysis of the bacterial cells was achieved by shearing (Nebulizer, Glas-Col Inc., Terre Haute, USA). A 10-20 mL sample from the bioreactor was first centrifuged at 10,000 x g for 10 minutes at 4°C. The supernatant was discarded, and the pellet resuspended in 5 mL of distilled water. The cells were then lysed by shearing in the Nebulizer for 15 minutes, using nitrogen at a pressure of 110 psi, in the closed-cycle mode for sample recycling. The lysed cell products were then centrifuged at 10,000 x g for 10 minutes at 4°C, and the supernatant collected using a Pipetman P1000 (Gilson Inc.). The cell-free extract was stored at –20°C if necessary.

3.5.2. DNA extraction

Phenol solution (pH 8.0, Sigma-Aldrich Inc., St-Louis, USA) and chloroform:isoamyl alcohol (24:1) were added to the cell free extract in a volume ratio of 2:1:1. This procedure was done to extract the proteins. The solution was mixed by inversion 6 times, before centrifugation for 5 minutes at 10,000 x g and 4°C. Following centrifugation, the aqueous phase containing the DNA and RNA was carefully pipetted into a clean tube, without touching the interface between both phases, which contained cell debris and other impurities. To the aqueous phase collected, a full volume of the chloroform:isoamyl alcohol mixture was added for a second extraction. The sample was mixed and centrifuged as described above. The aqueous phase was then pipetted into a clean tube, to

which was added 5M NaCl to a final concentration of 0.5M. Two volumes of isopropanol were added to this solution. This was carried out in order the precipitate the DNA. The sample was mixed by inversion 6 times before incubating for either 90 minutes at –70°C or overnight at –20°C. Following incubation, the sample was centrifuged for 20 minutes at 10,000 x g and 4°C. The supernatant was discarded and the pellet was washed with 1 mL of 70% ethanol by centrifugation for 10 minutes, at 10,000 x g and 4°C to clean the DNA pellet of all remaining salts. The ethanol was then discarded and the pellet air dried until all the remaining ethanol evaporated. The DNA pellet was resuspended in DNase, RNase free distilled water (Sigma-Aldrich) and stored at –20°C.

3.5.3. DNA purity and quantification

The ratio of the absorbance at 260nm over that at 280nm was used as an indicator of the purity of the DNA preparation. Samples were diluted 200-fold with distilled water, and absorbances were read at 260nm and 280nm, against distilled water. A ratio of absorbances between 1.8 and 2.0 indicates that the DNA sample is of good purity. A ratio below 1.8 indicates the presence of proteins and other contaminants, while a ratio greater than 2.0 means that there are still significant levels of RNA in the DNA preparation (Sambrook, Fritsch et al. 1989).

Provided the purity was adequate, the extracted DNA was quantified using absorbance at 260nm, using a calibration factor of 1 absorbance unit at 260nm per 50 ng double-stranded DNA / μL (Sambrook, Fritsch et al. 1989).

Another technique was used to quantify DNA samples at low concentrations (<20 μg/mL DNA). The "Saran Wrap" method consisted of quantifying fluorescent, ethidium bromide-stained DNA, by visualization under UV light at a 254nm wavelength (Sambrook, Fritsch et al. 1989). A sheet of Saran Wrap was placed over the glass plate of the UV transilluminator (Bio-Rad Inc., Carlsbad, USA). 2 μL volumes of the DNA samples were spotted on the Saran Wrap, along with 2 μL volumes of a series of DNA

standards of known concentrations. To each spot was added an equal volume of 2 μg/μL ethidium bromide in TE buffer pH 8.0 (10 mM Tris-Cl, 1 mM EDTA). Samples were mixed by pipetting up and down with the micropipettor. A picture was then taken under UV light, and using the range of DNA standards, a calibration curve was constructed relating the intensity of the spots to the respective DNA concentrations (Figure 3-6). However, only the linear portion of the curve could be used for quantification, therefore leaving only a small range to work with (0 to 5 ng/μL). Unfortunately, the method proved to have a high variability between samples, since it was observed that the standard solutions gave different normalized intensity values during each series of analyses, making the technique of limited value.

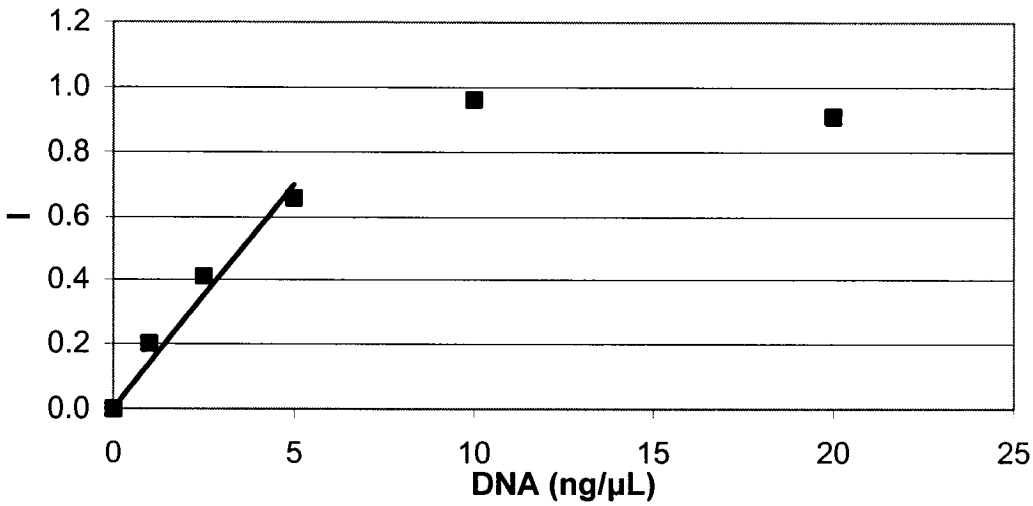

Figure 3-6: Calibration curve for ethidium bromide fluorescent quantification of DNA samples. The trendline was used to determine the correlation between intensity and DNA concentration.

3.5.4. Purification of activated sludge samples

Using the method outlined above, when DNA is extracted from activated sludge samples, other contaminants, such as humic acids, may be co-extracted. These contaminants might interfere with the absorbance reading at 260 nm, and can also inhibit the action of the *Taq* DNA polymerase in the PCR reaction (Young, Burghoff et al. 1993). Purification of the

DNA preparation can be achieved by migration of a DNA sample in a 1.5% agarose/ 2% polyvinylpolypyrolidone (PVPP) (wt/vol) gel in TAE 1X buffer (0.04 M Tris-acetate, 0.001M EDTA), using the Mini Sub-Cell GT and Wide Mini Sub-Cell GT electrophoresis systems (Bio-Rad Inc.). The PVPP forms hydrogen bonds with phenolic compounds, such as those found in humic acids, therefore retarding the electrophoretic migration of the contaminants. In the current work, a 15 µl sample of the DNA preparation was mixed with 3 µl of 6X loading buffer (0.25% bromophenol blue, 0.25% xylene cyanol FF and 30% glycerol) and loaded onto the gel. Migration was carried out at 80V for 70 minutes at room temperature using a PowerPac power supply (Bio-Rad Inc., models 300 and 1000). The gel was stained by incubating in a 50 µg/ml ethidium bromide solution for 2 minutes, and then destained for 2 minutes in 1 mM $MgSO_4$. Agitation during staining and destaining was achieved with an Orbitron rotator II gyratory plaque (Model 260250, Boekel Scientific, Feasterville, USA). The gel was then visualized under UV light with a transilluminator (Bio-Rad Inc.) and the genomic DNA bands were extracted from the gel using a sharp blade. Genomic DNA retrieved from the gel matrix was extracted using the QIAquick gel extraction kit (QIAGEN Inc, Mississauga, Canada) following the supplier's instructions. The recovered genomic DNA was quantified as described in section 3.5.3, and stored at –20°C.

3.5.5. Polymerase Chain Reaction (PCR) amplification

The Bio-Rad iCycler thermal cycler equipped with a 96-well reaction module was used for all PCR procedures. A region of 193 bp from the variable V3 region of the 16S rRNA gene (positions 341 to 534 in *Escherichia coli*) was amplified with primers annealing to conserved regions of the 16s rRNA gene. The conserved regions targeted by the primers were common to all species within the bacterial domain (Juck, Charles et al. 2000). The nucleotide sequences of the forward primer was: 5'- CGC CCG CCG CGC GCG GGC GGG GCG GGG GCA CGG GGG GCC TAC GGG AGG CAG CAG –3', and the reverse primer was: 5'- ATT ACC GCG GCT GCT GG –3' (Muyzer, De Waal et al. 1993). The 40 base-pair GC clamp in the forward primer was added to prevent complete

unwinding of the DNA fragment in the denaturing gel. A 250 ng quantity of genomic DNA, 50 pmol of each primer, 200 μmol of each deoxyribonucleoside triphosphate, 0.4 μg BSA, and 5 μL of 10X PCR buffer (500 mM KCl, 15 mM $MgCl_2$, 100 mM Tris-HCl pH 9.0) were added to a 0.2 mL thin wall PCR tube, filled to 49.75 μL with sterile, DNase-free, RNase-free water. Samples were initially denatured for 2 minutes at 94°C in the thermal cycler, after which 0.25 μL (1.25U) *Taq* DNA polymerase (Amersham Biosciences) was added to the reaction mixture. This hot-start technique was performed to minimize non-specific primer annealing to non-target DNA (Muyzer, De Waal et al. 1993). Amplification was carried out for 25 cycles, where each cycle consisted of: denaturation at 94°C for 1 minute, primer annealing at 55°C for 1 minute and strand elongation at 72°C for 1 minute. A final elongation step of 5 minutes at 72°C was allowed after the 25 cycles, before the temperature was decreased to 4°C to stop the reaction.

3.5.6. Agarose gel electrophoresis for PCR verification

In order to verify the efficacy of the PCR amplification, samples were run on a 1.5% (wt/vol) agarose gel in 1X TAE running buffer. A 5 μL volume of the PCR product was mixed with 1 μL of 6X gel loading buffer and loaded onto the gel. Migration was carried out at 80V for 70 minutes at room temperature. Staining of the gel was achieved by soaking the gel in a 50 μg/ml ethidium bromide solution for 5 minutes, and destained for 5 minutes in 1 mM $MgSO_4$ under constant agitation. The gel was then visualized under UV light using a transilluminator equipped with a digital camera. Band analysis was performed with image analysis software (Quantity One, Bio-Rad Inc.).

3.5.7. Denaturing gradient gel electrophoresis (DGGE)

DGGE was performed using the Dcode universal mutation detection system (Bio-Rad Inc.). A 8% (wt/vol) polyacrylamide gel in 1X TAE buffer was cast using a gradient delivery system (Bio-Rad, model 475) with a 30 to 60% denaturing gradient formed with

8% (wt/vol) acrylamide stock solutions (acrylamide- *N,N'*-methylenebisacrylamide, 37,5:1) and 7M urea and 40% deionized formamide as denaturing agents (Sigma-Aldrich Inc). This range was based on optimized conditions for separating the bands of interest (Data not shown). A 30 µL volume of the PCR products was mixed with 6 µl 6X gel loading buffer (see section 3.5.4) and loaded directly onto the gel. Electrophoresis was performed at a constant voltage of 160V for 6 hr at a constant temperature of 60°C. Staining, destaining, visualization and banding pattern analysis of the gel were done as described in section 3.5.6.

4. RESULTS

4.1. CAFFEINE CONSUMPTION BY *P. Putida* IF-3 – SCREENING STUDIES

4.1.1. Growth on caffeine as the sole source of carbon and nitrogen

Pseudomonas putida IF-3 was first grown on caffeine as the sole source of carbon and nitrogen in the bioreactor. Complete caffeine removal was observed for all cycles. As mentioned previously (Section 3.3), a cycle consisted of filling the reactor, from the 50% to the 100% level with growth medium, allowing biological reactions to occur, and draining half of the reactor volume. A typical result is shown in figure 4-1. Growth yields were calculated for five subsequent cycles, and averaged to give a yield on caffeine of 0.135 ± 0.03 g X/g S (Refer to section 7 for nomenclature). Caffeine concentrations were varied between 0.1 and 10.0 g/L, and it was determined that caffeine concentrations should be kept below 5.0 g/L to prevent high biomass formation that could lead to clogging of the aeration port. Carbon dioxide evolution was measured as the percent difference in carbon dioxide concentrations between the inlet air and the reactor offgas (ΔCO_2). This parameter was used for gross characterization of the metabolic activity of the culture. In figure 4-1, carbon dioxide evolution shows a single large peak, which can be directly linked to the active metabolic state of the growing culture. Average rates were calculated using data gathered immediately after caffeine consumption was observed (Equation 4-1). Thus, data in the lag phase were not considered. Biomass values used to calculate rates were determined by taking the biomass value at $\Delta t = ½$, where Δt was defined as the time required for substrate depletion. Using this equation, average degradation rates were calculated from these data for four subsequent cycles, resulting in a value of 0.976 ± 0.405 g S/ g X-h.

Equation 4-1:

$$r_S = \frac{-\Delta S}{\Delta t} \frac{1}{X\big|_{\Delta t/2}}$$

4.1.2. Addition of supplemental carbon source

In order to assess the capacity of the microorganism to target caffeine when other nutrient sources are present, glucose was added to the culture medium. Glucose was added at higher concentrations than caffeine, at a ratio of 2:1, on a molar basis, for most cycles. Both carbon substrates were degraded completely (Figure 4-2). As expected, glucose was degraded at a higher rate than caffeine. The average rates of degradation were 1.11 ± 0.33 g G / g X-h for glucose, and 0.22 ± 0.18 g S /g X-h for caffeine. However, figure 4-2 shows that caffeine was degraded concomitantly with glucose. Here again, carbon dioxide evolution shows only one broad peak. Caffeine breakdown was associated with nitrogen release, measured by Conway diffusion. The caffeine molecule ($C_{10}H_8O_2N_4$) has a molar carbon to nitrogen ratio of 5:2. Based on the empirical formula for biomass, $CH_{1.79}O_{0.5}N_{0.2}$ (Doran 1995), the C:N ratio associated with biomass formation is 10:2. Moreover, with equimolar concentrations of both carbon substrates, the carbon to nitrogen ratio increases to 7:2. Therefore, without even considering other carbon sinks, it is apparent that the culture was carbon-limited and led to the observed nitrogen accumulation in the culture broth.

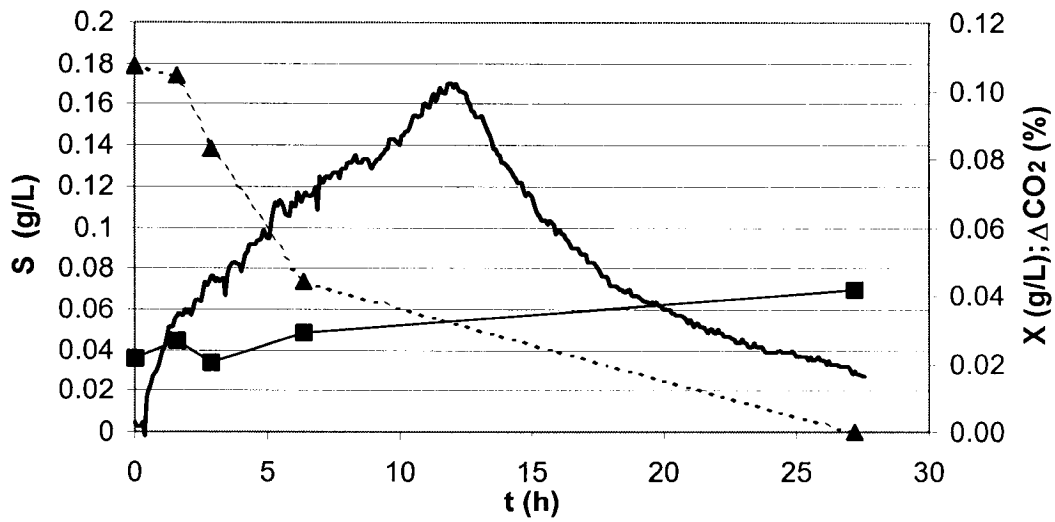

Figure 4-1: Caffeine degradation (-▲-) and biomass formation (-■-) of *Pseudomonas putida* IF-3 grown on caffeine as sole source of carbon and nitrogen. The solid line with no data points represents carbon dioxide evolution.

The increase in nitrogen measured at 2.25h is associated with caffeine depletion (Figure 4-2). The nitrogen remains associated with the breakdown products of caffeine for a period after the depletion of the caffeine molecule, accounting for the lag between when caffeine is degraded and nitrogen accumulation is noted. Increasing the glucose concentrations allowed all the excess nitrogen present in the culture broth to be consumed (Data not shown).

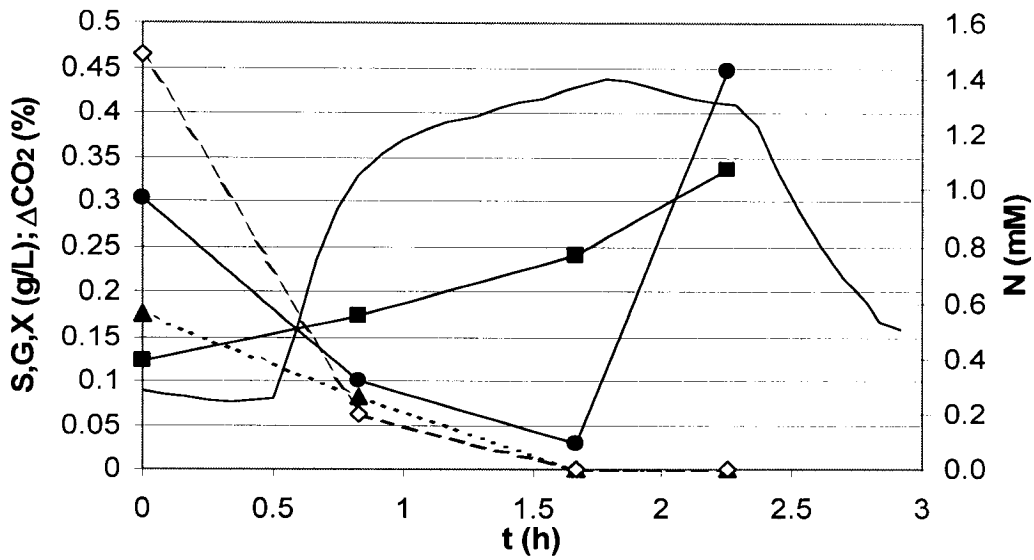

Figure 4-2: Caffeine (-▲-), glucose (-◊-) and biomass (—■—) concentrations during *Pseudomonas putida* IF-3 growth on caffeine and glucose. Ammonium concentrations (—●—) were monitored by Conway diffusion. The solid line represents carbon dioxide evolution.

4.1.3. Addition of supplemental nitrogen source

Ammonium sulfate was added to the culture medium to allow the bacteria to grow independently on either carbon substrate, without any dependence on the caffeine molecule for nitrogen. Caffeine and glucose were again removed completely from the broth, although total caffeine removal required more time. Figure 4-3 shows a typical cycle with caffeine, glucose and ammonium sulfate. The carbon dioxide pattern demonstrates two small peaks followed by a broader peak tailing off towards the end of

the cycle. Nitrogen was again released in the culture broth long after caffeine was completely degraded, indicating carbon limitation. Substrate removal rates were lower for both carbon substrates than those calculated for growth on caffeine and glucose only. Degradation rates obtained were 0.091 ± 0.058 g S / g X-h and 0.418 ± 0.243 g G / g X-h, respectively, based on equation 4-1.

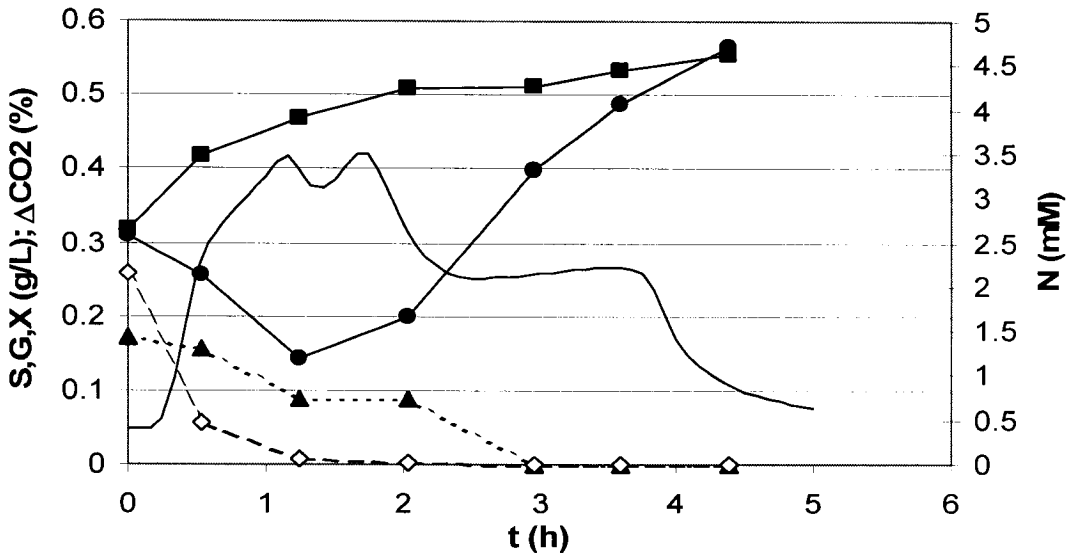

Figure 4-3: Caffeine (-▲-), glucose (-◊-) and biomass (-■-) concentrations during *Pseudomonas putida* IF-3 growth on caffeine, glucose and ammonium sulfate. Ammonium concentrations (-●-) were monitored by Conway diffusion. The solid line represents carbon dioxide evolution.

Table 4-1 summarizes all degradation rates calculated from cycles in the bioreactor experiments. Variability in the data was determined by calculating a 95% confidence interval. As can be seen in table 4-1, there is a large spread in the data for both caffeine and glucose rates, when *P. putida* IF-3 was grown on caffeine and glucose.

[Initial]							
S g/L	**G** g/L	**N_{ext}** g/L	**ΔX** g/L	**r_S** g S / g-h	**Average r_S** g S / g-h	**r_G** g G / g-h	**Average r_G** g G / g-h
0.168	-	-	0.023	0.621		-	-
0.179	-	-	0.020	0.647		-	-
0.150	-	-	0.016	1.011		-	-
0.182	-	-	0.025	1.625	0.976 +/- 0.405	-	-
0.159	0.451	-	0.255	0.073		1.507	
0.165	0.269	-	0.254	0.057		0.599	
0.455	0.521	-	0.529	0.19		0.977	
0.224	0.529	-	0.548	0.141		1.067	
0.169	0.315	-	0.159	0.279		0.997	
0.175	0.464	-	0.213	0.579	0.221 +/- 0.176	1.536	1.114 +/- 0.325
0.127	0.278	0.067	0.100	0.091		0.718	
0.173	0.259	0.067	0.237	0.141		0.308	
0.146	0.196	0.067	0.173	0.039	0.091 +/- 0.058	0.229	0.418 +/- 0.243

Table 4-1: Degradation rates calculated for bioreactor experiments. All experiments were run in carbon-limiting conditions.

4.2. CAFFEINE CONSUMPTION BY *P. putida* IF-3 – DETAILED STUDY

Based on the information gathered from the screening studies, a series of shake flask experiments were performed with different substrate concentrations to further quantify the effect of nutrient limitation on the metabolism of *P. putida* IF-3. Table 4-2 presents the conditions used for the experiments. The limiting nutrient was determined by stoichiometric analysis based on the following equation:

Equation 4-2: $aC_8H_{10}O_2N_4 + bC_6H_{12}O_6 + cO_2 + hNH_4^+ \rightarrow dCH_{1.79}O_{0.5}N_{0.2} + eCO_2 + fH_2O$

caffeine glucose ammonium biomass

From the experimental conditions (Table 4-2) and estimates of the growth yields from the screening experiments, the limiting nutrient was estimated (Appendix I). The results are shown in table 4-2. The percent nutrient in excess (E) was defined as:

Equation 4-3: $E = 100 \times (1 - [A]/[B])$

where [A] represents the stoichiometric amount of nutrient needed to close the mass balance and [B] represents the amount of nutrient added. Ratios were determined with the mass balance equations (Appendix I).

Flask no.	S g/L	G g/L	Next g/L	Limiting nutrient	% Excess nutrient
1-2	2			C-limited	95
3-4	0.25	2		C-limited	5
5-6		1	0.5	C-limited	69
7-8		1	0.1	N-limited	34
9	0	0	0	Abiotic	

Table 4-2: Conditions used in shake flask experiments. The medium was used as described in table 3-3 and supplemented with the appropriate carbon and nitrogen source.

4.2.1. Carbon limited culture

Under all carbon limited conditions, both caffeine and glucose were completely depleted (Figures 4-4, 4-5 and 4-6). There were significant amounts of free nitrogen left in the culture broth, as expected, for both conditions where there was a large amount of excess nitrogen (95% excess nitrogen for flasks 1-2 (Figure 4-4), and 69% excess nitrogen for flasks 5-6 (Figure 4-6)). As can be seen in figure 4-4, when grown on caffeine as sole source of carbon and nitrogen, the ammonium concentration increased after all carbon was depleted. This transient was not observed when *P. putida* was grown in carbon-limiting conditions on glucose and ammonium sulfate (Figure 4-6). More biomass was formed when glucose was included as a source of carbon, which was expected, since the biomass yield of *Pseudomonas putida* IF-3 on glucose is higher than the growth yield on caffeine (approximately 0.284 g X / g G for glucose compared to 0.135 g X / g S for caffeine).

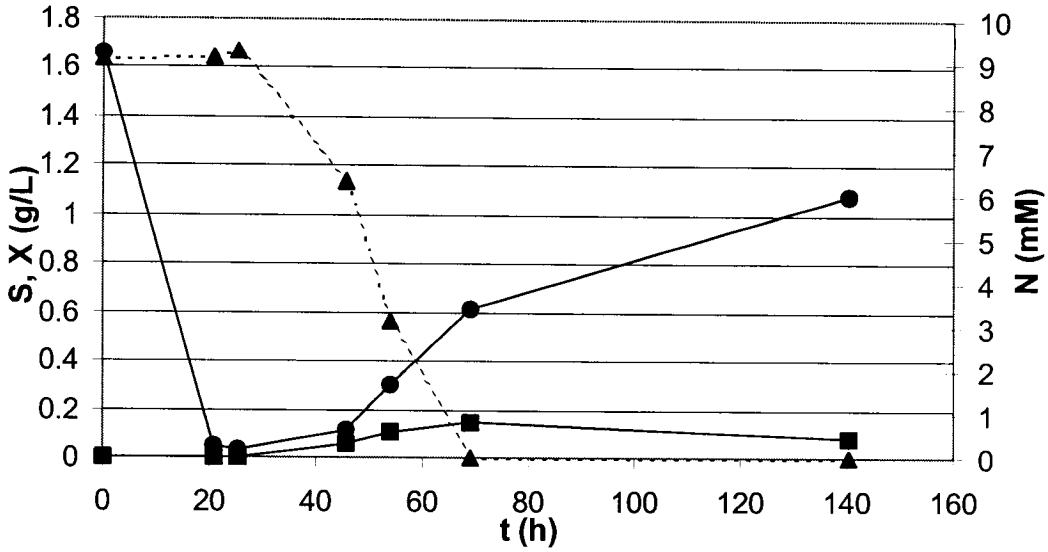

Figure 4-4: Caffeine (-▲-), biomass (-■-) and ammonium (-●-) concentrations during *Pseudomonas putida* IF-3 growth under carbon limitation (flask 2).

Growth on glucose and caffeine in cultures where nitrogen was provided in only slight excess (approximately 5%) was also studied (Figure 4-5). Both carbon sources were completely degraded, and little residual ammonium was observed in the culture broth. A peak in ammonium concentration occurred between the 25 and 55-hour marks, which can be attributed to the nitrogen release associated with caffeine breakdown. Ammonium concentrations decreased to low levels as glucose degradation was achieved, suggesting the bacteria used most of the nitrogen released by caffeine for biomass formation.

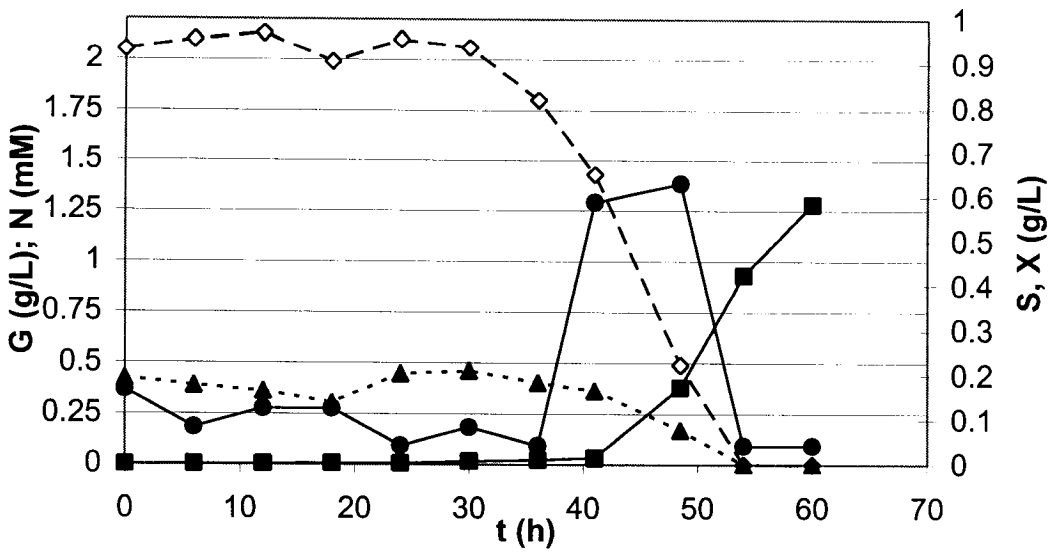

Figure 4-5: Caffeine (-▲-), glucose (-◊-), biomass (-■-) and ammonium (-●-) concentrations during *Pseudomonas putida* IF-3 growth under carbon limitation (flask 4).

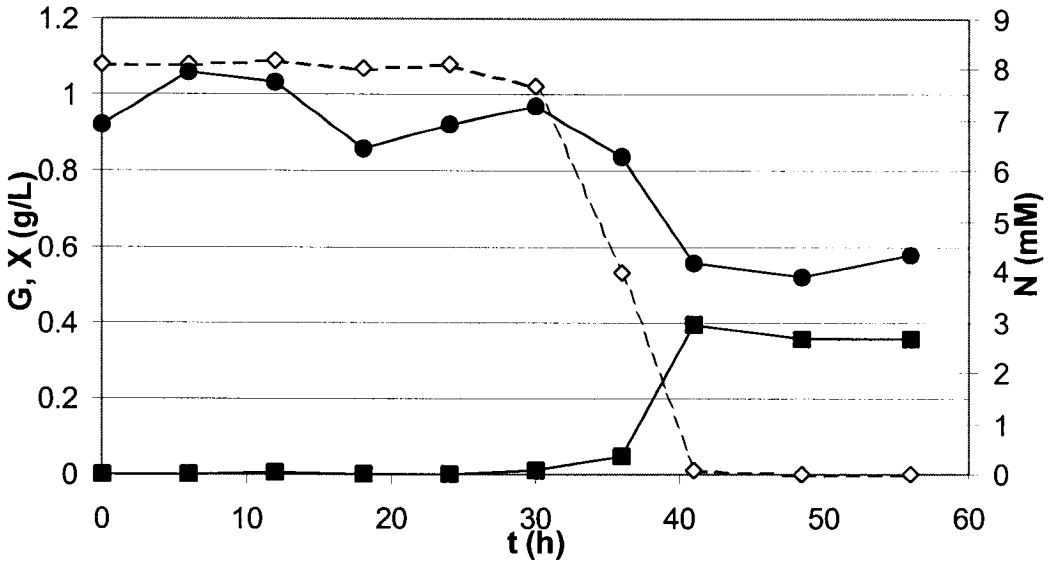

Figure 4-6: Glucose (-◊-), biomass (-■-) and ammonium (-●-) concentrations during *Pseudomonas putida* IF-3 growth under carbon limitation (flask 6).

4.2.2. Nitrogen limited culture

When grown under nitrogen-limiting conditions on glucose and ammonium sulfate, one would expect growth, and therefore carbon uptake, to stop as nitrogen became depleted. However, this was not observed, as can be seen in figure 4-7. Glucose, which was the carbon substrate supplied in excess, was completely removed by the bacteria. Glucose degradation rates obtained were higher than those obtained under carbon limitation for glucose and ammonium sulfate (Table 4-3).

In the abiotic control, no bacterial growth was observed, and caffeine concentrations remained constant (Data not shown).

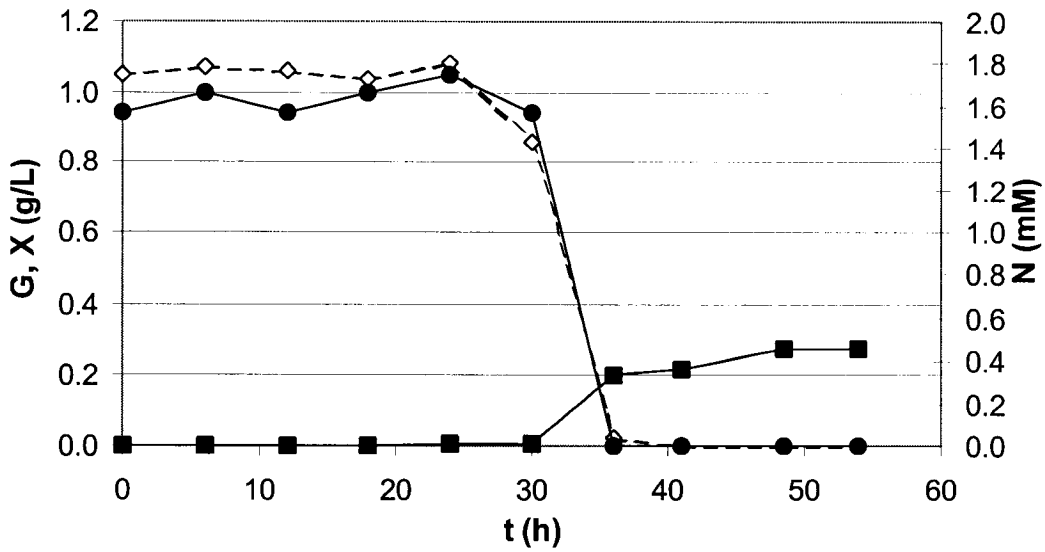

Figure 4-7: Glucose (-◊-), biomass (-■-) and ammonium (-●-) concentrations during *Pseudomonas putida* IF-3 growth under nitrogen limitation (flask 7).

4.2.3. Degradation rates

Substrate removal rates were calculated (see section 4.1.1) for all conditions outlined in table 4-2 and are presented in table 4-3. Caffeine degradation rates significantly

decreased when glucose was added. As for glucose, rates were highest when the culture was grown under nitrogen limitation on ammonium sulfate. The data also suggest faster glucose removal with a more readily available nitrogen source than with caffeine as the sole source of nitrogen.

#	Limiting substrate	S g/L	G g/L	N_{ext} g/L	r_S g S/ g X-h	Average r_S g S/ g X-h	r_G g G/ g X-h	Average r_G g G/ g X-h
1	C	2			0.546	0.517 +/-		
2	C	2			0.487	0.030		
3	C	0.25	2		0.060	0.061 +/-	0.292	0.352 +/-
4	C	0.25	2		0.062	0.001	0.411	0.060
6	C		1	0.5			0.464	0.464
7	N		1	0.1			0.565	0.577 +/-
8	N		1	0.1			0.588	0.010

Table 4-3: Substrate degradation rates calculated for carbon and nitrogen limitation shake flasks experiments. Experimental conditions are described in Table 4-2.

4.3. DENATURING GRADIENT GEL ELECTROPHORESIS (DGGE)

4.3.1. Pure cultures and defined microbial communities

Favourable conditions for denaturing gradient gel electrophoresis (DGGE) were first developed with DNA extracted from pure cultures. The objective was to gather information on the approximate melting conditions of the 16S rRNA fragments of pure cultures, and more specifically *Pseudomonas putida* IF-3, in order to monitor the presence of this organism after incorporation into a mixed culture.

Mixtures of known quantities of *Rhodococcus rhodochrous* and *P. putida* IF-3 were lysed, and subjected to DGGE analysis (see sections 3.5.1 to 3.5.7). Through systematic experimentation, a denaturing gradient of 30-60% was found to provide adequate separation of the fragments. Results obtained from this experiment differed from what is usually accepted in microbial ecology literature, where it is stated that the number of bands in a DGGE banding pattern corresponds to the number of predominant members in

the microbial community (Muyzer and Smalla 1998). It was assumed that each organism would give rise to a single band. As shown in figure 4-8, lane 2 shows a banding pattern comprised of 6 bands, and corresponds to the PCR-amplified fragment of *P. putida* IF-3 (Bands 1, 2, 4, 5, 7 and 8) while lane 1 shows the three-band pattern associated with *R. rhodochrous* (Bands 1, 8 and 9). The reproducibility of the banding patterns between gels was verified by loading the same samples on another gel. Figure 4-11 shows the same *P. putida* IF-3 pattern in lane 1 and the *R. rhodochrous* pattern in lane 3. Lane 2 shows the three-band pattern specific to *E. coli*.

4.3.2. Bias in the DGGE protocol

Denaturing gradient gel electrophoresis applied to environmental samples yields a community-scale view of all dominant bacterial species present in a sample (Muyzer and Smalla 1998). However, there are many preparation steps between sampling and running the denaturing gel, and biases can be introduced by a number of factors. First, the method used for cell lysis can lead to preferential lysis of certain types of bacteria over others. For example, preferential lysis of Gram-negative cells over Gram-positive type of cells can occur (Wintzingerode, Göbel et al. 1997).

Also, another step where bias could be introduced is in the enzyme kinetics of the PCR amplification. The use of DGGE for microbial ecology studies relies on the assumption that different DNA templates will amplify proportionally to their initial concentration (Morrison and Gannon 1994). Therefore, a band showing up as dominant on a gel picture (based on band intensity) should have a greater proportion of DNA in the extract, and hence a larger number of cells in the original community.

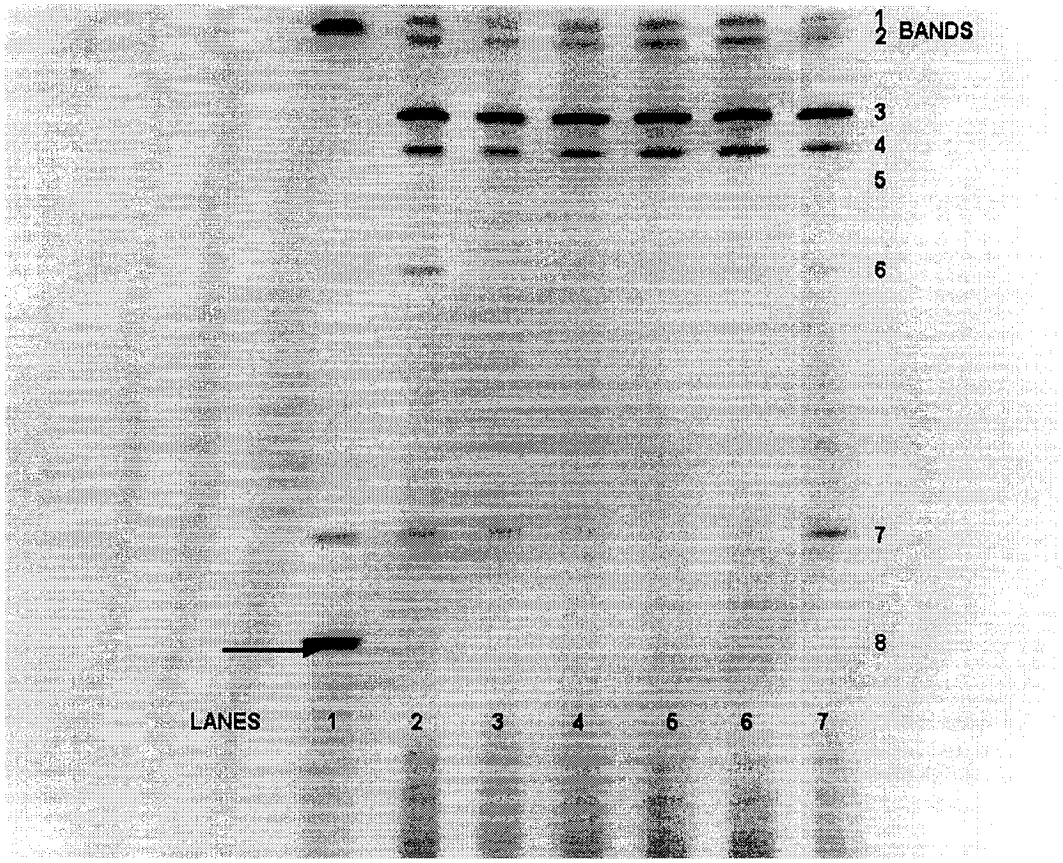

Figure 4-8: Parallel 30/60% DGGE of pure cultures samples, and defined mixtures of cultures (inverted display). The arrow indicates the strongest *R. rhodochrous* band present in defined mixed cultures of *P.putida* IF-3 and *R. rhodochrous*. Mixed cultures are as described below.

Lane	Sample
1	*R. rhodochrous*
2	*P. putida* IF-3
3	*P. putida* IF-3 at 2 g/L biomass + *R. rhodochrous* at 2 g/l biomass
4	*P. putida* IF-3 at 2 g/L biomass + *R. rhodochrous* at 1 g/l biomass
5	*P. putida* IF-3 at 2 g/L biomass + *R. rhodochrous* at 0.5 g/l biomass
6	*P. putida* IF-3 at 2 g/L biomass + *R. rhodochrous* at 0.1 g/l biomass
7	*P. putida* IF-3 at 0.1 g/L biomass + *R. rhodochrous* at 0.1 g/l biomass

Experiments were done to assess the potential for bias in which cells, grown in pure cultures and of different Gram type, *P. putida* IF-3 (Gram-negative) and *R. rhodochrous* (Gram-positive), were mixed prior to cell lysis. Several biomass concentrations of the cells were lysed, and the DNA was extracted and amplified as described in sections 3.5.1,

3.5.2 and 3.5.5. The experimental conditions are described in figure 4-8, for lanes 3 to 7. Samples were then run on DGGE. Decreasing the biomass concentration of one type of cell should decrease the intensity of its banding pattern in a proportional fashion. Lanes 3 to 7 of figure 4-8 show the results of the experiments. Band intensities were calculated with the Gel-Doc software. Intensities were then scaled between 0 and 1 by dividing each intensity by the maximum band intensity on the gel. Figure 4-9 shows the relative band intensities of lanes 3 and 7 from figure 4-8, where both samples were at equal biomass concentrations. For equal ratios of biomass (Lanes 3 and 7), differing only in total amount, banding pattern intensities were similar, but it can clearly be seen that the *P. putida* IF-3 bands were more intense than the strongest *R. rhodochrous* band (band 8). It is interesting to see that only one minor band for *R. rhodochrous* (band number 8) showed up in the mixed samples, while most of the IF-3 bands remained. These results suggest that bias has occurred, otherwise the *P. putida* IF-3 and *R. rhodochrous* banding patterns would have been completely additive, with all bands obtained with pure cultures present. This was not the case, and only one band remained for *R. rhodochrous*. A possible explanation for this would be that preferential lysis has occurred for Gram-negative cells such as *P. putida* IF-3, which would lead to higher DNA recovery for IF-3 over *R. rhodochrous*. The concentration of DNA recovered from *R. rhodochrous* cells was so low that only one dominant band could be seen.

The intensity of the *R. rhodochrous* band does decrease (Figure 4-8), as the biomass concentrations drop (Figure 4-10). However, the band intensities associated with the *P. putida* IF-3 pattern increase, despite the fact that the biomass concentration remains constant. Fortunately, the ratio of the intensities of *P. putida* IF-3's strongest band (number 5) to the *R. rhodochrous* band (number 8) increases proportionally to the biomass ratios, indicating the data are quantitative in this respect.

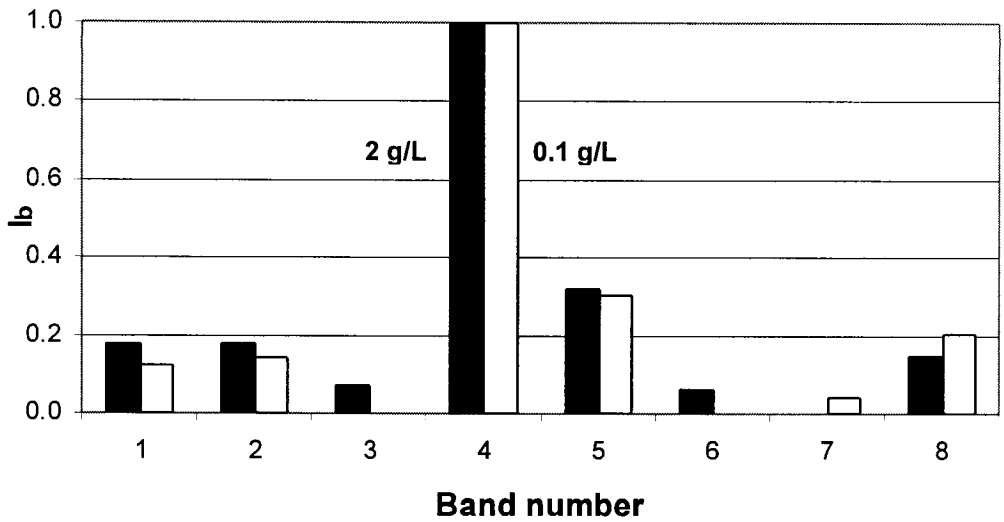

Figure 4-9: Relative band intensities associated with lanes 3 and 7 from figure 4-8. The sample loaded in lane 3 (black) was 2 g/L biomass for each cell type. Lane 7 (white) was 0.1 g/L biomass for each cell type. Band 8 can be attributed the major *R. rhodochrous* band. The other bands are attributed to the *P. putida* IF-3 banding pattern.

Lysis times were increased in an attempt to circumvent the possible effects of lysis on the results. Samples containing three different bacterial species were lysed for up to 40 minutes. Figure 4-11 shows the results produced by DGGE analysis. Although both *P. putida* IF-3 and *E. coli* patterns are present in the mixed samples, the *R. rhodochrous* (Gram +) bands do not show up at all, which reinforces the idea that there is indeed some strong bias. It also suggests a lack of repeatability for the lysis and PCR steps of the protocol, since the banding patterns of *P. putida* IF-3 and *R. rhodochrous* were additive in previous experiments (Figure 4-8).

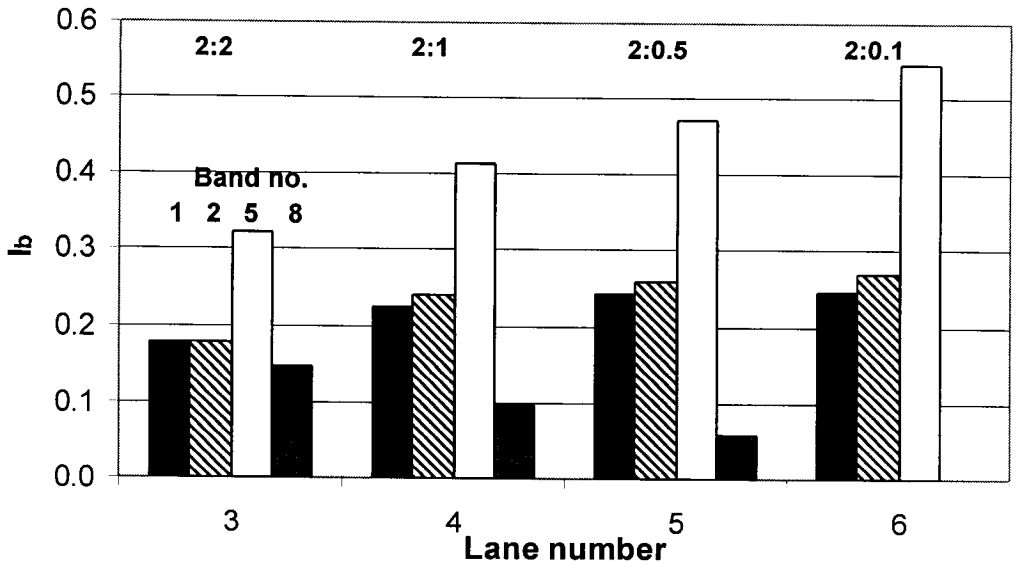

Figure 4-10: Relative band intensities of three of the *P. putida* IF-3 bands (Bands 1, 2 and 5), and the *R. rhodochrous* band (Band 8). Biomass ratios of *P. putida* IF-3 to *R. rhodochrous* are indicated in bold in the figure (in g/L).

Lanes 8 to 10 of figure 4-11 show activated sludge samples with and without *P. putida* IF-3 cells. The activated sludge sample gave a banding pattern comprised of many bands. However, when mixed with *P. putida* IF-3 cells, the resulting banding pattern was the one characteristic of *P. putida* IF-3, as can be seen by comparing lanes 8 and 10 with lanes 4 to 7. Doubling lysis time did not have any significant effect on the intensity of the banding patterns. Relative intensities of the bands were compared for lanes 4-5, 6-7 and 8-10, and band intensities did not increase systematically (data not shown). Therefore, a lysis time of 20 minutes was adequate for the experiments in this study.

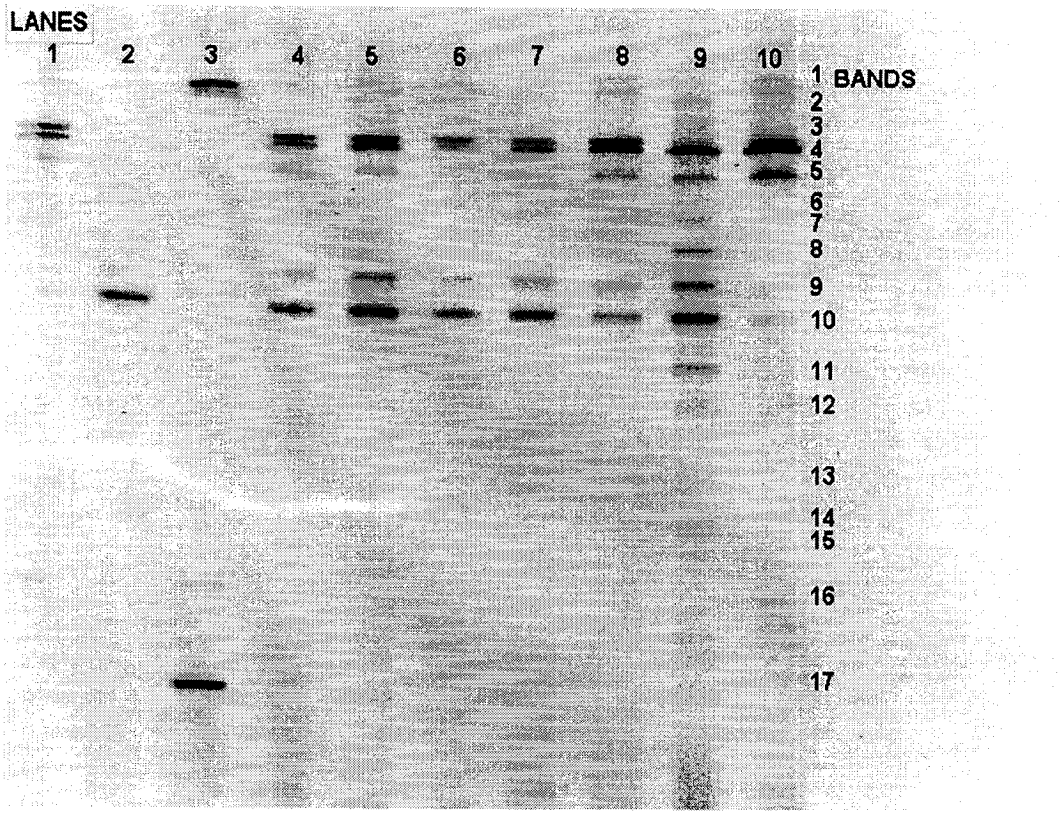

Figure 4-11: 30/60% DGGE with samples with differential lysis times (Inverted display).

Lane	Sample
1	*P. putida* IF-3
2	*E. coli* DE3
3	*R. rhodochrous*
4	Mixture of all three species at 1 g/L biomass each, lysed for 20 minutes
5	Mixture of all three species at 1 g/L biomass each, lysed for 40 minutes
6	Mixture of all three species at 0.5 g/L biomass each, lysed for 20 minutes
7	Mixture of all three species at 0.5 g/L biomass each, lysed for 40 minutes
8	Activated sludge sample + *P. putida* IF-3 at 0.5 g/L biomass, lysed for 20 minutes
9	Activated sludge sample lysed for 20 minutes
10	Activated sludge sample + *P. putida* IF-3 at 0.5 g/L biomass, lysed for 40 minutes

Since PCR must be carried out on all samples prior to interpreting the results, another possible cause of error would lie in this step, where different affinities of the *Taq* DNA

polymerase for specific templates could lead to preferential amplification of some fragments, independent of their starting concentration. Another set of experiments was carried out in order to study the potential problem. Theoretically, greater initial DNA template concentrations should yield greater product quantity, and therefore more intense bands when visualized on DGGE. Three different DNA templates (*P. putida, R. rhodochrous* and *E. coli*) were mixed in various proportions in PCR tubes and co-amplified to verify if these assumptions were correct. Results can be seen on figure 4-12, in lanes 4 to 7. *P. putida* IF-3 (Bands 1, 2, 3, 4, 6 and 7) and *R. rhodochrous* patterns (Bands 1, 7 and 8) did show up clearly in all lanes. Conclusions are hard to draw for *E. coli*, since its major band overlaps with one of the *putida* bands (Band 6, white arrow). However, lanes 6 and 7 were mixtures of all three organisms, and the overlapping band seems to have a greater intensity than in lanes 4 and 5, where *E. coli* was not amplified. This would indicate the presence of *E. coli* in the banding pattern. Intensity analysis revealed that *E. coli* did have an effect on band 5 (Figure 4-13). Intensity of band 5 increased in lanes 6 and 7 when E. coli was mixed with *P. putida* IF-3 and *R. rhodochrous*. The band intensity increased in lane 6, where 250 ng of each DNA template was mixed prior to PCR amplification, suggesting an increase in band intensity caused by additive *E. coli* DE3 and *P. putida* IF-3 bands. However, it was observed that band intensities obtained for the mixed samples were not proportional to the initial amount of template DNA. This can be seen by comparing the *R. rhodochrous* banding pattern obtained in lane 2 with the bands associated with *R. rhodochrous* in lanes 4 and 5. Since these PCR reaction tubes all contained 250 ng of *R. rhodochrous* DNA, it was assumed that the intensity of its banding pattern would be similar, but a significant decrease in band intensity was observed for lanes 4 and 5 (data not shown).

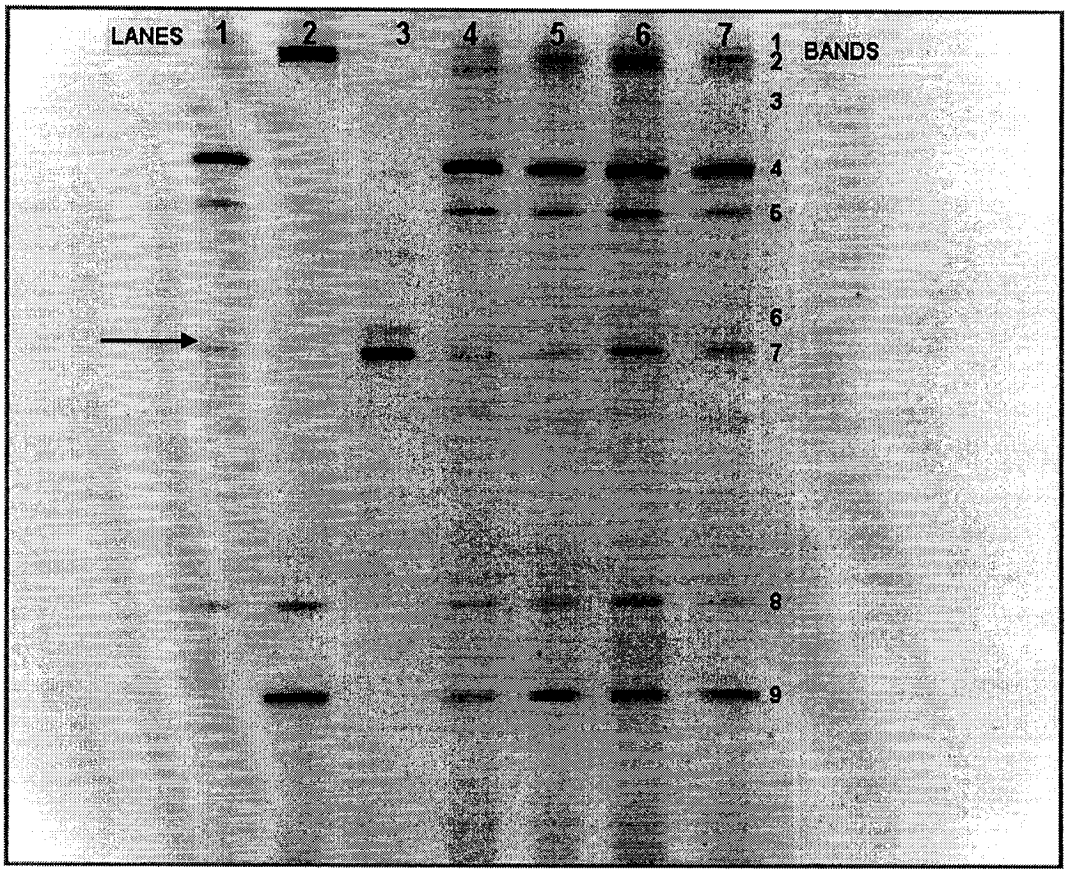

Figure 4-12: Parallel 30/60% DGGE with pure culture samples, and mixed DNA templates (Inverted display). Mixing was carried out prior to PCR amplification. The arrow indicates the overlapping *P. putida* IF-3 and *E. coli* DE3 band (Band 6).

Lane	Sample
1	*P. putida* IF-3, 250ng
2	*R. rhodochrous*, 250 ng
3	*E. coli* DE3, 250 ng
4	*P. putida* IF-3 + *R. rhodochrous*, 250 ng of each DNA template
5	*P. putida* IF-3 + *R. rhodochrous*, 125 ng of each DNA template
6	*P. putida* IF-3, *R. rhodochrous* and *E. Coli* DE3, 250 ng of each DNA template
7	*P. putida* IF-3, *R. rhodochrous* and *E. Coli* DE3, 125 ng of each DNA template

4.3.3. Bias caused by DGGE

Denaturing gradient gel electrophoresis can also introduce bias. It is important to determine a gradient range that yields the proper resolution. The choice of the denaturing gradient that is not well suited for the fragments under study can results in poor resolution of the banding patterns. For a gradient that is too broad, all bands will migrate to the center of the gel.

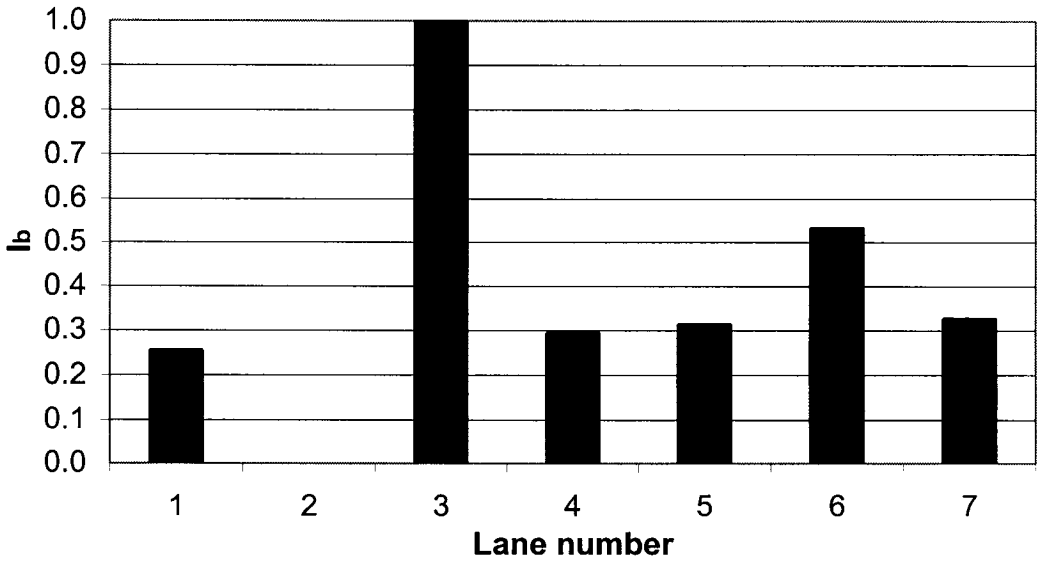

Figure 4-13: Banding intensity analysis of band number 5 (indicated by the white arrow in figure 4-12) associated with the *Escherichia coli* banding pattern.

A gradient whose maximum concentration is too low could lead to unwanted migration of all fragments to the bottom of the gel, with little or no melting of the fragments. Finally, a gradient whose maximum concentration is too high would give the opposite result, where most bands would be trapped at the top of the gel. To address these issues, an initial screening study was done to determine the optimum denaturing gradient range, by casting parallel gels with a gradient ranging from 0 to 100% denaturing agent. *P. putida* IF-3 and activated sludge samples were loaded, and migration was carried out as usual. The optimal gradient was determined by calculating the gradient range in which all

the bands were contained. A denaturing gradient of 30 to 60% was chosen as the optimal gradient for all subsequent DGGE gels (data not shown).

Another factor with the DGGE step is associated with gel loading. It is not possible to quantify the amount of DNA in the PCR products by absorbance (see section 3.5.3), because of interference caused by one component of the PCR reaction. Absorbance at 260 nm of all reaction components besides the DNA templates was measured, in order to determine which component was causing the interference (Table 4-4). It was clear that the dideoxynucleotide mix was the major component interfering with the reading, and to a lesser extent, the primers were also causing interference. Cleanup of the PCR products was attempted, with limited success (data not shown). Therefore, a constant volume of PCR product was loaded on the DGGE gels in an attempt to normalize the quantity of DNA loaded. The assumption made here was that every PCR-amplified sample started at the same initial template concentration, and should yield an approximately similar concentration after amplification. An approximate estimate of the DNA concentrations obtained after PCR amplification was obtained when the verification gel was run, where it can be qualitatively determined if all bands have the same intensity. Here again, pixel saturation must be taken into account, but relative abundance should be preserved as well, and give a good indication of the relative concentrations of PCR products.

Component	Volume	Total volume	Abs 260nm	A260/A280
	µL	mL	AU	
PCR buffer	5	1	0	0
dNTP mix	1	1	**0.4082**	1.786
Primers	1	1	0.0246	1.5625
BSA	1	1	0.0098	0.4872
Taq DNA polymerase	0.25	1	0.0004	0.1264

Table 4-4: Absorbance at 260nm of PCR components.

Analysis of the banding patterns using the image analysis software could also lead to undesired grouping of unrelated bands. Banding analysis was first achieved by detecting bands in every lane. The software detected a band when there was a localized change in intensity in the gel picture within a certain length and width. However, regions of

smearing on the gels were often detected as being bands, as were regions where the background noise was greater. Unequal background noise was due to the distribution of the UV light in the transilluminator plaque, yielding better UV lighting in the middle of the plaque than in the corners. Detected bands were then matched manually with similar bands in other lanes, based on a migration distance scale. The grouped bands were then assigned a variable number, for further analysis. "Smiling" can occur during migration, and lead to gels in which samples in the middle lanes migrate further than those in the side lanes. This has to be taken into account when banding analysis is achieved; otherwise it is impossible to match bands correctly.

4.4. GENETIC FINGERPRINTING OF MIXED CULTURES

4.4.1. Natural transients in the microbial community

The first step in working with mixed cultures was to assess the stability of the microbial consortium in the bioreactor when no external environmental pressure was applied. Due to the many possible interactions between the various microbial populations, it is probable that the community is always in flux (El Fantroussi, Verschuere et al. 1999). A mixed culture of activated sludge was first cultured in the bioreactor on activated sludge medium (table 3-4) in order to investigate if a stable microbial consortium could establish itself in the bioreactor, resulting from washout of certain bacterial types and acclimatizing of others into a small-scale ecosystem. Cycling was carried out twice per day. Samples taken from the bioreactor over a 17-day period were loaded onto a DGGE gel. Figure 4-14 shows samples from cycles 13 to 31. Those samples represent the microbial community between days 8 to 17 of the culture. A certain number of bands remained in all lanes. The intensity of other bands either increased or diminished as time went on, indicating transient conditions in the bioreactor. Banding pattern analysis was achieved using principle component analysis (PCA).

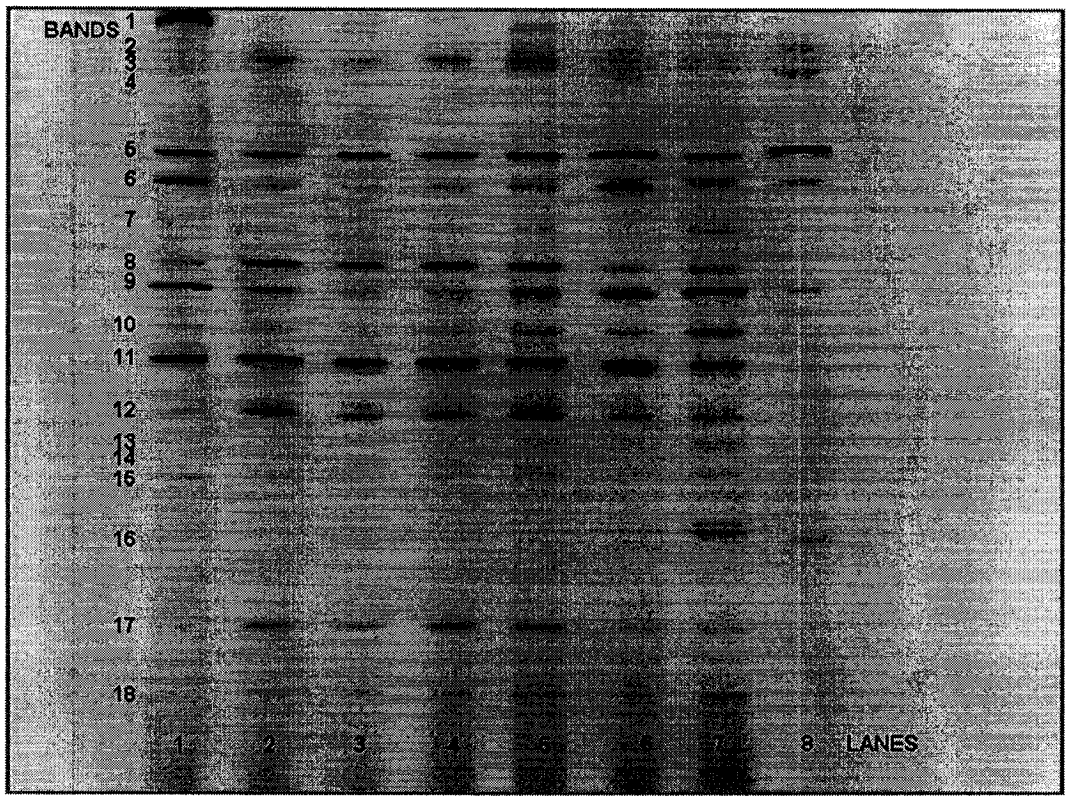

Figure 4-14: Parallel DGGE with mixed cultures samples (Inverted display).

Lane	Sample	Time (h)
1	Cycle 13, day 8	120
2	Cycle 19, day 11	192
3	Cycle 21, day 12	216
4	Cycle 24, day 13	252
5	Cycle 28, day 15	300
6	Cycle 30, day 16	312
7	Cycle 31, day 17	324
8	*P. putida* IF-3	

As a parameter of the structural diversity of the microbial population, the Shannon-Weaver index of bacterial diversity (***H***) was calculated using the following equation:

Equation 4-3: $$H = -\sum P_i \log P_i$$

where P_i is the importance probability of the bands in a lane. H was calculated using all bands in a gel lane that were detected by the image analysis software, and to which an intensity value was assigned. The importance probability, P_i, was calculated as:

Equation 4-4: $P_i = I_i/\sum I$

where I_i is the intensity value of band i, and $\sum I$ is the sum of all intensity values in a lane (Eichner, Erb et al. 1999).

The Shannon-Weaver index provides a quantitative measure of the diversity of the banding pattern. For a pattern comprised of 25 bands, assuming all bands had equal intensity, the maximum value for H would be 1.40. On the other hand, for the same banding pattern, assuming one dominant band (95% of the total intensity of the lane), the value for H would drop to 0.16. This calculation shows the range in which H might vary, and that minor bands do not have a significant influence on H values. Evaluation of the index is somewhat subjective, with the researcher looking for clear trends. In the work by Eichner, Erb *et al.* (1999), Shannon-Weaver index values dropped from 1.12 to 0.35 in 24 hours, while Ogino *et al.* (2001) observed changes in values from 1.07 to 0.72. Clearly, these changes are significant. Figure 4-15 shows the Shannon-Weaver index of bacterial diversity applied to lanes shown figure 4-14, over the time course of the experiment. The diversity index was calculated only for the first seven lanes, as the eighth lane was not loaded with a mixed culture sample. The number of bands per lane varied from 15 to 18. Associated Shannon-Weaver indexes ranged from 0.99 to 1.13, therefore suggesting little variability in the microbial community.

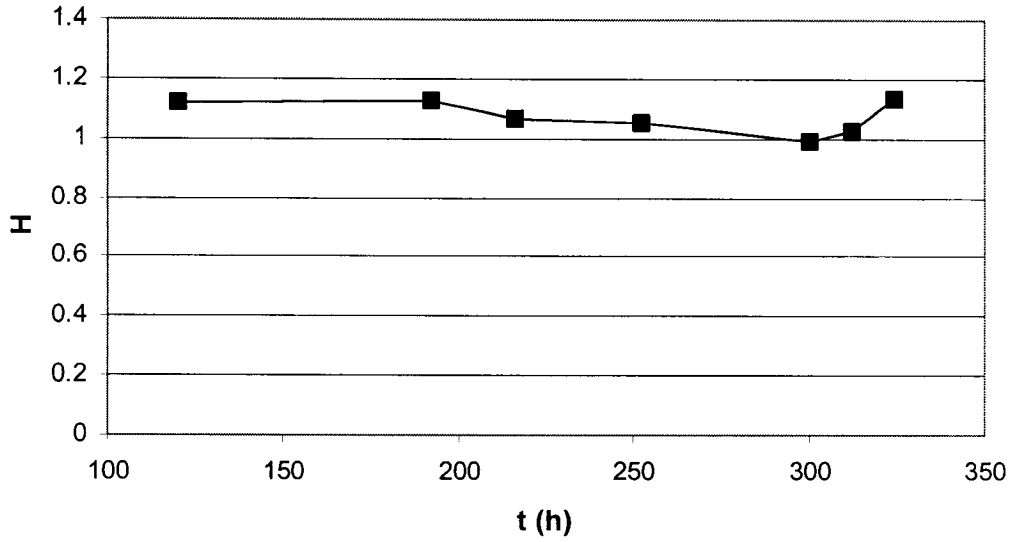

Figure 4-15: Shannon-Weaver index of bacterial diversity applied to lanes 1 through 7 of figure 4-14.

4.4.2. Effects of caffeine loading on microbial communities

Activated sludge was grown in the bioreactor on sludge growth medium at 30°C (Table 3-4). Samples were taken every two hours for the early phase of the cycle, then every 6 hours until the end of the cycle. Samples were analyzed for biomass growth, ammonium concentration and pH. Carbon dioxide evolution was also measured, as an indicator of active metabolism. Little variation in biomass and ammonium concentration was observed. The pH varied, ranging from 6.8 to 9.1, with an initial pH of 8.2. The only useful indicator of bacterial metabolism followed in these experiments was carbon dioxide evolution, where peaks could be observed, indicating an increase in bacterial activity.

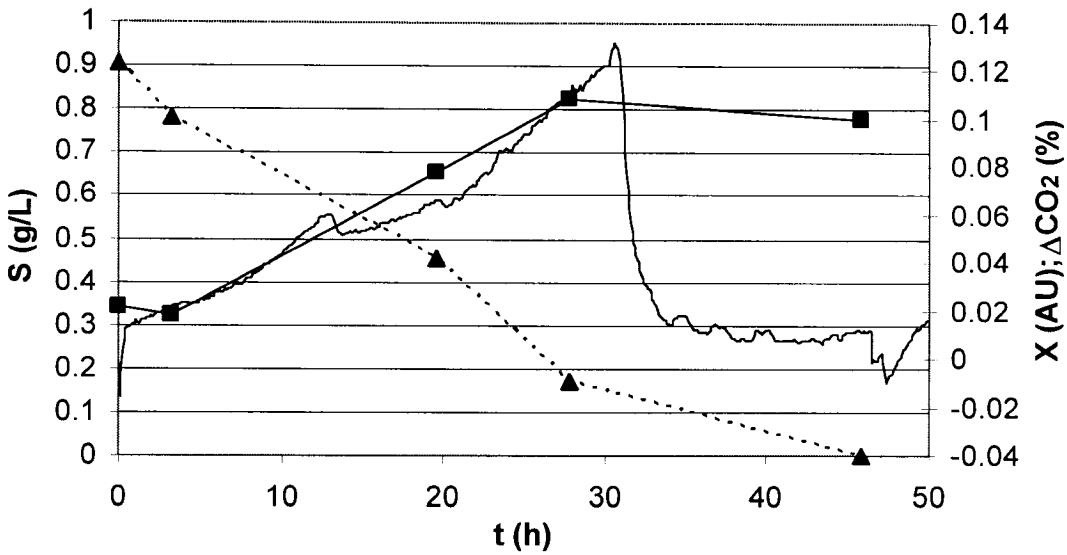

Figure 4-16: Caffeine (-▲-) and biomass (-■-) concentrations in the microbial consortium grown on activated sludge medium and spiked with 0.905 g/L caffeine (cycle 15). The solid line represents carbon dioxide evolution.

Cycling was usually carried out every 24 hours, after the carbon dioxide levels had peaked and subsequently fallen to basal levels. At this point, the culture was assumed to be starved for nutrient. Figure 4-16 shows a representative cycle. The microbial consortium was spiked with increasing caffeine concentrations in various cycles. The concentrations added ranged from 0.012 g/L to a maximum of 4.27 g/L, as measured by gas chromatography, after addition. Table 4-5 shows the caffeine amounts added over the course of the experiment, in addition to the activated sludge growth medium (Table 3-4). For other cycles, only activated sludge growth medium was used as the nutrient source. For caffeine cycles, cycling times, defined as the time needed to allow biological reactions to occur, varied significantly with the quantity of added caffeine. Complete caffeine removal was obtained for all cycles, although a considerable lag phase was observed for high caffeine loadings, reaching over 24 hours for cycle 19 (Figure 4-17). Cycles 15, 16 and 19 showed measurable biomass formation, as opposed to all other cycles at lower caffeine concentrations. Carbon dioxide release increased as the microbial consortium metabolized caffeine, coinciding with the observed cell growth. Denaturing

gradient gel electrophoresis was carried out with samples from most cycles of the reactor run (Figures 4-18 and 4-19).

Cycle	t	S
	h	g/L
1	0.0	-
2	24.7	-
3	48.6	-
4	73.7	0.051
5	102.2	-
6	129.0	-
7	145.5	0.012
8	168.4	-
9	192.5	0.200
10	220.0	-
11	242.4	-
12	267.8	0.201
13	294.6	-
14	312.2	-
15	339.1	0.905
16	386.2	1.536
17	436.6	-
18	479.6	-
19	480.3	4.267

Table 4-5: Caffeine amounts added during bioreactor experiments.

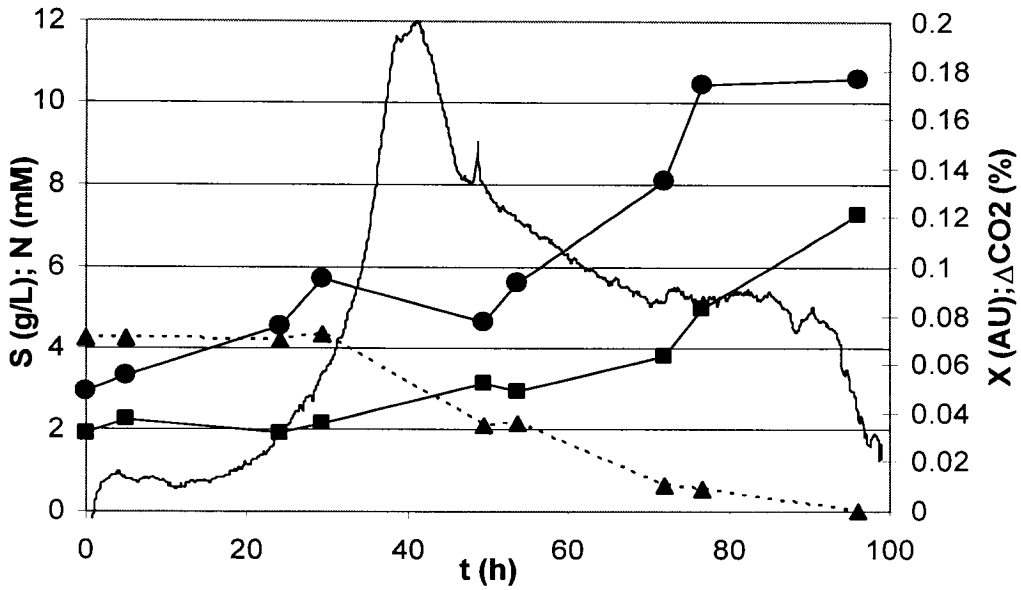

Figure 4-17: Caffeine (-▲-) and biomass (-■-) concentrations in the microbial consortium grown on activated sludge medium and spiked with 4.267 g/L caffeine (cycle 19). Ammonium concentrations (-●-) were monitored by Conway diffusion. The solid line represents carbon dioxide evolution.

Samples were loaded onto the gel in chronological order. Gel 1 (Figure 4-18) shows samples from cycle 1 to 14, with low caffeine loadings (0.012 g/L to 0.201 g/L). Gel 2 shows the remaining cycles, with the higher caffeine loadings (Figure 4-19). Lane 14 of both gels shows the *P. putida* IF-3 banding pattern used as an internal standard for band scaling. Banding patterns were analyzed by principle component analysis. The experiment was repeated with samples loaded in a randomized order to address the block effects that may have been introduced by having all the samples exposed to high caffeine concentrations on the same gel (data not shown). Qualitatively, there did not appear to be any block effects. However, technical problems did not allow using this data set for principle component analysis of the banding patterns, therefore the possible block effects could not definitely be eliminated prior to PCA.

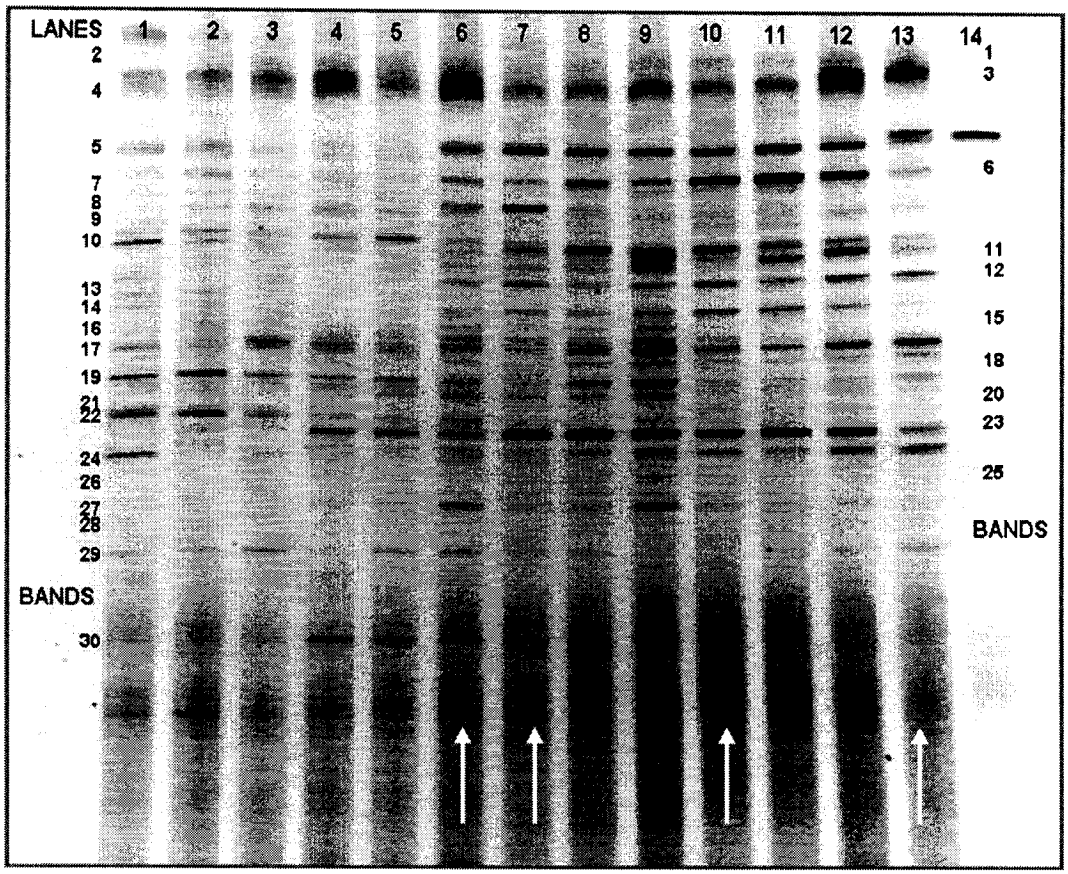

Figure 4-18: 30/60% DGGE, caffeine loading experiment on a mixed culture, gel 1 (Inverted display). Arrows indicate cycles where caffeine was added. Refer to table 4-6 for added caffeine concentrations.

Lane	Sample	Time (h)	Lane	Sample	Time (h)
1	Cycle 1, sample 1	0	8	Cycle 8, sample 1	168.4
2	Cycle 2, sample 1	24.6	9	Cycle 9, sample 1	192.5
3	Cycle 3, sample 1	48.6	10	Cycle 9, sample 3	216.3
4	Cycle 4, sample 2	101.5	11	Cycle 10, sample 1	220.0
5	Cycle 5, sample 1	102.2	12	Cycle 12, sample 1	267.8
6	Cycle 7, sample 1	145.5	13	Cycle 14, sample 1	312.2
7	Cycle 7, sample 2	167.7	14	*P. putida* IF-3	

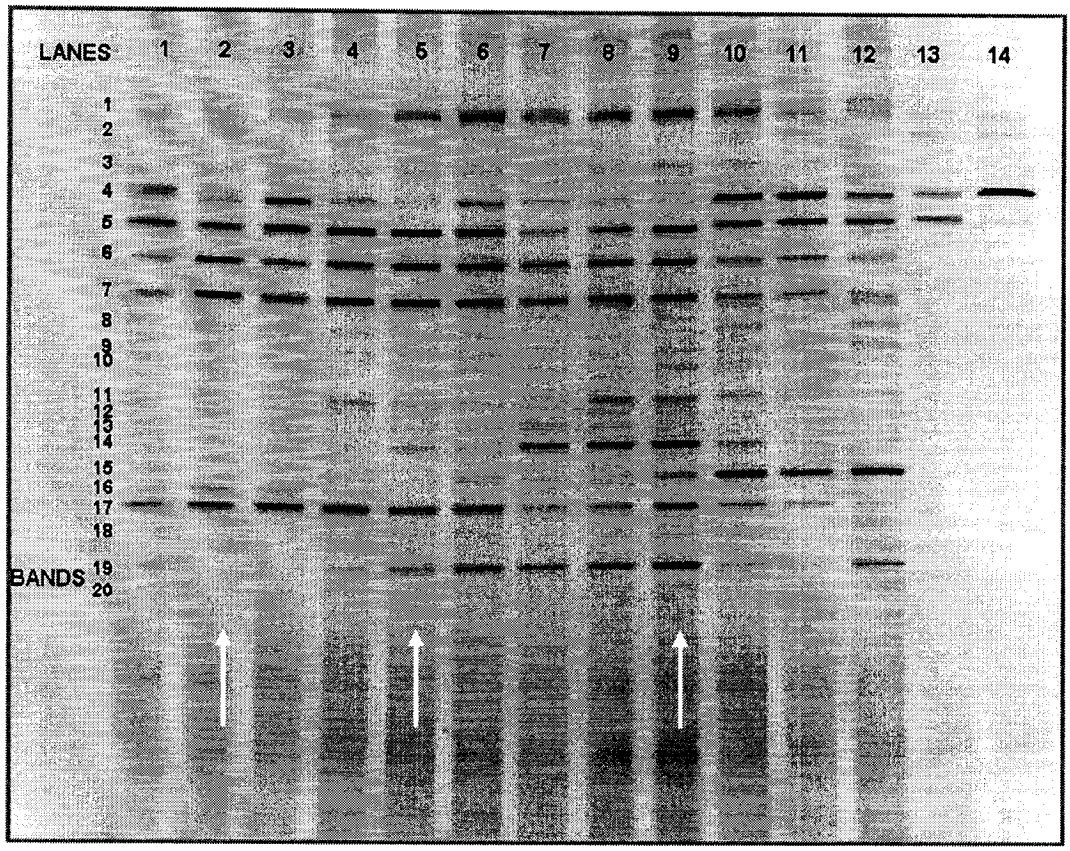

Figure 4-19: 30/60% DGGE, caffeine loading experiment on a mixed culture, gel 2 (Inverted display). Arrows indicate cycles where caffeine was added. Refer to table 4-6 for added caffeine concentrations.

Lane	Sample	Time (h)	Lane	Sample	Time (h)
1	Cycle 15, sample 1	339.1	8	Cycle 19, sample 1	480.3
2	Cycle 15, sample 3	358.7	9	Cycle 19, sample 3	504.3
3	Cycle 15, sample 4	367.0	10	Cycle 19, sample 5	529.8
4	Cycle 16, sample 2	389.3	11	Cycle 19, sample 7	552.4
5	Cycle 16, sample 3	407.4	12	Cycle 19, sample 9	576.4
6	Cycle 16, sample 5	436.6	13	Caffeine-degrading m-o.	
7	Cycle 18, sample 1	479.6	14	*P. putida* IF-3	

From the results, it was obvious that the mixed culture had the ability to grow on caffeine. In order to isolate any organism with caffeine-degrading abilities from others present in the mixed culture, a sample was plated on an agar plate containing caffeine as the only source of carbon and nitrogen. Following incubation at 30°C for several days,

colonies appeared. A single colony was picked from the plate and used as inoculum for a 150 mL shake flask. DNA was extracted from the culture, amplified by PCR and loaded onto the gel. Lane 13 of gel 2 (Figure 4-19) shows the banding pattern of the caffeine-degrading indigenous microorganism present in the activated sludge. Its banding pattern is composed of four distinct bands, with migration distances similar to the first four bands of *Pseudomonas putida* IF-3. However, band intensities differ from the intensities of the first four *P. putida* IF-3 bands.

The Shannon-Weaver index of bacterial diversity (***H***) was also calculated for lanes in figures 4-18 and 4-19 (Figure 4-20). ***H*** was calculated for the first 13 lanes of gel 1 (Figure 4-18), and for the first 12 lanes of gel 2 (Figure 4-19). Values ranged between 1.04 and 1.20, suggesting small variations in the microbial community, but no drastic changes were observed. Moreover, upon addition of large amounts of caffeine (0.905, 1.536 and 4.267 g/L, blank squares), no significant changes in the bacterial diversity index were observed.

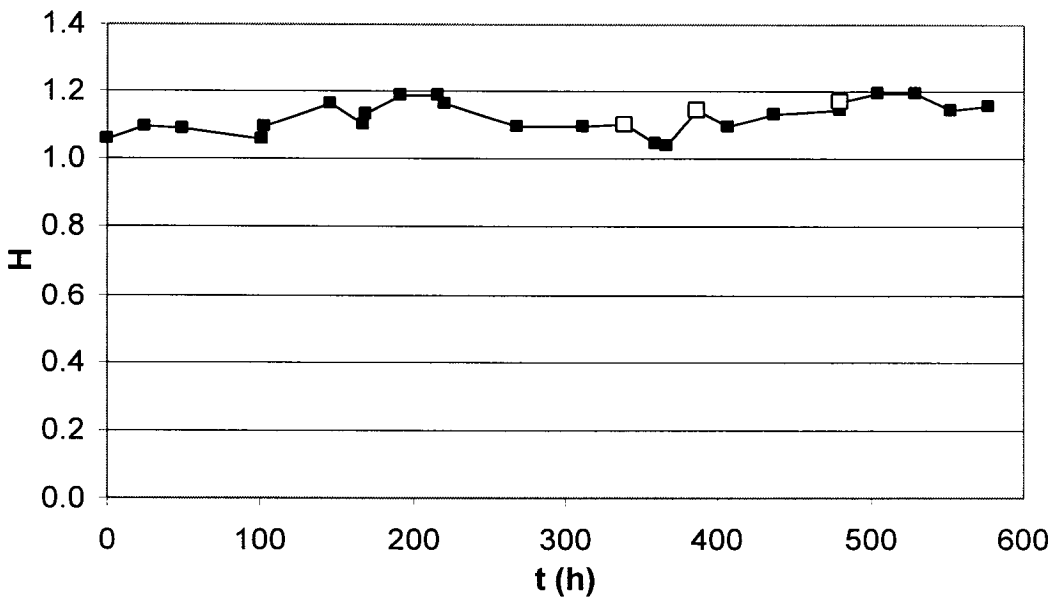

Figure 4-20: Shannon-Weaver index of bacterial diversity in caffeine loading experiments. Values were calculated for lanes 1 to 13 of figure 4-18, and lanes 1 to 12 of figure 4-19. Open squares represent addition of 0.905, 1.536 and 4.267 g/L caffeine, respectively.

4.4.3. Principal component analysis (PCA) of DGGE banding patterns

A multivariate data analysis technique, principal component analysis (PCA), was used to detect trends and relationships in the banding patterns. PCA is a multivariate analysis technique that extracts latent variables, from the original data set, that are linear combinations of the originals. (Ogino, Koshikawa et al. 2001). The method extracts systematic variations in a multivariate data matrix (Eriksson, Johansson et al. 1999). The first principal component (PC1) is selected so that it points in the direction of greatest variation in the original data set. Subsequent components are selected based on the amount of variance explained, in decreasing order, subject to the constraint that they are orthogonal (CAMO 1998). This creates a new set of coordinate axes where the principal components are orthogonal to each other, with each containing less information than its predecessor.

Data gathered from the mixed culture experiments were combined prior to analysis by PCA (Figures 4-18 and 4-19). Data from the caffeine-free control (Figure 4-14) were also incorporated, to decouple the effects of caffeine on transients in microbial populations from natural transients occurring in the mixed cultures.

Banding patterns were analyzed with image analysis software (Quantity One, Bio-Rad Inc.). The software detected bands automatically, and a report relating migration distances and band intensities was produced. *Pseudomonas putida* IF-3 was loaded on all gels, and its banding pattern used as reference. Migration distances (*Rf*) were then scaled with respect to the *Pseudomonas putida* IF-3 banding pattern, where the first band of the pattern was attributed an *Rf* value of 0, and the sixth band a value of 1. Intensities were scaled between 0 and 1, with respect to the most intense band of the *Pseudomonas putida* IF-3 pattern (Band number 3, Figure 4-8) that was given a value of 1. This scaling allowed comparison of bands and lanes run on different gels. Each band was treated as a unique variable. Other variables considered are presented in Table 4-6.

Variable Label	Variable
t	Time
H	Shannon-Weaver Index
S	Caffeine concentration
S_c	Cumulative caffeine concentration added
1-24	Band number

Table 4-6: Variables used for PCA analysis of banding patterns.

The data set used for PCA therefore consisted of 28 variables, corresponding to the intensities of the 24 possible bands, time, Shannon-Weaver index of bacterial diversity, caffeine concentrations as measured when samples were taken, and the cumulative amount of caffeine added. The cumulative caffeine concentration refers to the total amount of caffeine added during the time course of the experiment, and is used to capture the general history of caffeine exposure of the culture. Band numbering, as shown in figures 4-14, 4-18 and 4-19 differs slightly from the actual band numbering used in the data set. Since band normalization was achieved with the *P. putida* IF-3 banding pattern, the variable number of the six bands had to be identical for all three gels. Therefore, some minor adjustments were made to fit all three IF-3 patterns, resulting in bands having a value of 0 for all samples in the control data set. Samples, or experimental observations, consisted of the 8 lanes of figure 4-14, and the 14 lanes each of figures 4-18 and 4-19, for a total of 36 samples. All variables were weighted based on the standard deviation, and centered about the average. Sample notation was based on the source of the data, the gel number, and the time at which the sample was taken. The letters indicate the origin of the sample, where "C" is for the control data set, and "GA" and "GB" indicate data run on gels 1 and 2 of the caffeine loading experiment. The numeric sequence at the end of the label indicates the time (in hours) that the sample was taken. The suffix "IF-3" represents P. putida IF-3 samples, while the suffix "CD" represents the indigenous caffeine-degrading bacteria.

PCA results are presented in score and loading plots. A score plot is a representation of the data in the principal component (PC) space. The loading plot shows the location of

each of the individual variables on the principal components. It describes how much each variable contributes to the variation in the data (CAMO 1998).

A PCA was carried out with the 6 variables associated with the *P. putida* IF-3 banding pattern only (Bands 3, 5, 7, 8, 13 and 22), using the Unscrambler multivariate data analysis software (CAMO ASA, Woodbridge, USA). Cumulative caffeine concentration was also used as a variable. 71% of the variance was explained by the first 2 principal components (Figure 4-23). Figure 4-21 shows that three clusters were formed: one with GA samples from time 0 to time 102 hours, one with the other GA samples, and the third one with all GB samples. These clusters can be explained by examining the loading plot. From the results, GA samples have greater intensities of band 5, while GB samples are leveraged by bands 3, 8 and 22 (Figure 4-22).

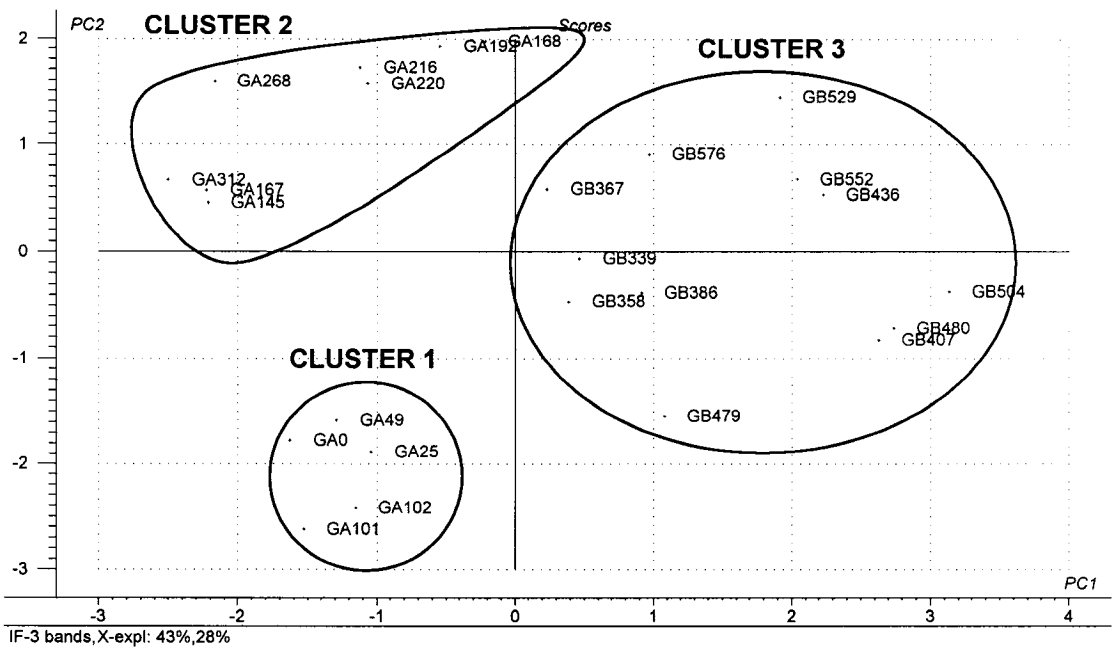

Figure 4-21: PCA score plot of the *P. putida* IF-3 variables, along with the variable associated with cumulative caffeine concentration (S_c).

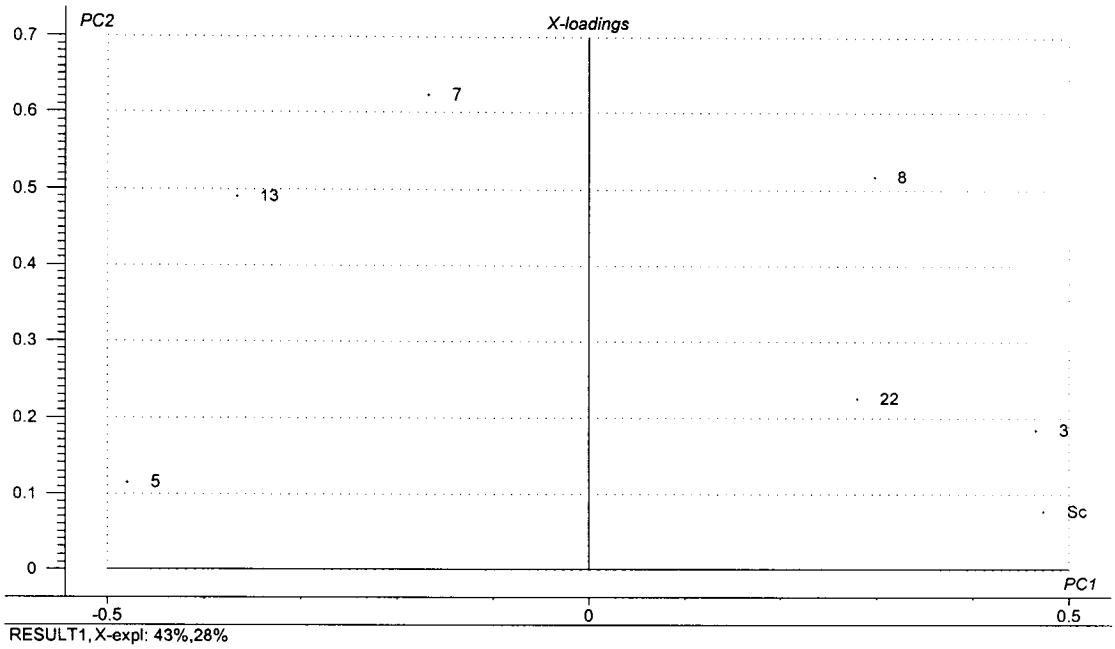

Figure 4-22: PCA loading plot of the *P. putida* IF-3 variables, along with the variable associated with cumulative caffeine concentration (S_c).

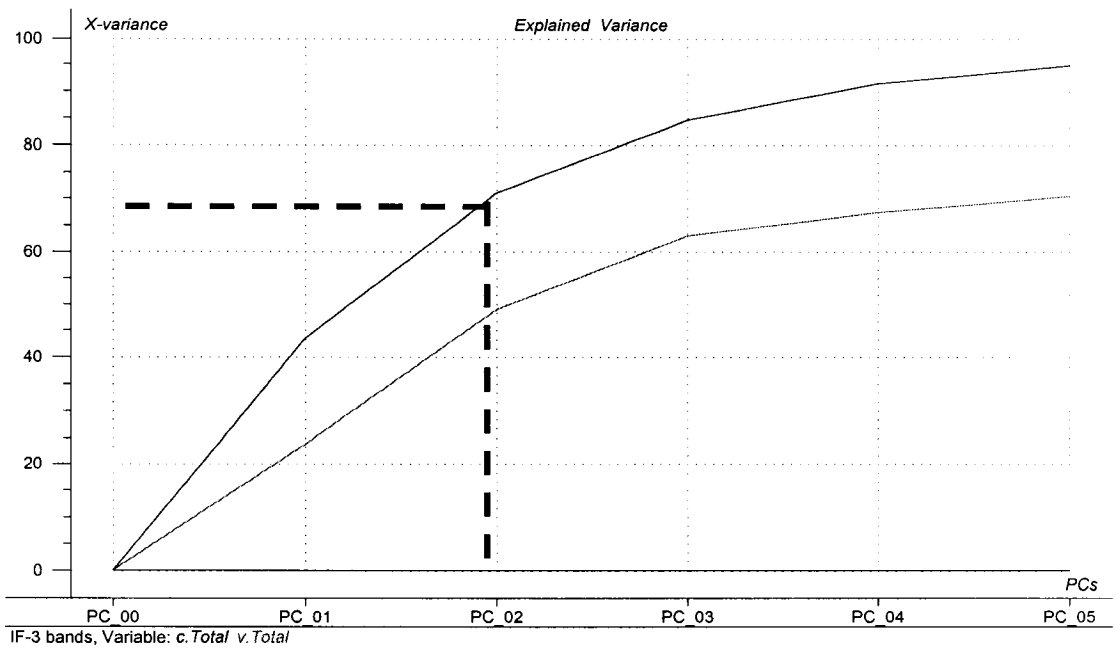

Figure 4-23: PCA explained variance of the *P. putida* IF-3 variables, along with the variable associated with cumulative caffeine concentration (S_c).

All data was then analyzed by PCA. The variables associated with time, Shannon-Weaver index, caffeine and cumulative caffeine concentrations were not included. Approximately 40% of the variance was explained by the first two PCs (Figure 4-26). Again it is clear

that three clusters are formed in the score plot (Figure 4-24). A first cluster is composed of all mixed culture samples of the control set. The second cluster is associated with all *P. putida* IF-3 samples, along with the sample for the indigenous caffeine-degrading bacteria (See section 4.4.2). Finally, a third cluster is associated with all mixed culture samples from the caffeine loading mixed culture experiments. Therefore, there seem to be strong differences between the banding patterns of the control and caffeine experiments. The loading plot is shown in figure 4-25.

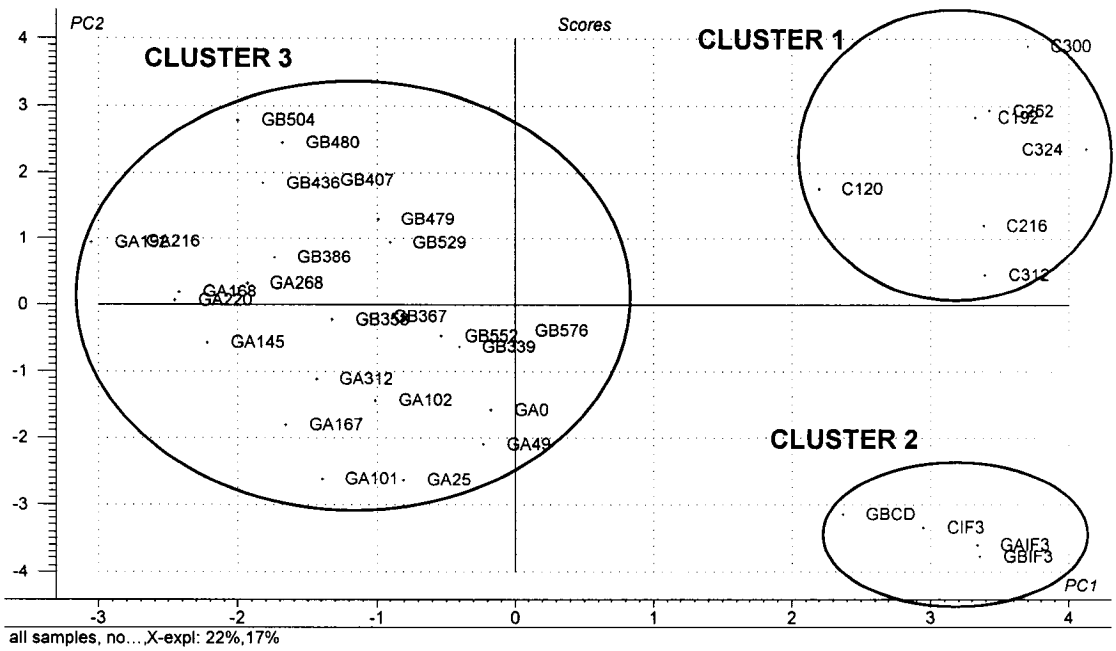

Figure 4-24: PCA score plot for all samples, without variables associated with time, Shannon-Weaver index, instantaneous caffeine and cumulative caffeine concentrations.

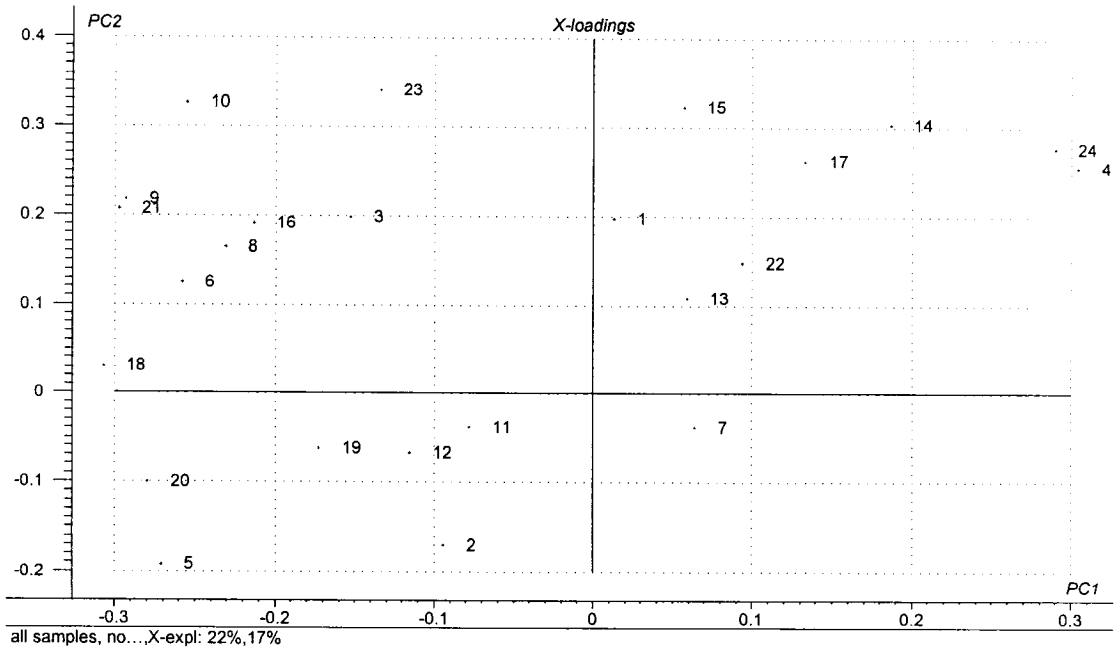

Figure 4-25: PCA loading plot for all samples, without variables associated with time, Shannon-Weaver index, instantaneous caffeine and cumulative caffeine concentrations.

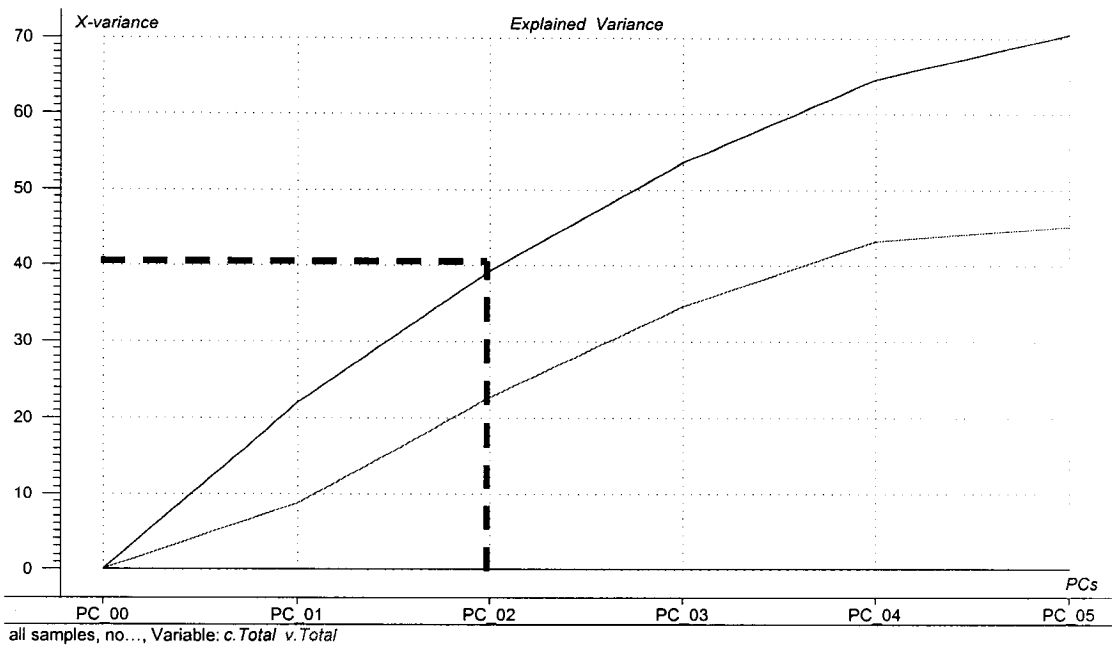

Figure 4-26: PCA explained variance for all samples, without variables associated with time, Shannon-Weaver index, instantaneous caffeine and cumulative caffeine concentrations.

A third PCA was run in which the control data set was left out. Again, only the variables associated with the mixed culture samples of the caffeine experiments were considered. Approximately 45% of the variance was explained by the first two principal components (Figure 4-29). The data are more spread out in the score plot, with samples from gel 1 (Denoted "GA" in the score plots) all located in the two left quadrants, while samples from the second gel (Labeled "GB" in the score plots) are all located in the two right quadrants (Figure 4-27). There seems to be a trend in the data with respect to time, as GA samples trend as sample time increases. Sample GA312, the last sample of gel 1, is located at a significant distance from GB339, the first sample of gel 2. This indicates a break in the apparent trend with time, which id then re-established with the samples on gel B. It therefore appears that here is a block effect between the data on both gels. Figure 4-28 shows the loading plot for this analysis.

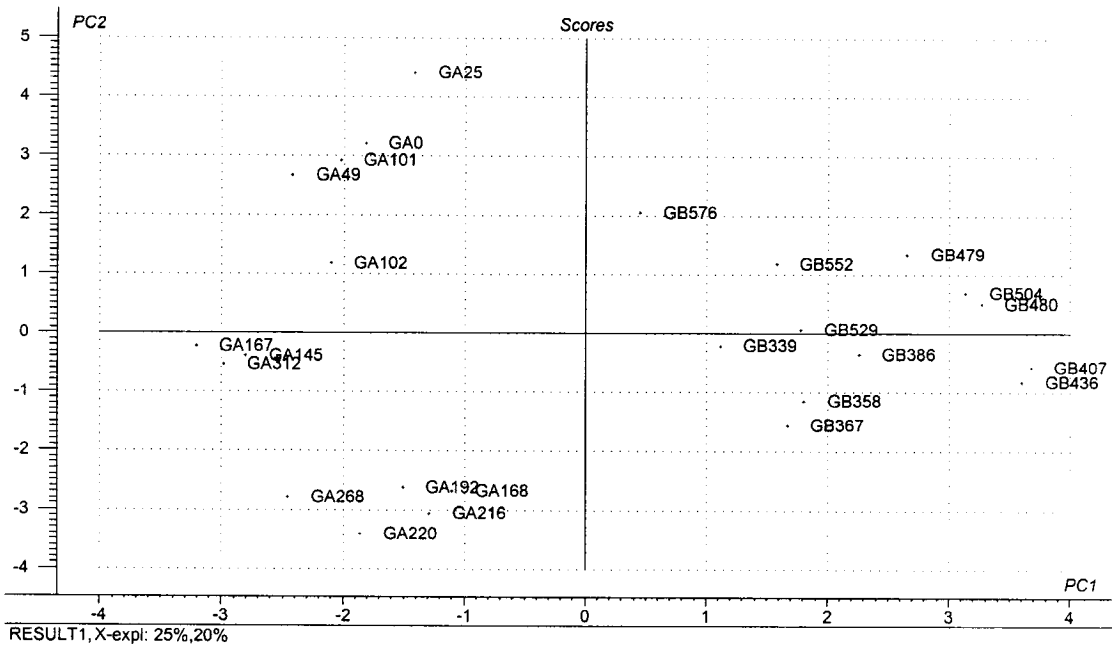

Figure 4-27: PCA score plot without control data, without variables associated with time, Shannon-Weaver index, instantaneous caffeine and cumulative caffeine concentrations.

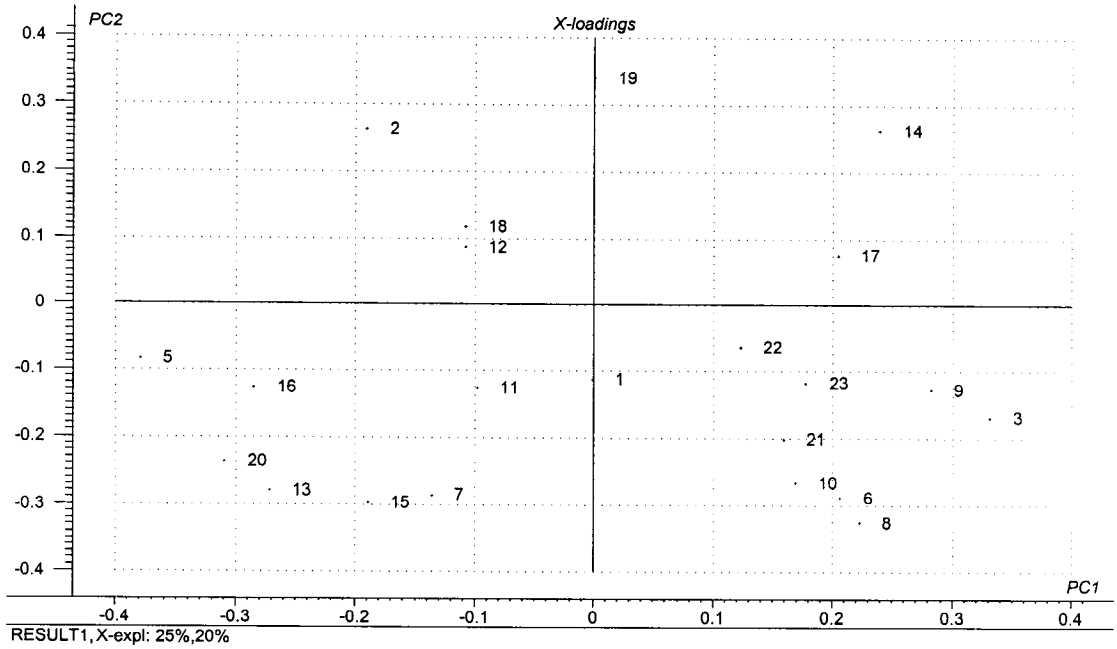

Figure 4-28: PCA loading plot without control data, without variables associated with time, Shannon-Weaver index, instantaneous caffeine and cumulative caffeine concentrations.

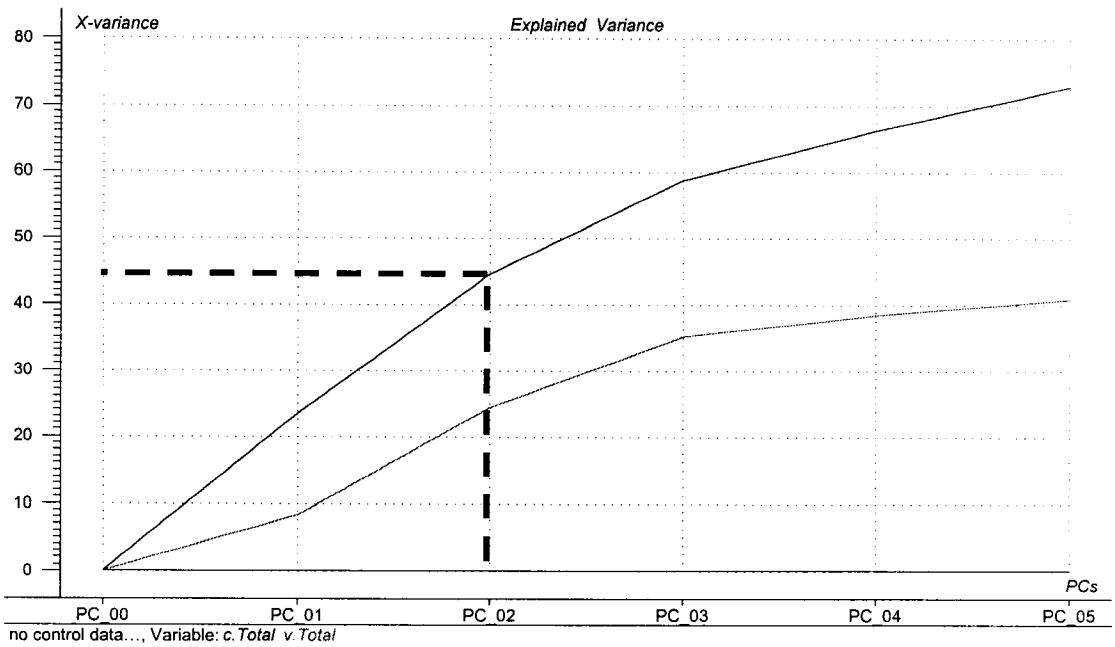

Figure 4-29: PCA explained variance without control data, without variables associated with time, Shannon-Weaver index, instantaneous caffeine and cumulative caffeine concentrations.

Another analysis was done with the same data set to which the cumulative caffeine concentrations was included as a variable. This was performed in order to investigate if that variable would play a significant role when added into the mathematical analysis. Approximately 45% of the variance was explained by the first two PCs (Figure 4-32). Two clusters can be seen from figure 4-30, one associated with gel 1 samples (GA), the other one with gel 2 samples (GB). The score plot looks similar to the one obtained previously. Loadings plot places the caffeine variable ($\mathbf{S_c}$) in the cluster associated with GB samples (Figure 4-31).

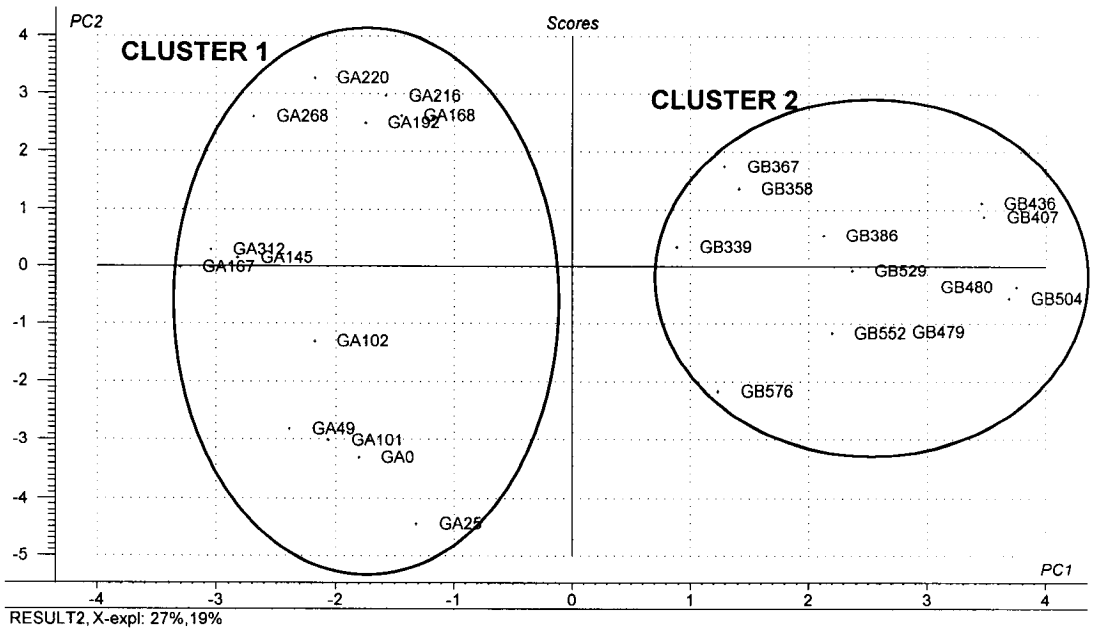

Figure 4-30: PCA score plot without control data, with the variable associated with cumulative caffeine concentration.

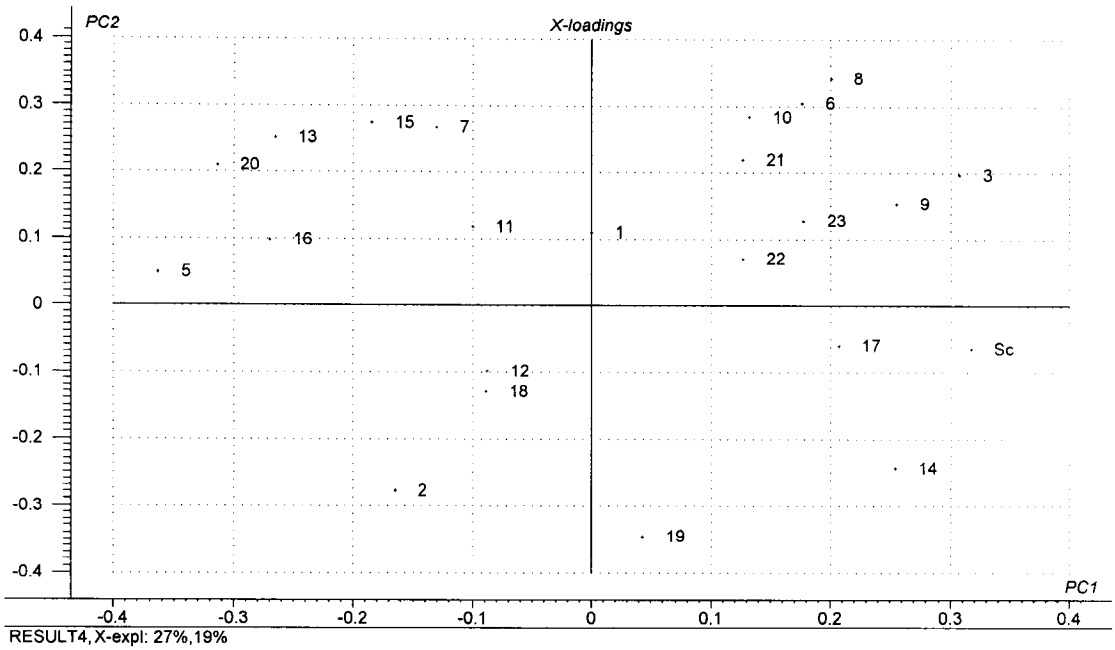

Figure 4-31: PCA loading plot without control data, with the variable associated with cumulative caffeine concentration (S_c).

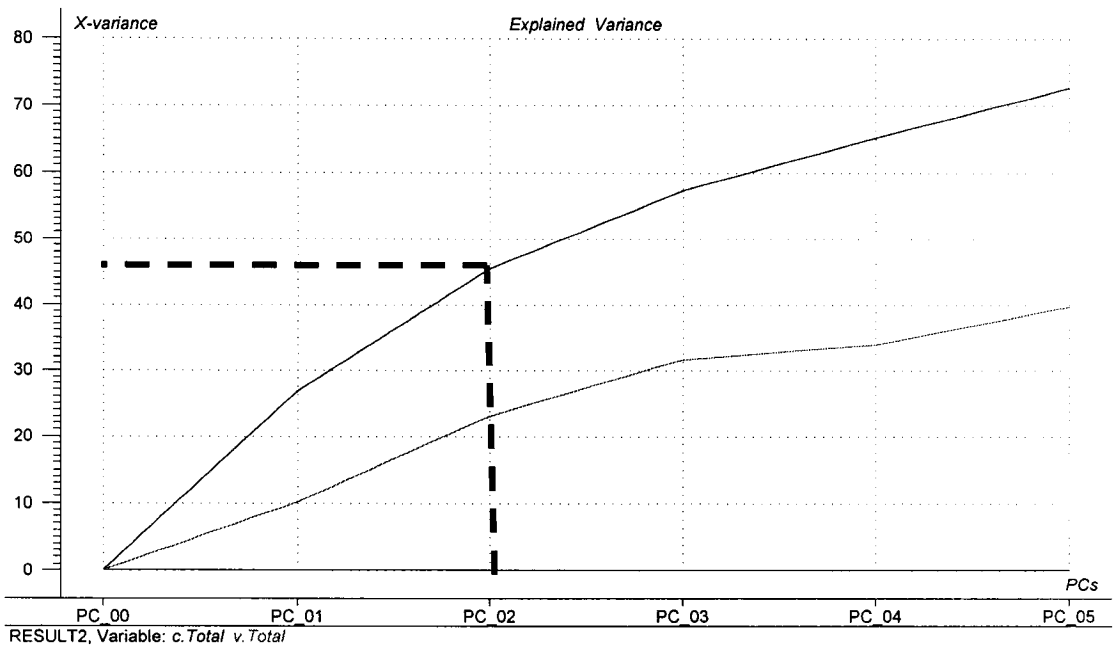

Figure 4-32: PCA explained variance without control data, with the variable associated with cumulative caffeine concentration.

In order to determine the importance of all control variables, a final PCA was run with the samples associated with the caffeine experiments, and all variables, including time, Shannon-Weaver index, caffeine and cumulative caffeine concentrations. Two principal components explained 45% of the variance (Figure 4-35). Figure 4-33 shows the score plot, where there is again heavy clustering between both gel samples. Loading plot shows that the time, Shannon-Weaver index, caffeine and cumulative caffeine concentrations variables are all located within near distance from each other, and that the cluster associated with GB samples is linked to these control variables (Figure 4-34).

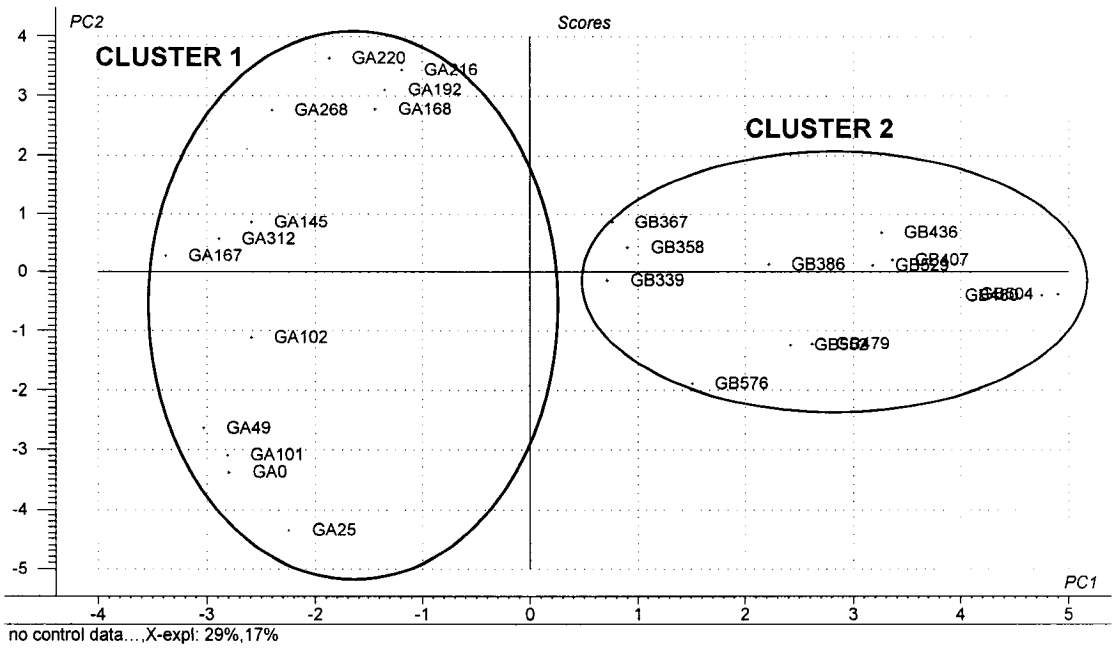

Figure 4-33: PCA score plot without control data, with the variables associated with time, Shannon-Weaver index, caffeine and cumulative caffeine concentrations.

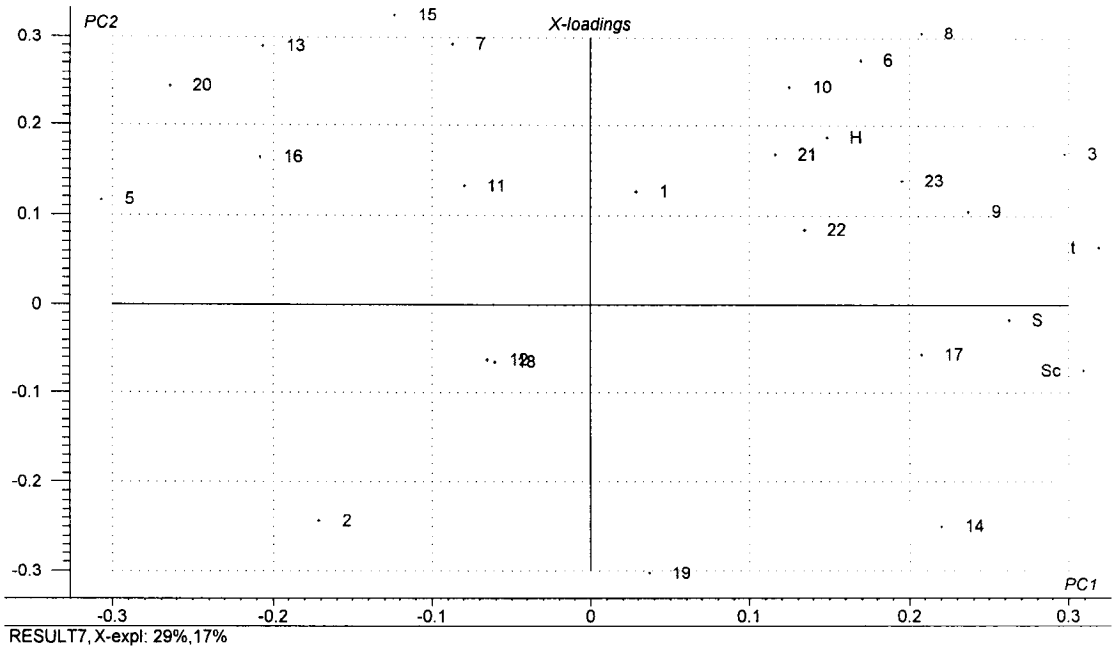

Figure 4-34: PCA loading plot without control data, with the variables associated with time (**t**), Shannon-Weaver index (**H**), caffeine (**S**) and cumulative caffeine concentrations ($\mathbf{S_c}$).

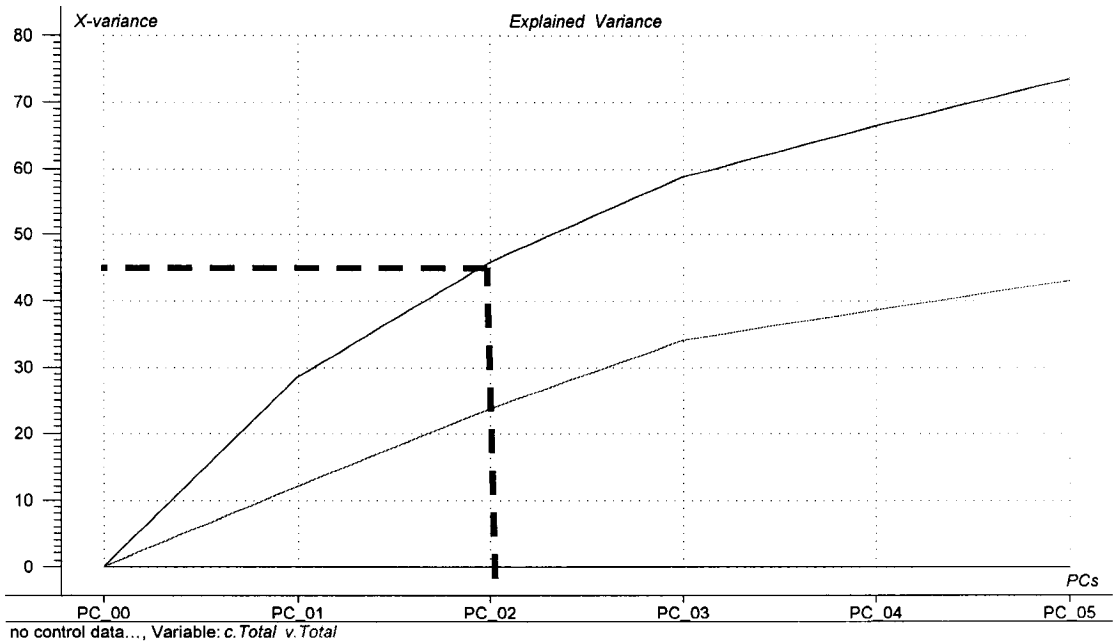

Figure 4-35: PCA explained variance without control data, with the variables associated with time, Shannon-Weaver index, caffeine and cumulative caffeine concentrations.

5. DISCUSSION

5.1. CAFFEINE DEGRADATION POTENTIAL

5.1.1. Growth of *P. putida* IF-3 on caffeine

Growth experiments with *Pseudomonas putida* IF-3 both in shake flasks and in the bioreactor showed that total caffeine removal could be achieved, when caffeine was used as the sole source of carbon and nitrogen (Figures 4-1 and 4-4). Various caffeine concentrations were tested, and complete caffeine consumption occurred in each experiment. Due to the chemical composition of the caffeine molecule, which has a molar carbon to nitrogen (C:N) ratio of 2:1, growth with caffeine as the sole source of carbon and nitrogen led to nitrogen accumulation, mainly as ammonium, since the C:N ratio needed for biomass formation for that type of microorganism would be on the order of 5:1, excluding the expense of carbon generated by carbon dioxide production during growth. However, such experimental conditions are not representative of those that would be generated if caffeine-containing coffee by-products were discarded as effluent streams, since other carbon and nitrogen sources would likely be available to promote bacterial growth. Therefore, it was essential to establish the effects of additional nutrient sources in addition to caffeine. Degradation rates obtained were higher when cells were grown in the bioreactor, as oxygen transfer is better achieved than in shake flasks, and can promote faster aerobic metabolism (Tables 4-1 and 4-3).

The average rate obtained with the bioreactor work shows more variability than the degradation rate obtained with shake flasks. This can be explained by the fact that initial caffeine concentrations were significantly lower (10-fold) in the bioreactor work, therefore yielding less biomass. Consequently, the smaller biomass levels in the range of 0.016-0.025 g/L (compared to 0.133-0.143 g/L for similar shake flask experiments) increased the variation in the results obtained, as the relative error in these numbers was the same.

5.1.2. Addition of supplemental carbon source

Degradation rates were suspected to vary significantly upon addition of other carbon and nitrogen sources, based on the assumption that the bacteria will have different affinities for different substrates. It then became plausible that caffeine removal could be maximized by working in a nitrogen limited environment, where *P. putida* IF-3 would be forced to break down the caffeine to allow nitrogen release, which would be necessary for metabolism of the other carbon sources present in the culture broth. Upon addition of glucose to the culture broth, it was observed that the bacteria degraded caffeine to generate excess nitrogen, and then used this nitrogen along with the carbon from the glucose for biomass growth (Figures 4-2 and 4-5). Therefore, diauxic growth was not observed here, as both carbon substrates were degraded concomitantly, although at a slower rate with respect to caffeine. As expected, caffeine degradation rates decreased significantly upon addition of another carbon source, for both bioreactor and shake flask experiments (Table 5-1). Both types of experiments were carried under carbon limitation. However, growth on caffeine and glucose in shake flasks was carried out with little excess nitrogen (5% excess) (Figure 4-5). As observed earlier for other conditions (Section 5.1.1), degradation rates observed for growth on caffeine and glucose were significantly lower for both carbon sources in the shake flask experiments, as compared to the rates obtained in the bioreactor work (Tables 4-1 and 4-3). Carbon sources did get depleted completely, suggesting either carbon uptake for carbon dioxide formation, or for cell maintenance needs. Since the culture was in slight nitrogen excess, there might have also been small discrepancies between the numbers expected from the model and the actual values obtained.

Ammonium accumulation and biomass formation continued to occur in the culture broth after complete caffeine and glucose removal (Figure 4-2). This can be explained by the presence of carbon and nitrogen-containing compounds, such has uric acid, ureidoglycine and ureidoglycolic acid, which are intermediates of the caffeine degradation pathway. These compounds can support bacterial growth, and also release nitrogen in the culture

medium as they are metabolized. No ammonium accumulation was observed with shake flasks under light carbon limitation, where all the available nitrogen released from caffeine was used directly by the bacteria for growth on glucose (Figure 4-5).

As seen in table 4-1, there was a large spread in the degradation rate calculated for caffeine when cells were grown on caffeine and glucose. This can be partly explained by two factors. First, a high level of free nitrogen in the culture broth carried from the previous cycle could decrease the caffeine degradation rate, since exposure to free nitrogen could allow biomass formation on glucose without the need to breakdown the caffeine molecule to release nitrogen. Such a case would not happen if the level of free nitrogen at the end of the previous cycle was low. For example, for the last two cycles where *P. putida* IF-3 was grown on caffeine and glucose (Table 4-1), for similar initial caffeine concentrations (0.169 and 0.175 g/L, respectively), degradation rates significantly differed (0.279 and 0.579 g S / g X-h). The cycle with the lower degradation rate had an initial ammonium concentration at t=0 of 5.37×10^{-3} mM in the culture broth, while the other cycle, at t=0, had 9.68×10^{-4} mM ammonium in the broth. However, such a hypothesis could not be verified with all samples, because ammonium concentrations were not measured in earlier experiments.

An acclimatization period for the cells, upon exposure to caffeine, which is thought to have inhibitory effects on their RNA and protein synthesis, could explain the lower rates obtained in the beginning of the run (Putrament, Rabanowska et al. 1972).

In caffeine-containing culture medium comprised of more than one carbon and nitrogen source, which is a more realistic situation, the degradation rates observed were significantly lower for caffeine than for the other carbon sources (Table 5-1). To assess the biodegradation potential in complex environments it was necessary to decouple the nitrogen released from various sources. Thus, material balances were made to assess the nutrient status of *Pseudomonas putida* IF-3. Glucose was added to allow consumption of the excess nitrogen to give an indication of the quantity of caffeine that could be removed relative to the quantity of other carbon sources present, under nitrogen limiting

conditions. Due to its chemical structure as a reducing sugar, glucose was expected to be more easily degradable than caffeine. Therefore it was a good way to test the affinity of *P. putida* IF-3 for caffeine. The biomass produced and the nitrogen status, after depletion of a predetermined amount of caffeine and glucose, were determined, based on experimental growth yields on caffeine (0.135 g bacteria / g caffeine), and glucose, (0.284 g bacteria / g glucose).

	Limiting substrate	**S** g/L	**G** g/L	**N_{ext}** g/L	**Average r_S** g S/ g X-h	**Average r_G** g G/ g X-h
Bioreactor	C	x			0.976 +/- 0.405	
Flask	C	x			0.517 +/- 0.030	
Bioreactor	C	x	x		0.247 +/- 0.207	1.160 +/- 0.381
Flask	C	x	x		0.061 +/- 0.001	0.352 +/- 0.060
Flask	C		x	x		0.464
Flask	N		x	x		0.577 +/- 0.010
Bioreactor	C	x	x	x	0.091 +/- 0.058	0.418 +/- 0.243

Table 5-1: Relative caffeine and glucose degradation rates obtained in the study.

Based on equation 4.2 and with known initial concentrations caffeine and glucose, and growth yields for both carbon substrates, material balances were carried out for carbon, nitrogen, hydrogen and oxygen to yield four equations with five unknowns. A fifth equation was developed with the yields. (See appendix 1).

Although the carbon balances were closed to within 20% for most reactor cycles, the nitrogen balance could not be closed within that same margin of error in most cases. The discrepancy between the expected numbers and the experimental data sets obtained can be explained in part by the method used for nitrogen quantification. Conway diffusion can only account for nitrogen released as ammonium, therefore not taking into account all other nitrogen forms that could have been present in the culture broth. Ureidoglycine, ureidoglycolic acid and urea, for example, are all nitrogen-containing compounds that could have been released as intermediates in the caffeine degradation pathway (Figure 1-2). However, as these compounds are further degraded, intramolecular nitrogen is released as ammonium, (figure 4-3). Thus, ammonium concentrations continued to increase for a period after caffeine has been depleted. Based on the ammonium

concentrations in the broth measured later on in the cycle, the nitrogen balance closed to within 15% error. Unfortunately, nitrogen accumulation measurements were not performed for most cycles, and therefore, the nitrogen data could not be completely interpreted in all cases.

5.1.3. Addition of ammonium sulfate as external nitrogen source

The addition of an external nitrogen source to allow independent growth on glucose without forcing the bacteria to break down caffeine was investigated. Ammonium sulfate was added, and taken into account in the material balances (Equation 4.2, and appendix 1). As observed in figure 4-3, diauxic growth did not occur in this situation either, which implies that caffeine was being degraded at the same time as glucose, and that its degradation was independently regulated in terms of nitrogen needs by the bacteria. Degradation rates obtained after addition of ammonium sulfate were lower than those obtained with caffeine and glucose in carbon limitation in the bioreactor, but remained higher than the rates obtained in similar shake flask experiments (Table 5-1). The decrease in the caffeine degradation rate was to be expected, since addition of an external nitrogen source would eliminate the need for the bacteria to breakdown caffeine to retrieve nitrogen.

Carbon dioxide evolution in figure 4-3 showed an interesting pattern. The first peak observed can be attributed to an initial glucose degradation burst, promoted by the presence of an external nitrogen source at the beginning of the cycle. The second small peak would then be attributed to subsequent caffeine degradation, once the initial glucose removal burst has faded. Finally, the last observable peak occurs once both carbon substrates have disappeared, and is linked to biomass growth on carbon and nitrogen-containing intermediates of the caffeine pathway (Figure 1-2). Therefore, addition of ammonium sulfate allowed the growth of the bacterium on both carbon substrates to be decoupled.

Growth of *P. putida* IF-3 on glucose and ammonium sulfate was also investigated (Figures 4-6 and 4-7), both under carbon-limiting (69% excess nitrogen) and nitrogen-limiting (34% excess carbon) conditions. Glucose was completely removed from the culture broth in both experiments, and associated with a decrease in the ammonium concentration in the broth. Degradation rates calculated were higher in nitrogen-limiting conditions (Table 5-1). The opposite scenario was expected, as the presence of excess nitrogen in the culture broth was thought to allow faster glucose metabolism. Bacterial growth on glucose was expected to stop once the nitrogen was depleted. Surprisingly, all glucose was consumed for nitrogen-limiting conditions. All carbon released from glucose does not go into biomass, as cellular metabolism produces carbon dioxide. Moreover, the cell has other energy requirements under nitrogen limitation besides cell growth, such as for maintenance and repair, and that could also explain the total removal of glucose from the broth. When glucose was used as sole source of carbon (Figures 4-6 and 4-7), less biomass was formed in the nitrogen-limiting environment, with an equal carbon amount in the beginning. These results imply that the rate-limiting step in the process would be the nitrogen release from caffeine into the growth medium. Thus, it is not surprising to find lower degradation rates under nitrogen limitation, where the rate-limiting step exerts more of an effect than in nitrogen sufficient cultures, where readily available nitrogen allowed minimizing the effect of the rate limitation. Data obtained from these experiments were checked for consistency by carrying out the mass balances, and biomass numbers were off by 30% error (Appendix 1). The biomass obtained was always lower than predicted, suggesting that growth yields used in the model as observed for the bioreactor were not adequate for shake flask experiments, due to less efficient mixing and aeration.

5.1.4. Degradation rates

Overall, the highest degradation rates for caffeine were observed with caffeine as the sole source of carbon and nitrogen in the bioreactor (Table 5-1). Upon addition of glucose as an external carbon source, caffeine degradation rates decreased significantly, both with

the bioreactor work and the shake flask experiments. Rates were again lowered upon addition of an external nitrogen source allowing independent growth of *Pseudomonas putida* IF-3 on glucose. Therefore, in complex effluents comprised of multiple nutrient sources, maximizing caffeine removal by *P. putida* IF-3 could be better achieved by minimizing the presence of external nitrogen. Glucose degradation rates were higher in a nitrogen-limited environment. It would have been interesting to run all conditions in the bioreactor, to provide better process control (mixing, aeration, temperature control, online metabolic state).

5.2. DENATURING GRADIENT GEL ELECTROPHORESIS (DGGE)

5.2.1. DGGE of pure cultures

Standard analysis of banding patterns found in microbial ecology literature assumes that each band present on a DGGE gel is directly linked to a single organism present in the sample (Muyzer and Smalla 1998). However, it is clearly not a reliable assumption. Figures 4-8 and 4-11 show that pure cultures of *P. putida* IF-3, *E. coli* and *R. rhodochrous*, grown in shake flasks and plated to verify the absence of contamination, presented patterns containing up to six bands when run on a denaturing gel. This is confirmed in the literature, where it has been shown that there can be more than one 16S rRNA gene of different sequence in a DNA preparation from a pure culture (Wang, Zhang et al. 1997). Therefore, after PCR amplification of these fragments, resolving them with DGGE yields a number of bands proportional to the numbers of different 16S rRNA genes (Clayton, Sutton et al. 1995; Rainey, Ward-Rainey et al. 1996; Wang, Zhang et al. 1997). From these results, it is more accurate to look for species-specific banding patterns than specific bands only, even though looking for one major band per organism would be a valuable method for identifying known organisms in a microbial consortium. In this study, the banding pattern of *P. putida* IF-3 was composed of six easily identifiable bands (Figures 4-8 and 4-11). Therefore, when *P. putida* was incorporated in a mixed culture, this pattern should be visible if the microorganism could establish itself in the microbial

community. Banding patterns were also obtained for other bacterial species, such as *R. rhodochrous* and *E. coli*, each having a unique banding pattern. The repeatability of the pure culture banding patterns was excellent, as shown in figure 5-1, where the six-band patterns of *Pseudomonas putida* IF-3 from four different samples are plotted. Migration distances were scaled between 0 and 1, with 0 corresponding to the first of the six bands, and 1 corresponding to the last band. As expected, the relative intensities of the bands were also repeatable. The fourth and fifth bands are the ones that show more variability in terms of both migration distances and relative band intensity. A 95% confidence interval was calculated to determine the variability in the data. The data point with the highest variability is the fourth one, with an average intensity of 0.345 +/- 0.06. All other data points had lower variability, therefore suggesting good repeatability.

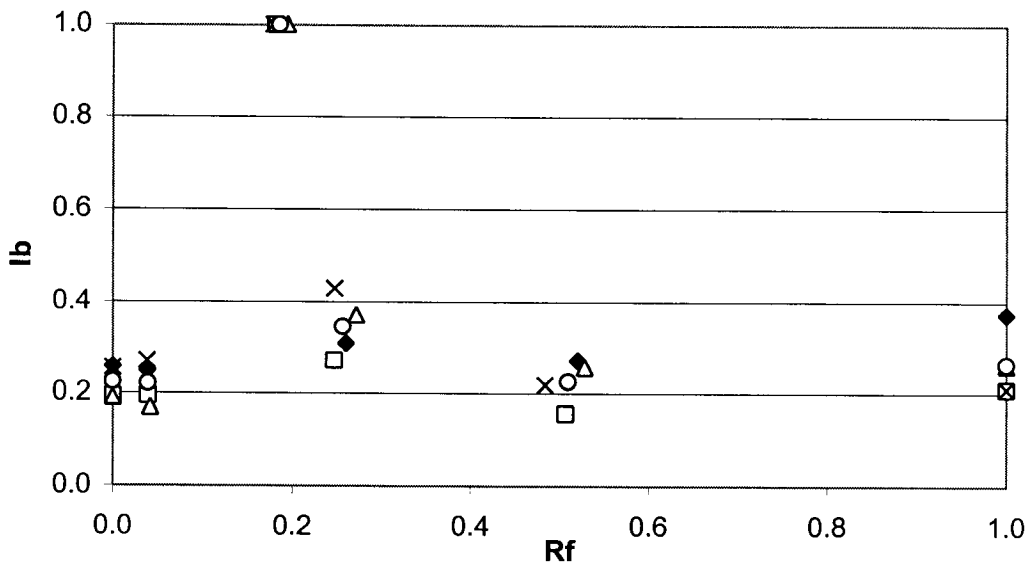

Figure 5-1: Repeatability of the *P. putida* IF-3 six band pattern. Four different samples of P. putida IF-3 are plotted in terms of migration distances and relative band intensities. Circles (○) represent data points of average migration distance and average intensity.

5.2.2. Bias and causes of errors

The lysis and PCR amplification steps of the DGGE procedure can create biases that may affect the overall interpretation of the results (Sections 4.3.2 and 4.3.3). Preferential lysis can lead to a DNA preparation that might not be representative of the genomic diversity present in the sample, if cells were lysed with different efficiencies. Therefore, the results shown on DGGE gels could represent only a fraction of all the microorganisms that were present when the sample was taken, most likely the Gram-negative bacteria. This can lead to an important loss of information, since the most active microorganisms in a treatment system, even if they are present in large cell numbers, can resist cell lysis, resulting in a banding intensity that is not proportional to the cell numbers in the sample.

Figure 4-8 shows that the banding patterns of both *P. putida* IF-3 and *R. rhodochrous* were not additive when mixed at equal biomass concentrations (Lanes 3 and 7), where only one band can be seen for *R. rhodochrous*. Therefore, preferential lysis might have occurred with Gram-negative cells over Gram-positive cells, leading to a banding pattern on the DGGE that was not proportional to the initial cell numbers from each cell type. Increasing lysis time did not solve the problem (Figure 4-11). However, when band intensities were compared relatively to their biomass concentrations (Figure 4-10), the ratio of intensities of *P. putida* IF-3's major band (number 5) to the *R. rhodochrous* band (number 8) increased proportionally to the biomass ratios. These results were obtained after scaling of the intensities with a calibration factor, however. Such results suggest that there is bias, but that it might be constant. Therefore, assuming a constant bias in the lysis or PCR amplification steps, DGGE analysis of mixed cultures would yield a community profile that would be representative of the genomic diversity of the DNA preparation.

It is important to note though, that the overall amount of DNA that can be recovered from each cell can vary between bacterial species. Therefore, the 2:1 ratio in band intensity between *P. putida* IF-3's band number 5 and the *R. rhodochrous* band could be explained in part by natural differences in DNA quantities recovered from each cell type rather than preferential lysis (Figure 4-10).

Another source of error is associated with PCR amplification. The problem here lies in the fact that preferential amplification of certain templates could lead to a result that is not representative of the original population mixture. In this case, the results obtained from DGGE are related to the bacterial species lysed, and to the DNA templates from those bacteria that actually amplified. Therefore, it might not provide a reliable community-scale view of the evolution of the bacterial community. As such, one could be looking at only a small fraction of the total organisms, and moreover, a fraction that is not necessarily representative of what evolved in the bioreactor. However, from the results obtained (Figure 4-12), there is no evidence that the PCR reaction was preferential to a small number of templates. However, even if amplification did occur for all three DNA templates, the intensity of the banding patterns were definitely not proportional to the initial amount of template DNA, as shown by comparison of the *R. rhodochrous* banding patterns in pure and mixed samples (Figure 4-8). These results reinforce the idea of induced bias prior to DGGE.

Because post-PCR DNA quantification could not be achieved for reasons mentioned earlier (Section 4.3.3), a constant volume of PCR product was loaded onto DGGE gels, instead of a consistent DNA quantity. This can lead to misinterpretation of intensity readings. Assuming that the same initial template concentrations will yield similar amplicon concentrations is not a reliable assumption, mainly because of the variability between two identical PCR amplifications. Experimental errors, when working with volumes in the microliter range, can have dramatic effects on the outcome on the amplification. Adding slightly different volumes of DNA polymerase, primers and free nucleotides can modify the kinetics of the reaction, therefore altering the yields of double-stranded PCR products obtained. Therefore, the actual quantity of DNA loaded onto the gel can differ from one sample to another, independently of the fact that the volumes were equal. Moreover, the only way to verify if DNA quantities seem consistent is by running the PCR verification gel, where saturation effects can lead to misinterpretation. Consequently, the intensity of the banding patterns on DGGE can be less for some samples, and therefore induce errors in the pattern analysis. Normalization

of the banding patterns with respect of migration distances and relative band intensities was achieved to circumvent the problems mentioned above.

5.3. EFFECT OF CAFFEINE ON MIXED CULTURES

5.3.1. Background flux of the mixed culture

An experiment was performed to quantify the change in community structure of the mixed culture, in the absence of the environmental stress caused by caffeine. As can be seen in figure 4-14, a number of bands were present on all lanes, corresponding to the last 9 days of the reactor run, indicating some stabilization of the major bacterial species present. Although the major bands seem to remain present from cycle to cycle, there is a noticeable change in the banding patterns with time, suggesting transient metabolism occurring in the bioreactor, as opposed to a stable microbial community. The Shannon-Weaver index of bacterial diversity (***H***) was calculated as an indicator of structural diversity within a microbial community (Figure 4-15). Values did not vary appreciably, ranging from 0.99-1.13, indicating stable maintenance of a rather diverse microbial community. Reduced diversity caused by the dominance of a small number of organisms would have led to smaller ***H*** values. This was not observed here, indicating the maintenance of diversity in the bacterial community over the 200 hours presented in figure 4-14.

It is important to keep in mind that the results must be interpreted in light of the many biases that exist. Therefore, the observations and data gathered from DGGE must be considered with a certain degree of latitude.

Consistent with the results observed, it is difficult to make a case that a unique and time invariant bacterial community could be maintained over long periods of time with regards to the individual populations, under any circumstances. For example, a competition model offers a realistic view of one interaction that could exist, in which there are some

variations in the dominance, and hence in numbers, of some organisms relative to others, because of the continuous competition over nutrients. Some bacterial species, particularly well adapted for metabolizing certain nutrients present in the culture broth, could dominate in the earlier stages of growth, gaining an advantage. However, other bacteria may be better adapted to feed off metabolites released in this first consumption step, therefore using the nutrients released by the first organisms to feed without spending the energy required for the breakdown of the initial molecule. The latter type of opportunistic bacteria would then have an advantage over the first, and increase in numbers (Shuler and Kargi 1992). Many other interactions are possible such as antagonism, where one type of bacteria would produce, through the metabolism of available substrates, a toxin or inhibitor to another type of bacteria present, therefore slowing its metabolism. Commensalism is the opposite scenario, where products released by one type of bacteria promote growth of the other bacteria present. Since many different interactions can exist between bacterial strains in mixed cultures, it is more likely to see transient changes in a bacterial community than a stabilized number of bacterial species (Shuler and Kargi 1992).

5.3.2. Effects of caffeine loadings on a mixed culture

Caffeine pulses were added periodically to the bioreactor growth medium to study the effects of the alkaloid on the mixed culture obtained from activated sludge. Complete caffeine removal was obtained for all caffeine additions, suggesting the presence of an indigenous caffeine-degrading microorganism. The strong resemblance between banding patterns of *P. putida* IF-3 and the indigenous caffeine-degrading organisms suggests a high similarity between the organisms. The organism isolated from activated sludge could quite possibly be of the *Pseudomonad* genus. DNA sequencing of the PCR-amplified 16S rDNA fragment would be a useful tool to identify the organism. Furthermore, although microbial caffeine degradation has only been demonstrated by a relatively small number of microorganisms, complete enzymatic caffeine removal by the organisms found in activated sludge from the wastewater treatment plant clearly shows

the wide variety of enzymatic processes that can be undertaken by bacterial cells. This result provides evidence that such a microbial process can be achieved in the environment by a large number of naturally present bacterial species, and that the presence of caffeine may not be as problematic as anticipated (Putrament, Rabanowska et al. 1972).

Subsequent caffeine additions resulted in changes in the banding patterns over time, suggesting a metabolic response to the environmental stress in the microbial community. Shannon-Weaver index values did not vary appreciably throughout the 575-hour long experiment, suggesting little variation in the number of species in the microbial community over time (Figure 4-20). Addition of caffeine at high concentrations did not seem to affect the health of the microbial community, since diversity index values did not decrease significantly. The indigenous caffeine-degrading organism present in the mixed culture might have played a protective role in the consortium, by removing the undesirable compound. Consequently, maintenance of a relatively diverse microbial consortium could be achieved even in the presence of high caffeine concentrations.

5.3.3. PCA of DGGE banding patterns

The first analysis by PCA was performed considering only the variables associated with the *P. putida* IF-3 banding pattern, and the cumulative amount of caffeine added. Of the total, 71% of the variance was explained by the first two principal components (Figure 4-23). Data were separated in three clusters (Figure 4-21). The first cluster could be linked to the first 5 samples of gel 1, which represent samples that were not exposed to caffeine. Upon addition of small amounts of caffeine, another cluster was formed with the remaining GA samples (Cluster 2). Finally, the last cluster was formed with all GB samples, which are the samples associated with exposure to high caffeine concentrations. Since all samples from gel 1 are located in the left quadrants, and all samples from gel 2 located in the right quadrant, there is evidence of a block effect associated with the different gels. This block effect was most probably the reason why the two latter clusters

are completely separated, since there was not a big difference in caffeine exposure between the last samples of gel 1 and the first samples of gel 2 (Table 4-5). Loading plot shows correlations between bands 3, 8 and 22 and high caffeine concentrations (Figure 4-22), a strong negative correlation for band 5 and a slight negative correlation for bands 7 and 13. These results also clearly show a strong negative correlation between bands 3 and 5.

The data set was then analyzed considering all samples, but excluding the variables associated with time, Shannon-Weaver index and caffeine. In this manner, any trends extracted are a result only of the information contained within the banding patterns. Considering only two principal components, 40% of the total variance was explained (Figure 4-26). Looking at the score plot clearly indicates the formation of three major clusters (Figure 4-24). The biggest cluster is comprised of all GA and GB samples, which originated from the same experiment. However, most GB samples are located in the upper part of the cluster, and GA samples are mostly located in the bottom part, which suggest that the data associated with each gel are indeed different. By analyzing the loading plot (Figure 4-25), bands that draw both parts of the clusters apart are bands that have an important presence in only one of the two gels. For example, bands 5 and 20 for gel 1 (Bands 4 and 23 in figure 4-18), and bands 10 and 23 for gel 2 (Bands 10 and 19 in Figure 4-19). Data from the control experiment are also clustered together. It is interesting to note that all bands that were added in the control data set to line up the *P. putida* IF-3 patterns for all gels, are located in the same lower-left quadrant of the loadings plot except band 6 (Bands 2, 11, 12, 19 and 20). These bands all had a value of 0 for the control data. This also contributed to the clustering effect. Finally, the patterns associated with *Pseudomonas putida* IF-3, which were loaded once onto every gel, clustered together along with the indigenous caffeine-degrading bacteria isolated from the mixed culture. The statistical analysis, without the variables associated with time, Shannon-Weaver index and caffeine allowed determining differences in the raw data, without any mathematical influence from those variables. Because of the clustering obtained in the score plot, it can be clearly seen that there were some major differences in the data treated, more specifically in the banding patterns. Exposure to caffeine caused all

samples to group together, and all the control samples did cluster together as well. However, that effect could also be caused by the difference in time between both mixed cultures. The control experiment was run three months earlier than the caffeine experiment, and transient fluctuations in the microbial populations in their natural habitat might have contributed to the difference in banding patterns obtained. Furthermore, bands 4 and 24, located at the far right in the loading plot, contribute to separate the control cluster from the rest of the data. Both bands were only present in the control data set, which explains this contribution. It is not surprising to see the indigenous caffeine-degrading bacteria (noted "GBCD" in figure 4-24) clustered with the internal standards, since its banding pattern was found to be similar to the first four bands of the *P. putida* IF-3 pattern.

An analysis was then carried out considering only data from gels 1 and 2. The plot score shows a wider spread in the data, but there is still heavy clustering between gels (Figure 4-27). This can be explained by looking at the impact of specific bands from the loading plot (Figure 4-28). For example, band 14 (upper right quadrant) has more weight on GB since it is present in 9 lanes of gel 2, and it is only present in two lanes of gel 1. GA would be more leveraged by bands 5, 13 and 20 (lower left quadrant), which are more important in the banding patterns of gel 1 lanes than they are in the gel 2 banding patterns.

Block effects due to combining data from two different gels are observed in the score plot obtained from this PCA. GA312, the last sample of gel 1 (Figure 4-18, lane 13) is very distant in the plot from GB339, which is the first sample of gel 2 (Figure 4-19, lane 1). Since both samples are linked by time, they should be closer together. The data should follow some chronological trend, which they seem to do for gel 1 only. Numerical values of the score plot obtained for the first principal component are plotted against time in figure 5-2. Arrows indicate samples GA312 and GB339, the last sample from gel 1 and the first sample from gel 2, respectively. There is a large difference in scores between these two samples, induced by running two separate gels. The block effects should not detract from the importance of this plot. From the figure, it is apparent that the banding

pattern trends with the amount of caffeine in solution. As caffeine is consumed, the pattern reacts accordingly, providing compelling evidence of the influence of caffeine on the community structure.

The analysis was the repeated, but including the cumulative caffeine concentration variable. This was done to determine if the actual values of the caffeine data would play a significant role in the PCA, or if its effects could be denoted without the need to add it in the analysis. Score plot shows a clustering effect similar to the one seen in the last analysis, with GA samples on the left side and GB on the right side (Figure 4-30).

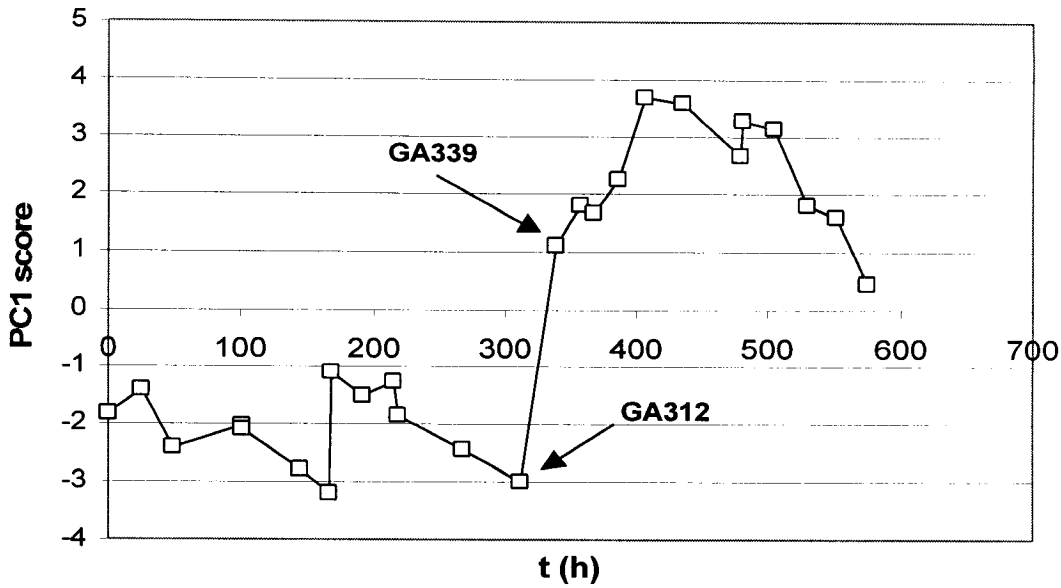

Figure 5-2: Plot of the numerical results of the first principal component in the PCA score plot without control data, without variables associated with time, Shannon-Weaver index, instantaneous caffeine and cumulative caffeine concentrations (Figure 4-27).

Interestingly, upon analysis of the loading plot (Figure 4-31), the location of the cumulative caffeine concentration (noted S_c) suggests that gel 2 samples seem to trend with higher caffeine concentrations, which was to be expected. Also, bands 3 and 5, which correspond to the band locations of the first two *P. putida* IF-3 patterns, seem to be strongly negatively correlated, since their physical distance in the loading plot is rather

large. Principal component analysis was very helpful in detecting such hidden trends in the data, as this would not have been noticed without the analysis. These results would suggest that the intensity of band 3 would be higher at high caffeine concentrations, while the intensity of band 5 would increase at lower caffeine concentrations. Band intensities as a function of the cumulative caffeine concentration added were plotted for these two bands (Figure 5-3). Trendlines were drawn, and it can be clearly seen that there is a trend between cumulative caffeine concentrations and increasing band intensities for band 3, while the opposite scenario occurred for band 5. Therefore, there is a definitive effect of caffeine on the mixed cultures, since exposure to higher concentrations could result in transient shifts in microbial populations.

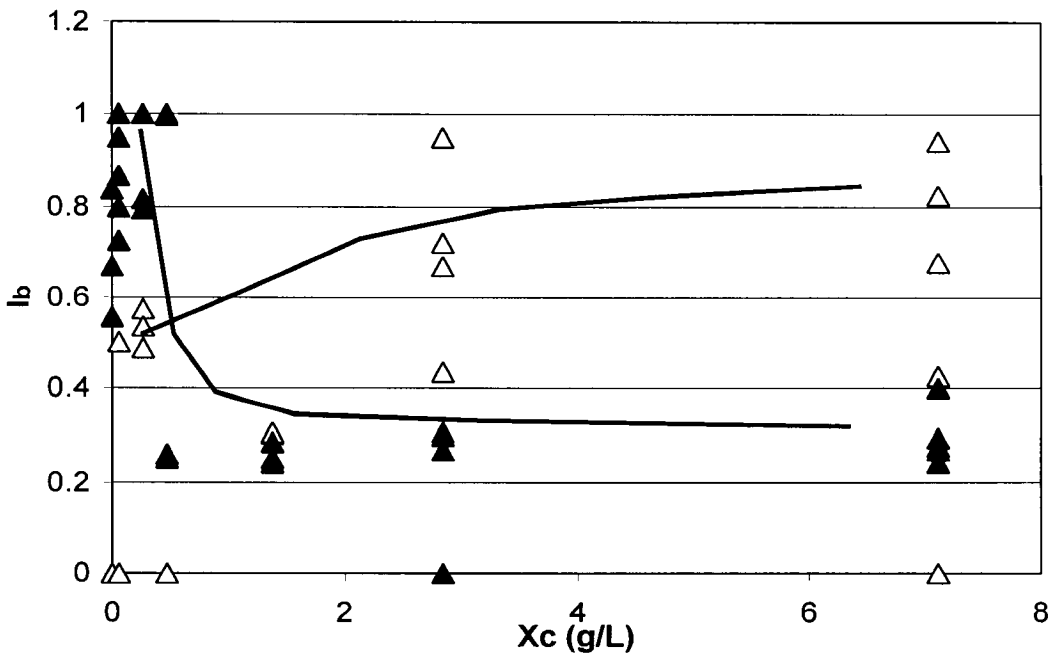

Figure 5-3: Band intensity variation upon cumulative caffeine addition for bands 3 (Δ) and 5 (▲) of the gel 1 and gel 2 banding patterns. Bands 3 and 5 correspond to bands 1 and 3 for figure 4-18, and bands 1 and 2 for figure 4-19.

Time, Shannon-Weaver index, caffeine and cumulative caffeine concentrations were then included. This was done to understand if all these variables exerted the same influence on the samples. Heavy clustering was still observed, separating GA and GB samples, with

GB samples correlating with the control variables (Figure 4-33). Time, Shannon-Weaver index, caffeine and cumulative caffeine concentrations were all situated rather closely in the loading plot, suggesting all these variables contain the same amount of information (Figure 4-34). Therefore, in the previous analysis, exchanging the cumulative caffeine concentration variable for any other of the variables mentioned above would not have changed the overall interpretation of the results.

As the gels were loaded with samples collected in chronological order, the natural transients in microbial communities over time could not be decoupled from the effects of caffeine. To circumvent this problem and also to prevent false interpretation of the data due to chronological loading on the gels, the experience was repeated with samples loaded in a random order. However, technical difficulties prevented proper analysis of the gels, and no data could be extracted from this experiment. Having said this, it is difficult to imagine that the score plot shown above would have yielded data that followed the expected caffeine concentration profiles, had the dependence been introduced artificially as a result of the order the samples were loaded.

In conclusion, banding pattern analysis by principle component analysis allowed a better understanding of the transient changes observed on a microbial consortium upon addition of caffeine. First, heavy clustering is taking place between the three data sets, namely the control data, gel 1 data and gel 2 data sets. These results suggest significant differences in banding patterns obtained with and without exposure of the mixed culture to caffeine. However, upon DGGE analysis, mixed cultures of the same origin sampled at significantly distant times will yield banding patterns with appreciable differences, due to the natural shifts in microbial communities in their habitat. Therefore, it was difficult to decouple what effects could be attributed to caffeine only from the overall transients observed with the mixed culture aging with time. Therefore, data from both caffeine gels could not be linked together with respect to time. Moreover, time, Shannon-weaver index, instantaneous and cumulative caffeine concentrations all carried the same information.

However, samples from gel 2, which were exposed to high caffeine concentrations, were clearly correlated to caffeine exposure. Also, PCA allowed detection of trends in specific bands, which seemed to demonstrate a strong correlation to caffeine exposure. Band 3 showed an increase in intensity upon addition of caffeine at high concentration, indicating a positive correlation, while band 5 was negatively correlated to cumulative caffeine concentration. Other bands showed similar responses to caffeine additions.

6. CONCLUSIONS

- Total caffeine removal was achieved by *Pseudomonas putida* IF-3 when used as the sole source of carbon and nitrogen. Such cultures led to ammonium accumulation, because of the high nitrogen content of the caffeine molecule.
- Upon addition of other carbon and nitrogen sources, complete caffeine degradation occurred without diauxic growth, but degradation rates varied upon the nature of the substrate added, and the nutrient limitation status of the culture. It was observed that the caffeine rates were lower than glucose degradation rates, therefore suggesting a lower affinity for caffeine than for other easily available carbon substrates.
- Addition of an external nitrogen source resulted in a decrease in both caffeine and glucose degradation rates.
- Degradation rates obtained were higher when cultures were exposed to carbon-limiting conditions, compared to nitrogen limitation. Therefore, the breakdown of the caffeine molecule in order to release nitrogen is suspected to be the rate-limiting step in the process.
- Maximizing caffeine removal in the presence of other carbon and nitrogen sources can be achieved by keeping the external nitrogen levels low, in order to promote caffeine breakdown.
- Monitoring changes and overall health of microbial populations using DGGE can be achieved, but interpretation of the results must consider the different sources of error that can result from the multiple steps in the protocol. Inherent biases in the lysis and PCR amplification steps can lead to banding patterns that do not represent all major bacterial species present in the population.
- Banding intensities can vary between samples. To circumvent this problem, proper scaling and band normalization is necessary in order to allow the user to compare bands in a gel, and lanes between different gels.
- Addition of a sample with a repeatable and easily identifiable banding pattern on each gel provides a good basis for reliable scaling.

- Analysis of genomic DNA of a pure culture by DGGE often results in multiple bands. The banding pattern is repeatable. This finding is in contrast to the prevailing assumption that a single DGGE band is associated with a single organism.
- Organisms that can achieve biological caffeine degradation appear to be more prevalent than previously thought. Such an organism was found and isolated from activated sludge from a wastewater treatment plant in the Montreal region.
- The indigenous caffeine-degrading microorganism might have played a protective role for the microbial consortium, from the effects of caffeine. Therefore, bioprotection might have occurred without the need for bioaugmentation with *Pseudomonas putida* IF-3.
- Principal component analysis revealed significant differences in the banding patterns obtained for the control mixed culture experiment and the caffeine-exposed mixed culture experiment. Although the number of species contained in the culture did not change appreciably, the relative amounts of the organisms trended with the amount of caffeine in the mixture.

7. RECOMMENDATIONS

7.1. CAFFEINE CONSUMPTION STUDIES

- All growth experiments would be best carried out in a bioreactor, to provide better process control (mixing, aeration, temperature control, online metabolic state). It was shown that degradation rates obtained were higher when cells were grown in the bioreactor, most probably since oxygen transfer was better compared to shake flasks, thus promoting faster aerobic metabolism (Tables 4-1 and 4-3).

- The discrepancy in substrate degradation rates (Table 5-1) can be partly explained by the fact that a high level of free nitrogen in the culture broth was carried from previous cycles for some of the cycles only. This could decrease the caffeine degradation rate, since exposure to free nitrogen could allow biomass formation on glucose without the need to breakdown the caffeine molecule to release nitrogen. Therefore, maintaining low free nitrogen levels at the beginning of each cycle would allow better comparison between degradation rates, theoretically decreasing the discrepancy in biomass numbers obtained.

- From the model used to determine the amounts of nutrients needed for growth on each substrate, nitrogen balances were not closed to less than 10%. The discrepancy between the expected numbers and the experimental data sets obtained can be explained in part by the method used for nitrogen quantification. Conway diffusion can only account for nitrogen released as ammonium, therefore not taking into account all other carbon-bound nitrogen intermediates that were released in the culture broth. Unfortunately, nitrogen accumulation measurements were not performed for most cycles, and therefore, the nitrogen data could not be completely interpreted in all cases. A more sensitive method to quantify total nitrogen release would have been of great help. Furthermore, for shake flask experiments, the biomass numbers obtained were always lower than predicted,

suggesting that the growth yields used in the model as observed for the bioreactor were not adequate for shake flask experiments, due to less efficient mixing and aeration. Experimental growth yields for shake flasks should be calculated.

7.2. DGGE AND GENETIC FINGERPRINTING

- From the DGGE results obtained with pure cultures, it is more accurate to look for species-specific banding patterns than specific bands only, even though looking for one major band per organism would be a valuable method for identifying known organisms in a microbial consortium. This conclusion is valid for pure culture DGGE work as well as for mixed culture work.

- The method used for cell lysis, was not as efficient as expected. After lysis using the Nebulizer, it was found that preferential lysis can lead to a DNA preparation that might not be representative of the genomic diversity present in the sample, if cells were lysed with different efficiencies. Preferential lysis might have occurred with Gram-negative cells over Gram-positive cells, leading to a banding pattern on the DGGE that was not proportional to the initial cell numbers from each cell type. Lysozyme and bead beating methods were also used, but did not provide better results. Ideally, a cell lysis technique that would act independently of the cell wall structure would help in solving the problem.

- It is important to note though, that the overall amount of DNA that can be recovered from each cell can vary between bacterial species. Figure 4-12 showed that the intensity of the banding patterns were definitely not proportional to the initial amount of template DNA, as shown by comparison of the *R. rhodochrous* banding patterns in pure and mixed samples (Figure 4-8). These results reinforce the idea of induced bias prior to DGGE.

- We were not able to quantify PCR products using absorbance measurements, due to the interference of PCR reagents at 260 nm (Table 4-4). Therefore, the actual quantity of DNA loaded onto the gel can differ from one sample to another, independently of the fact that the volumes were equal. Moreover, the only way to verify if DNA quantities seem consistent is by running the PCR verification gel, where saturation effects can lead to misinterpretation. A PCR cleanup kit to wash out all non-amplified nucleotides would allow quantification of PCR products, thus equal DNA quantities could be loaded on the DGGE gel, which is a step up towards quantification of the banding patterns.

- Addition of an internal standard for DGGE is a god way to ensure proper scaling of the banding patterns, when gel to gel comparison are to be made.

8. NOMENCLATURE

All units are as mentioned below unless otherwise noted in the text.

DW : Cell dry weight (g/L).

$\mathbf{V_{HCl}}$: Volume of 0.02N HCl added (μL).

$\mathbf{N_{ext}}$: Ammonium sulfate concentration (mg/L).

I : Normalized average intensity.

DNA : DNA concentration (ng/μL).

S : Caffeine concentration (g/L).

$\mathbf{S_c}$: Cumulative caffeine concentration (g/L).

G : Glucose concentration (g/L).

X : Biomass concentration (g/L).

t : Time (h).

$\mathbf{r_S}$: Caffeine degradation rate (g S/ g X-h).

$\mathbf{\Delta CO_2}$: Percent difference in carbon dioxide concentration between the air inlet and the reactor offgas (%).

N : Ammonium ion concentration (mM).

$\mathbf{r_G}$: Glucose degradation rate (g G/ g X-h).

Ib : Relative band intensity.

Rf : Relative migration distance of a band.

H : Shannon-Weaver index of bacterial diversity.

P_i : Importance probability of the bands in a lane.

I_i : Intensity value of band i.

E : Percent nutrient in excess in the experiment.

[A] : Stoechiometric amount of nutrient needed to close the mass balance.

[B] : Stoechiometric amount of nutrient added in the experiment.

9. REFERENCES

Amann, R. I., W. Ludwig, et al. (1995). "Phylogenetic identification and *in situ* detection of individual microbial cells without cultivation." Microbiological reviews **59**: 143-169.

Asano, Y., T. Komeda, et al. (1993). "Microbial production of theobromine from caffeine." Biosci. biotech. biochem. **57**(8): 1286-1289.

Ashihara, H. and A. Crozier (1999). Biosynthesis and metabolism of caffeine and related purine alkaloids in plants. Advances in botanical research. A. press. **30:** 117-205.

Barone, J. J. and H. Roberts (1984). Human consumption of caffeine. Caffeine: perspectives from recent research. P. B. Dews. New-York, Springer-Verlag**:** 59-73.

Blecher, R. and F. Lingens (1977). "The metabolism of caffeine by a *Pseudomonas putida* strain." Hoppe-Seyler's Z. Physiol. Chem. **358**: 807-817.

Braham, J. E. (1979). Coffee pulp in other species. Coffee pulp: composition, technology and utilization. J. E. Braham and R. Bressani. Ottawa, IDRC 108e, International development research center**:** 51-54.

Braham, J. E. and R. Bressani (1979). Coffee pulp: composition, technolgy and utilization. Ottawa, IDRC 108e, international development research center.

Bressani, R. (1979). Antiphysiological factors in coffee pulp. Coffee pulp: Composition, technology and utilization. J. E. Braham and R. Bressani. Ottawa, IDRC 108e, International development research center**:** 83-88.

Bressani, R. (1979). The by-products of coffee berries. Coffee pulp: composition, technology and utilization. J. E. Braham and R. Bressani. Ottawa, IDRC 108e, international development research center**:** 5-10.

Bressani, R. (1979). Potential uses of coffee-berry by-products. Coffee pulp: composition, technology and utilization. J. E. Braham and R. Bressani. Ottawa, IDRC 108e - International development research center**:** 17-24.

Cabezas, M. T., A. Flores, et al. (1979). Use of coffee pulp in ruminant feeding. Coffee pulp: composition, technology and utilization. J. E. Braham and R. Bressani. Ottawa, IDRC 108e, International development research centre**:** 25-38.

CAMO (1998). The Unscrambler, user manual, CAMO ASA.

Clark, R. J. (1985). Coffee; botany, biochemistry and production of beans and beverage. M. N. Clifford and K. C. Willson. London, Croom Helm**:** 230-250.

Clarke, R. J. and R. Macrae (1987). Coffee vol. 2 Technology. London, Elsevier applied science publishers.

Clayton, R. A., G. Sutton, et al. (1995). "Intraspecific variation in small-subunit rRNA sequences in GenBank: Why single sequences may not adequately represent prokaryotic data." International journal of systematic bacteriology **45**(3): 595-599.

Conway, E. J. (1957). Microdiffusion analysis and volumetric error. London, Lockwood.

Curatolo, P. W. and D. Robertson (1983). "The health consequences of caffeine." Annals of Internal medicine **98**: 641-653.

Curatolo, P. W. and D. Robertson (1984). The cardiovascular effects of caffeine. Caffeine: perspectives from recent research. P. B. Dews. New-York, Springer-Verlag**:** 77-85.

Davis, K. (1996). Coffee: A guide to buying, brewing and enjoying., St-Martin's press.

Derman, A. I., W. A. Prinz, et al. (1993). "Mutations that allow disulfide bond formation in the cytoplasm of *Escherichia coli.*" Science **262**: 1744-1747.

Dews, P. B. (1984). Caffeine: perspectives from recent research. New-York.

Doran, P. M. (1995). Bioprocesses engineering principles. London, Academic Press.

Eichner, C. A., R. W. Erb, et al. (1999). "Thermal gradient gel electrophoresis analysis of bioprotection from pollutant shocks in the activated sludge microbial community." Applied and environmental microbiology **65**(1): 102-109.

El Fantroussi, S., L. Verschuere, et al. (1999). "Effect of phenylurea herbicide on soil microbial communities estimated by analysis of 16S rRNA gene fingerprints and community-level physiological profiles." Applied and environmental microbiology **65**(3): 982-988.

Elias, L. G. (1979). Chemical composition of coffee-berry by-products. Coffee pulp: composition, technology and utilization. J. E. Braham and R. Bressani. Ottawa, IDRC 108e, international development research center**:** 11-16.

Eriksson, L., E. Johansson, et al. (1999). Introduction to multi- and megavariate data analysis using projection methods (PCA & PLS). Umea, Sweden.

Fortin, N., R. R. Fulthorpe, et al. (1998). "Molecular analysis of bacterial isolates and total community DNA from kraft pulp mill effluent treatment systems." Canadian journal of microbiology **44**: 537-546.

Friedman, J. and G. R. Waller (1985). "Allelopathy and autotoxicity." The international biometric society: 47-50.

Glück, M. and F. Lingens (1987). "Studies on the microbial production of theobromine and heteroxanthine from caffeine." Applied microbiology and biotechnology **25**: 334-340.

Hakil, M., S. Denis, et al. (1998). "Degradation and product analysis of caffeine and related dimethylxanthines by filamentous fungi." Enzyme and microbial technology **22**: 355-359.

Iwamoto, T., K. Tani, et al. (2000). "Monitoring impact of in situ biostimulation treatment on groundwater bacterial community by DGGE." FEMS Microbiology Ecology **32**: 129-141.

Jarquin, R. (1979). Coffee pulp in swine feeding. Coffee pulp: composition, technology and utilization. J. E. Braham and R. Bressani. Ottawa, IDRC 108e, International development research center: 39-49.

Juck, D., T. Charles, et al. (2000). "Polyphasic microbial community analysis of petroleum hydrocarbon-contaminated soils from two northern Canadian communities." FEMS Microbiology Ecology **33**: 241-249.

Koide (1996). Caffeine demethylate gene-containing DNA fragment and microbial process for producing 3-methyl-7-alkylxanthine. United States, Amano Pharmaceutical Co.

Kurtzmann, R. H. and S. Schwimmer (1971). "Caffeine removal from growth media by microorganisms." Experimencia **127**: 481-482.

Liu, W.-T., T. L. Marsh, et al. (1997). "Characterization of microbial diversity by determining terminal restriction fragment length polymorphism of genes encoding 16S rRNA." Applied and environmental microbiology **63**(11): 4516-4522.

Lodish, Baltimore, et al. (1995). Molecular cell biology. New York, De Boeck University.

Lundsberg, L. S. (1998). Caffeine consumption. Caffeine. G. A. Spiller. New York, CRC Press: 199-224.

Macnaugton, S. J., J. R. Stephen, et al. (1999). "Microbial population changes during bioremediation of an experimental oil spill." Applied and environmental microbiology **65**(8): 3566-3574.

McLeod, M. N. (1974). "Plant tannins. Their role in forage quality." Nutrition abstracts and reviews. **44**: 804-815.

Mesarch, M. B., C. H. Nakatsu, et al. (2000). "Development of catechol 2,3-dioxygenase-specific primers for monitoring bioremediation by competitive quantitative PCR." Applied and environmental microbiology **66**(2): 678-683.

Molina, M. R., G. de la Fuente, et al. (1974). "Decaffeination. A process to detoxify coffee pulp." Journal of agriculture, food and chemistry **22**(6): 1055-1059.

Morrison, C. and F. Gannon (1994). "The impact of the PCR plateau phase on quantitative PCR." Biochimica et biophysica acta **1219**: 493-498.

Muyzer, G. (1999). "DGGE/TGGE a method for identifying genes from natural ecosystems." Current opinion in microbiology **2**: 317-322.

Muyzer, G., E. De Waal, et al. (1993). "Profiling of complex microbial populations by denaturing gradient gel electrophoresis analysis of polymerase chain reaction-amplified genes coding for 16S rDNA." Applied and environmental microbiology **59**(3): 695-700.

Muyzer, G. and K. Smalla (1998). "Application of denaturing gradient gel electrophoresis (DGGE) and temperature gradient gel electrophoresis (TGGE) in microbial ecology." Antonie van Leeuwenhoek **73**: 127-141.

Nitschke, L., H. Wagner, et al. (1996). "Biological treatment of wastewater containing glycols from de-icing agents." Water research **30**(3): 644-648.

Ogino, A., H. Koshikawa, et al. (2001). "Succession of microbial communities during a biostimulation process as evaluated by DGGE and clone library analyses." Journal of applied microbiology **91**: 625-635.

Ogita, S., H. Uefuji, et al. (2003). "RNA interference: Producing decaffeinated coffee plants." Nature **423**(6942): 823.

Orue, C. and S. Bahar (1985). "Utilization of solid coffee waste as a substrate fro microbial protein production." Journal of food science and technology **22**: 10-16.

Penaloza, W., M. R. Molina, et al. (1985). "Solid-state fermentation: an alternative to improve the nutritive value of coffee pulp." Applied and environmental microbiology **49**(2): 288-393.

Putrament, A., H. Rabanowska, et al. (1972). "Specificity of caffeine effects. Inhibition by caffeine of RNA and protein synthesis in yeast and *Escherichia coli.*" Molecular and general genetics **118**: 373-379.

Rainey, F. A., N. L. Ward-Rainey, et al. (1996). "*Clostridium paradoxum* DSM 7308 contains multiple 16S rRNA genes with heterogeneous intervening sequences." Microbiology **142**: 2087-2095.

Rolz, C., R. de Leon, et al. (1988). "Biological pretreatment of coffee pulp." Biological reviews **26**: 97-114.

Roussos, S., M. A. Aquiahuatl, et al. (1994). "Caffeine degradation by *Penicillium verrucosum* in solid state fermentation of coffee pulp: critical effect of additional inorganic and organic nitrogen sources." Journal of food science and technology **31**(4): 316-319.

Roussos, S., M. de los Angeles Aquiahuatl, et al. (1995). "Biotechnological management of coffee pulp - isolation, screening, characterization, selection of caffeine-degrading fungi and natural microflora present in coffee pulp and husk." Applied microbiology and biotechnology **42**: 756-762.

Sambrook, J., E. F. Fritsch, et al. (1989). Molecular cloning, a laboratory manual. Plainview, New York, Cold Spring Harbor laboratory press.

Santegoeds, C. M., T. G. Ferdelman, et al. (1998). "Structural and functional dynamics of sulfate-reducing populations in bacterial biofilms." Applied and environmental microbiology **64**(10): 3731-3739.

Schneegurt, M. A. and C. F. J. Kulpa (1998). "The application of molecular techniques in environmental biotechnology for monitoring microbial systems." Biotechnology and applied biochemistry **27**: 73-79.

Shuler, M. L. and F. Kargi (1992). Bioprocess engineering: Basic concepts. Englewood Cliffs, Prentice Hall PTR.

Sideso, O., F.P., A. Marvier, C., et al. (2001). "The characteristics and stabilization of a caffeine demethylase enzyme complex." International journal of food science and technology **36**: 693-698.

Somogyi, J. C. and U. Näegli (1976). "Antithiamine effect of coffee." International journal for vitamin and nutrition research **46**: 149-153.

Spiller, G. A. (1984). The methylxanthine beverages and foods: chemistry, consumption and health effects. New York.

Spindel, E. R. and R. J. Wurtman (1984). Neuroendocrine effects of caffeine in rat an man. Caffeine: perspectives from recent research. P. B. Dews. New York, Springer-Verlag: 119-128.

Vallaeys, T., E. Topp, et al. (1997). "Evaluation of denaturing gradient gel electrophoresis in the detection of 16S rDNA sequence variation in rhizobia and methanotrophs." FEMS Microbiology Ecology **24**: 279-285.

Waller, G. R., D. Kumari, et al. (1986). Caffeine autotoxicity in *Coffea arabica* L. The science of allelopathy. P. A.R. and C. S. Tang. New York, John Wiley and sons: 243-269.

Wang, Y., Z. Zhang, et al. (1997). "The actinomycete *Thermobispora bispora* contains two distinct types of transcriptionally active 16S rRNA genes." Journal of bacteriology **179**(10): 3270-3276.

Wilson, J. G. and W. J. Scott Jr. (1984). The teratogenic potential of caffeine in laboratory animals. Caffeine: perspectives from recent research. P. B. Dews. New York, Springer-Verlag: 165-187.

Wintzingerode, F. V., U. B. Göbel, et al. (1997). "Determination of microbial diversity in environmental samples: pitfalls of PCR-based rRNA analysis." FEMS Microbiology reviews **21**: 213-229.

Woese, C. R. (1987). "Microbial evolution." Microbiological reviews **51**: 221-271.

Woolfolk, C. A. (1975). "Metabolism of N-methylpurines by a *Pseudomonas putida* strain isolated by enrichment on caffeine as the sole source of carbon and nitrogen." Journal of bacteriology **123**: 1088-1106.

Young, C. C., R. L. Burghoff, et al. (1993). "Polyvinylpyrrolidone-Agarose Gel Electrophoresis Purification of Polymerase Chain Reaction-Amplifiable DNA from Soils." Applied and environmental microbiology **59**(6): 1972-1974.

Zuluaga, V. J. (1989). Utilizacion integral de los subproductos del café. Proceedings of I seminario international sobre biotechnologica en la agroindustri cafetalera (I SIBAC), Xalapa, Mexico.

APPENDIX 1: MASS BALANCE EQUATIONS

From equation 5-1, the overall equation of the mass balance process was:

$$aC_8H_{10}O_2N_4 + bC_6H_{12}O_6 + cO_2 \rightarrow dCH_{1.79}O_{0.5}N_{0.2} + eCO_2 + fH_2O + gNH_3$$

caffeine glucose biomass

This equation can be divided in two:

(1) $aC_8H_{10}O_2N_4 + cO_2 \rightarrow dCH_{1.79}O_{0.5}N_{0.2} + eCO_2 + fH_2O + gNH_3$

caffeine biomass

Where **a** is the known caffeine concentration (in mol/L).

(2) $bC_6H_{12}O_6 + cO_2 + gNH_3 \rightarrow dCH_{1.79}O_{0.5}N_{0.2} + eCO_2 + fH_2O$

glucose biomass

Where **b** is the known glucose concentration (in mol/L).

MW caffeine: 194.17 g/mol
MW glucose: 180.16 g/mol
MW biomass: 24.6 g/mol
MW NH3: 17.024 g/mol

$\mathbf{Y}_{X/S}$ = 0.135 g X / g S = 1.065 mol X / mol S (experimental)

$\mathbf{Y}_{X/G}$ = 0.284 g X / g G = 2.078 mol X / mol G (experimental)

For equation (1):

(1) $aC_8H_{10}O_2N_4 + cO_2 \rightarrow dCH_{1.79}O_{0.5}N_{0.2} + eCO_2 + fH_2O + gNH_3$

caffeine biomass

Material balances:

C: $8a = 0c + 1d + 1e + 0f + 0g$
H: $10a = 0c + 1.79d + 0e + 2f + 3g$
O: $2a = -2c + 0.5d + 2e + 1f + 0g$
N: $4a = 0c + 0.2d + 0e + 0f + 1g$
$\mathbf{Y}_{X/S} = d/a = 1.065a = 0c + 1d + 0e + 0f + 0g$

Two matrices were built in Excel, matrix A with the material balance unknowns, and matrix B for the constants. Values were obtained by multiplying both matrices in the following way:

[A]-1 x [B] = [RESULTS]

Example:

With a starting caffeine concentrations at 0.25 g/l = 1.29E-03 mol/L.

MATRIX A

c	d	e	f	g
0	1	1	0	0
0	1.79	0	2	3
-2	0.5	2	1	0
0	0.2	0	0	1
0	1	0	0	0

MATRIX B

1.03E-02
1.29E-02
2.58E-03
5.15E-03
1.37E-03

[caffeine]	0.25	g/L
	1.29E-03	mol/L

MATRIX A INVERTED

c	d	e	f	g
1	0.25	-0.5	-0.75	-1.048
0	0	0	0	1
1	0	0	0	-1
0	0.5	0	-1.5	-0.595
0	0	0	1	-0.2

X

MATRIX B

1.03E-02
1.29E-02
2.58E-03
5.15E-03
1.37E-03

RESULTS

Mol/L	Component	g/L
6.93E-03	O2	**0.222**
1.37E-03	Biomass	**0.034**
8.93E-03	CO2	**0.393**
-2.10E-03	H2O	**-0.038**
4.88E-03	NH3	**0.083**

These values could used to predict biomass formation on caffeine only. By putting the NH3 value obtained from (1) on the left side of equation (2), we can determine the amount of biomass that can be formed on glucose with the available nitrogen released from the caffeine. The overall result will also tell what nutrient will be limiting the culture.

For equation (2):

(2) $bC_6H_{12}O_6 + cO_2 + gNH_3 \rightarrow dCH_{1.79}O_{0.5}N_{0.2} + eCO_2 + fH_2O$
glucose biomass

Material balances:

C: 6b = 0c + 0g + 1d + 1e + 0f
H: 12b + 3(NH_3 from(1)) = 0c - 3g + 1.79d + 0e + 2f
O: 6b = -2c + 0g + 0.5d + 2e + 1f
N: 1(NH_3 from(1)) = 0c - 1g + 0.2d + 0e + 0f
$\mathbf{Y}_{X/G}$ = d/b = 3.662b = 0c + 0g + 1d + 0e + 0f

Two matrices were built in a similar fashion as for equation (1).

Example:

With a starting glucose concentration at 1 g/L = 5.55E-03 mol/L.

MATRIX A

c	d	e	f	g
0	1	1	0	0
0	1.79	0	2	-3
-2	0.5	2	1	0
0	0.2	0	0	1
0	1	0	0	0

MATRIX B

3.33E-02
8.12E-02
3.33E-02
4.88E-03
2.03E-02

[glucose] 1 g/L
5.55E-03 mol/L

MATRIX A INVERTED

c	d	e	f	g
1	0.25	-0.5	0.75	-1.348
0	0	0	0	1
1	0	0	0	-1
0	0.5	0	1.5	-1.195
0	0	0	1	-0.2

X

MATRIX B

3.33E-02
8.12E-02
3.33E-02
4.88E-03
1.15E-02

RESULTS

Mol/L	Component	g/L
2.12E-02	O2	**0.679**
1.15E-02	Biomass	**0.284**
2.18E-02	CO2	**0.958**
2.64E-02	H2O	**0.476**
2.57E-03	NH3	**0.044**

From the values obtained it was possible to determine the reaction totals.

TOTALS

Mol/L	Component	g/L
1.29E-03	Caffeine	**0.250**
5.55E-03	Glucose	**1.000**
2.81E-02	O2	**0.901**
3.07E-02	CO2	**1.351**
2.43E-02	H2O	**0.438**
1.29E-02	Biomass	**0.318**
2.57E-03	NH3	**0.044**

The model therefore predicts formation of 0.318 g/L biomass, with 0.25 g/L caffeine and 1 g/L glucose as starting carbon and nitrogen sources. It can also be noted that cultures run under these conditions will not go into nitrogen limitation, since there is an overall nitrogen accumulation as ammonium of 2.57E-03 mol/L.

Addition of ammonium sulfate as supplemental nitrogen source.

When $(NH_4)_2SO_4$ was added to the culture broth, an additional ammonium term was added on the left side of the overall mass balance equation to give:

$$aC_8H_{10}O_2N_4 + bC_6H_{12}O_6 + cO_2 + h(NH_4)_2SO_4 \rightarrow dCH_{1.79}O_{0.5}N_{0.2} + eCO_2 + fH_2O + gNH_3$$

caffeine glucose NH_4 sulfate biomass

Material balances were performed as described above to allow determination of the biomass and leftover ammonium concentrations, from known initial caffeine, glucose and ammonium sulfate concentrations.